

Pressure sensitive adhesives from renewable resources

Zur Erlangung des akademischen Grades eines

DOKTORS DER NATURWISSENSCHAFTEN

(Dr. rer. nat.)

Fakultät für Chemie und Biowissenschaften

Karlsruher Institut für Technologie (KIT) - Universitätsbereich

genehmigte

DISSERTATION

von

Dipl.-Chem. Wiebke Jutta Maaßen

aus

Weingarten (Ravensburg)

Dekan: Prof. Dr. Willem Klopper

Referent: Prof. Dr. Michael A. R. Meier

Korreferent: Prof. Dr. C. Barner-Kowollik

Tag der mündlichen Prüfung: 21.10.2015



Dieses Werk ist lizenziert unter einer Creative Commons Namensnennung 3.0 Deutschland Lizenz (CC BY 3.0 DE): <http://creativecommons.org/licenses/by/3.0/de/>

Die vorliegende Arbeit wurde im Zeitraum von August 2010 bis Juni 2015 unter Anleitung von Prof. Dr. Norbert Willenbacher (Institut für Mechanische Verfahrenstechnik und Mechanik) und Prof. Dr. Michael A. R. Meier (Institut für Organische Chemie) des Karlsruher Institut für Technologie (KIT) angefertigt.

VORWORT

„Viele Missverständnisse entstehen dadurch, dass ein Dank nicht ausgesprochen, sondern nur empfunden wird.“

Ernst R. Hauschka

Aus diesem Grunde möchte ich gebührenden Dank meinen Mentoren Prof. Dr. Norbert Willenbacher und Prof. Dr. Michael A. R. Meier aussprechen. Norbert dafür, dass er mir die Möglichkeit geboten hat dieses interessante, angewandte und umfangreiche Thema zu bearbeiten und mir bei aufkommenden Problemen in der materiellen Charakterisierung zur Seite stand. Mike danke ich sehr für die problemlose Integration in seine Arbeitsgruppe, die vielen Tipps und Tricks in Sachen Synthese und die motivierenden Worte wenn es mal nicht voranzugehen schien. Beiden danke ich für ihr Vertrauen in meine selbständige Arbeit innerhalb beider Gruppen und gruppenübergreifend und für ihre herausragende Menschlichkeit, die immer wieder bei diversen Seminaren und Ausflügen positiv zum Ausdruck kam.

Der Fachagentur für Nachwachsende Rohstoffe (FNR) danke nicht nur ich für die finanzielle Unterstützung und Förderung des innerhalb dieser Arbeit beantragten und genehmigten Forschungsvorhabens.

Dem Kooperationspartner tesa SE sei ein wertvoller Dank ausgesprochen, ohne dessen Beteiligung das Projekt nicht möglich gewesen wäre. Dazu bedanke ich mich namentlich recht herzlich bei Herrn Dr. Bernd Lühmann, Herrn Dr. Ingo Neubert und Herrn Dr. Alexander Prenzel für die informellen und erkenntnisbringenden Diskussionsrunden.

Eine Reihe wichtiger Menschen nahmen *maß-*geblich am Gelingen dieser Arbeit Anteil, darum danke ich auch besonders den Kollegen, denen ich bei ihrer Projektfindungsphase behilflich sein konnte - insbesondere denjenigen, denen ich in den Mittagspausen zur Alltagsbelustigung beitrug - welche kein BBQ verschmähten, obgleich winterliche Temperaturen herrschten - diejenigen, die mit ihrer Kaffeetasse zum höchst wissenschaftlichen Informationsaustausch ins Nachbarbüro einkehrten - und den vielen, die sich so viel Mühe mit meinen immer wiederkehrenden Fragen gaben. Danke euch allen für die unvergesslichen Erfahrungen inner- und außerhalb

der Arbeitsbereiche. Danke für privaten Austausch und nicht zu vergessen hoch zu Ross, Hossa! Hossa!

Frau Dr. Yana Rüdener geb. Peykova setzte für mich den Grundstein in Sachen Kleben, deshalb gilt ein besonderer Dank ihrem liebevollen und stets erfreulichen Wesen. Ihr und ihrer Familie wünsche ich alles Gute.

Herrn Dr. Oliver Kreye besten Dank für die Einführung in die Monomer Synthese - er stand mir während dieser Jahre mit all seinem Wissen mit Rat und Tat zur Seite.

Eine herzliche Umarmung für Frau Sabrina Müller, ihre offene Tür und ihre großartige Unterstützung in allen Belangen. All diejenigen die denken die Müllermilch macht's, kennen den Müller'schen Kaffee noch nicht!

Größter Dank gebührt meinen Eltern, die mit Sicherheit nach meiner Geburt schon wussten, dass ihre 'Lütte' noch Großes vollbringen würde und die mir dazu das Studium der Chemie ermöglichten, um mir in jeder Hinsicht ihre Unterstützung zukommen zu lassen. Meiner geliebten Schwester Claudia und ihrer außerordentlichen Familie herzlichen Dank für die rettenden Trosttelefonate zu Prüfungszeiten. Meinem lieben Bruder und seiner außerordentlichen Familie vielen Dank für die wertvolle technische Beratung in Sachen PC-Technik und Datenrettung.

„Das Beste kommt zum Schluss“ und herzlichster Dank kommt aus tiefstem Herzen für die eine Person, die mich durch all die Zeit bestärkt hat auch noch die letzten Schritte zur Fertigstellung dieser Arbeit zu tun. Ich kann, ob du es glaubst oder nicht, selbst mit Worten nicht ausdrücken wie unendlich dankbar ich für dich, Stefan Oelmann, in meinem Leben bin.

In Gedenken an meine Großeltern.

ZUSAMMENFASSUNG

Ein wichtiges Segment des Klebstoffmarktes stellen die sogenannten Haftklebstoffe (pressure sensitive adhesives, PSAs) dar, die für unterschiedlichste Anwendungen, wie z.B. Etiketten, Klebebändern und -folien oder Bauklebstoffen sowohl industriell als auch im Hausgebrauch eingesetzt werden. Aufgrund der steigenden Nachfrage von nachwachsenden Rohstoffen, versucht man in aktueller Forschung erdölbasierte Klebstoffe durch erneuerbare Materialien mit ähnlichen oder verbesserten Klebeeigenschaften zu ersetzen.

In dieser Arbeit werden neue Einblicke in die Klebeeigenschaften von bio-basierten PSAs präsentiert. Drei unterschiedliche Homopolymere auf Basis nachwachsender Fettsäuremethylester aus heimischen Pflanzenölen wurden dazu in Bezug auf ihre mechanischen wie auch adhäsiven Eigenschaften charakterisiert.

Die entsprechenden Monomere sowie Polymere wurden im Arbeitskreis von Prof. Dr. M. A. R. Meier (Institut für Organische Chemie, IOC, KIT) synthetisiert. Diese Monomere konnten mittels freier radikalischer Polymerisation zu Polymeren mit hohen Molekulargewichten umgesetzt werden. Zusätzlich wurden Polymere mittels Miniemulsionspolymerisation als stabile Dispersionen hergestellt. Die Verarbeitungs- und Adhäsionseigenschaften wurden in der Arbeitsgruppe von Prof. Dr. N. Willenbacher (Institut für Mechanische Verfahrenstechnik und Mechanik, MVM, KIT) charakterisiert.

Die Polymere zeigten typische Abhängigkeiten der Adhäsion von Molekulargewicht und Vernetzungsgrad, welche durch rheologische Studien als auch Tack- und 90° Schältests charakterisiert wurden. Das Acrylierte Methyl Oleat Monomer (**4ac**, AMO) und dessen Polymer (**P4ac**, p(AMO)) wurden hierfür im Detail untersucht. Unter anderem konnte durch Erhöhung der Trocknungszeit ein Übergang von Kohäsions- zu Adhäsionsbruch beobachtet werden, welcher sich mittels der unterschiedlichen Messmethoden darstellen lässt. Insbesondere sollte evaluiert werden, ob sich aufgrund der Hydrophobie der Monomere spezifische Vorteile gegenüber herkömmlichen erdölbasierten Produkten bezüglich der Haftung auf hydrophoben Substraten wie Polyolefinen ergeben. Im Allgemeinen zeigten die synthetisierte Polymere gute adhäsive Eigenschaften im Vergleich zu kommerziellen erdölbasierten Produkten und darüber hinaus verbesserte Eigenschaften auf niederenergetischen Oberflächen.

ABSTRACT

Pressure-sensitive adhesives (PSAs) represent an important segment of the adhesives market. They find many applications, i.e. as labels, tapes and foils, or special construction adhesives. Due to an increasing demand for renewable products, current research aims to replace petrochemical-based adhesives with renewable materials while maintaining or improving adhesive performance.

In this work, novel insights into the adhesive performance of bio-based pressure sensitive adhesives are presented. Three different homopolymers based on fatty acids derived from native vegetable oils as renewable feedstock were characterized in terms of their mechanical and adhesive properties.

Appropriate monomers and polymers were synthesized in the group of Prof. Dr. M. A. R. Meier (Institute for Organic Chemistry, IOC, KIT). Derived monomers were polymerized *via* free radical polymerization resulting in high molecular weight polymers with adhesive properties. Polymers were also obtained as aqueous dispersions by means of miniemulsion polymerization. The processing and adhesive properties were characterized in the group of Prof. Dr. N. Willenbacher (Institute of Mechanical Engineering and Mechanics, MVM, KIT). The polymers displayed the typical dependence of molecular weight and degree of crosslinking on the adhesive performance, which was quantified by rheological studies as well as probe-tack and 90° peel measurements. In particular, the monomer Acrylated Methyl Oleate (**4ac**, AMO) and the thereof derived polymer (**P4ac**, p(AMO)) were intensively studied. By increasing curing time at a given temperature, it was possible to show the change in the debonding behavior from cohesive towards adhesive failure. The same trend was also observed in tack and peel tests. Furthermore, specific advantages concerning the adhesion on hydrophobic substrates, such as polyolefins, compared to conventional petroleum-based products were investigated. The described polymers generally showed good PSA performance compared to a common industrial standard and display improved adhesion to the low surface energy substrate.

TABLE OF CONTENT

VORWORT	I
ZUSAMMENFASSUNG	III
ABSTRACT	IV
TABLE OF CONTENT	V
1. INTRODUCTION	1
2. FUNDAMENTALS AND STATE OF THE ART	4
2.1 Adhesives	4
2.1.1 Adhesives classification system	4
2.1.2 Pressure sensitive adhesives	6
2.2 Principles of adhesion	10
2.2.1 Bond formation	11
2.2.2 Bond separation	20
2.2.3 The stages of debonding by cavity nucleation	23
2.3 Evaluation methods of adhesive performance	28
2.3.1 Shear resistance.....	28
2.3.2 Peel test	28
2.3.3 Probe tack	32
2.3.4 Rheology of PSAs	34
2.4 Principles of polymer synthesis	41
2.4.1 Step growth polymerization	41
2.4.2 Chain growth polymers.....	42
2.4.3 Homogeneous bulk-/solution polymerization	47
2.4.4 Heterogeneous Polymerization.....	48
2.5 Appropriate polymers from renewable resources	52
2.5.1 Plant oils as renewable raw material	52

2.5.2 PSAs from renewable feedstock.....	54
3. RESULTS AND DISCUSSION	57
3.1 Synthesis of the acrylated fatty acid methyl esters	57
3.1.1 Three-step procedure	58
3.1.2 Two-step procedure.....	60
3.1.3 One-step procedures.....	61
3.2. Synthesis of poly(fatty acid methyl esters)	66
3.2.1 Polymer synthesis in solution/bulk.....	66
3.2.2 Modification of the polymer.....	70
3.2.3 Copolymer synthesis	71
3.2.4 Polymer synthesis in miniemulsion.....	72
3.3 Adhesive performance	74
3.3.1 Viscoelastic properties.....	74
3.3.2 Tack and peel performance	76
3.3.3 Influence of molecular weight on tack and peel.....	78
3.4 Tailoring adhesion behavior via curing	80
3.4.1 Effect of curing on shear modulus	80
3.4.2 Effect of curing on tack and peel	82
3.5 Adhesion to low energy substrates.....	86
3.6 Water resistance	89
4. EXPERIMENTAL PART	91
4.1 Materials and methods	91
4.2 Monomer synthesis	95
4.2.1 Monomer synthesis in a three-step procedure (A, B, C)	95
4.2.2 Monomer synthesis in a two-step procedure (procedure A, D)	102
4.2.3 One-step synthesis pathway (procedure E).....	104
4.3 Polymer synthesis	107

4.3.1 Solvent-/bulk polymerization.....	107
4.3.2 Saponification of the polymer side chain	107
4.3.3 Miniemulsion polymerization.....	107
4.3.4 Synthesized polymers	108
4.4 Preparation of polymer films.....	112
4.5 Experimental procedure	113
4.5.1 Determining tack.....	113
4.5.2 Determining peel	115
4.5.3 Determining viscoelastic properties	116
5. OUTLOOK AND CONCLUDING REMARKS	118
6. INDEX OF CONTENTS	121
List of Abbreviations and Symbols	121
List of Figures	128
List of Schemes	130
List of Tables.....	131
References.....	132
7. APPENDIX.....	151
List of Publications and Conference Contributions.....	151

1. INTRODUCTION

Sustainability is an important criterion in product design and development. To be considered truly sustainable, something may not negatively impact the overall ecosystem. The market demands more sustainable materials and industrial solutions. Specifically, renewable resources that can replace fossil resources are in high demand. A change from fossil feedstock to renewable resources offers a great opportunity for industrial applications, as renewables are believed to be capable of fulfilling highly challenging tasks^[1-3] There are numerous examples of renewable resources, which can substitute fossil born ones in many industrial processes as well as our everyday lives such as: in the energy sector, the textile industry, paints and coatings, pharmacy and of course in chemistry. The use of oils and fats as renewable raw materials is well established and a subject of continued investigation.^[4] The structural diversity of fatty acids depends on the oil source. It enables the design of a multitude of monomers, fine chemicals, and polymers, which can be derived in a straightforward fashion. Especially oils with high content of only one fatty acid, such as high oleic oils with a content of oleic acid exceeding 90%, have large potential for the substitution of petrochemicals currently in use.^[5,6]

If one considers an application where renewables currently play an important role, the energy sector comes to mind first; however, renewables are also present in the consumer products market. Companies and products advertise with various bio- and eco-labels, which stand for environmentally-friendly manufacture and/or utilization of renewable resources. In a simple walk through a supermarket reveals products ranging from detergents and cleaning products to food and cosmetics that all claim to be the most environmentally friendly one. On the contrary, daily used products the customer is less aware of are largely neglected in this regard. Adhesive are such an example.

Adhesives play an important role in both industrial and consumer products. The consumer is able to choose among many different types of adhesives, which are variable in their properties and thus able to cover many applications. The demand for adhesives has increased more than 25 % in the period from 2003 to 2013^[7] Pressure sensitive adhesives (PSAs) cover a production volume of about 200,000 tons per year in Europe (one-third as water based dispersions), which are used in approximately

1. Introduction

25,000 different industrial products. PSAs represent a macromolecular system that remains permanently tacky at room temperature and is able to adhere under slight pressure to any given substrate in a very short time without any phase transition or chemical reaction.^[8] Depending on the application, it can be designed to be completely removable from the surface. The global market shows a wide range of different products such as sticky tapes, stamps, and different kinds of labels.^[9] Typically, PSAs are specifically formulated to give optimum flexibility and, at the same time, a tack and peel strength adjusted to the desired application. A sufficiently low viscosity is needed to wet the surface of the substrate and generate initial adhesion, whereas a high elasticity is required to sustain loads (cohesion) and to enable a clean removal.

The main raw materials used are natural rubber, styrene-butadiene-styrene (SBS), polyisobutylene (PIB), nitrile rubber (NBR), polyurethanes, or polyacrylates. Major commercial PSAs are made from petroleum-based acrylate monomers (i.e. *n*-butyl acrylate or 2-ethylhexyl acrylate), which are optionally copolymerized with some vinyl compounds.^[10] One can tune the adhesive behavior in a wide range by selecting suitable co-monomers affecting the glass transition temperature or the surface energy and most importantly by adjusting the molecular weight as well as the degree of cross-linking and branching in the final product. It is thus possible to tailor tack and peel, as well as creep and shear properties.

Sustainability also plays an important role in the adhesive sector. In the year 2011, more than half of all adhesives in use were water based systems and the demand for replacing solvent borne adhesives towards new water based technologies continues to grow. Ecology-driven adaptations concentrate on production techniques as well as the substitution of adhesive types. Adhesive production by means of promoting renewable raw materials can lead to an independence of crude oil, as well as an improved CO₂ balance.

The motivation for this work is the challenge of producing pressure sensitive adhesives on the basis of renewable raw materials such as plant oils. This involves both the evaluation of the synthesis of these bio-based adhesives and their precursors as well as their characterization. In particular, the focus is on the use of domestic high oleic rapeseed and sunflower, since they provide oleic acid at competitive prices and in high

purity. Figure 1 shows the chemical structure of the thus derived renewable monomers used for this study. Using such starting materials, the derived adhesives can also be optimized for adhesion to low-energy surfaces in order to create an alternative to the market controlling oil-based products with improved application profile.

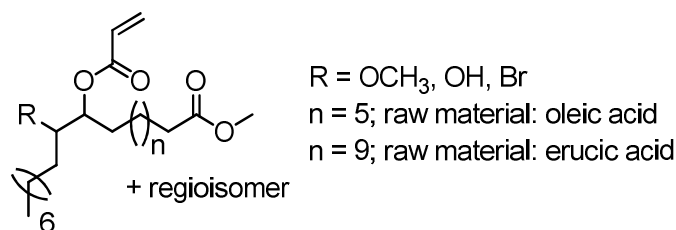


Figure 1. Chemical structure of synthesized and characterized acrylic monomers.

The aim of displacing oil-based PSAs requires a systematic study of the synthesized polymers. Therefore, the adhesive properties of PSAs, such as tack, peel strength, and viscoelastic behavior were studied in detail. The influence of the substrate surface roughness and the surface energy was also investigated. The copolymerization of an acrylic comonomer and the dependence on cross-linking was shown to be an important factor influencing the adhesion and forcing the transition of cohesive to adhesive failure. Characterization of the mechanical properties was achieved by means of the probe tack test in combination with image observation. The experimental setup allows observation of the debonding process, thereby tracking cavitation and fibrillation during separation from the substrate. Peel data results from a FINAT No. 2 methods based measurement, where an adhesive strip is peeled in a 90° angle off a glass substrate, are also discussed. The viscoelastic properties were determined by rheological oscillatory shear measurements.

2. FUNDAMENTALS AND STATE OF THE ART

2.1 Adhesives

Adhesives associated with sealants are of widespread interest and are known for many centuries. The very first adhesives consisted of natural materials such as bees wax, tree sap, or tar. Later on, animal protein and natural latex were developed. With the manifestation of the chemical industry and strides in synthetic polymer processing, the range of adhesive formulations expanded enormously. Modern life is unimaginable without them.

The automotive and aircrafts industries gave important impulses by implementing this key technology. The automotive and aircraft industries have an acute interest in weight reduction and thus construction methods based on bonding technologies are of high importance. In a modern aircraft, up to 30 % of all components are joined by adhesive bonds. In a modern car, the classic bonding techniques are usually used in combination with adhesive bonding. Nowadays, cars contain up to 18 kg of adhesive material.

2.1.1 Adhesives classification system

Adhesives are a part of everyday life: for small repair jobs, as office equipment, or for craftsmanship. Common adhesives however remain hidden and are generally out of sight to consumers. Adhesives are used extensively in the medical sector in form of everything from simple bandages to advanced medical applications (i.e. transdermal patches that allow a controlled drug delivery into the human body). Accordingly, adhesives can be classified in many different ways, for instance by bonding mechanism, chemistry type, or by application (i.e. structural vs. non-structural). Additionally, adhesives can be classified according to elastic properties taking in to account the mechanic moduli for rigid adhesives being in the range of 10^9 Pa. Elastomers show mechanical moduli of around 10^6 Pa and slightly cross-linked polymer melts in general around 10^4 Pa.^[11]

A typical classification, which gives a good overview, comprises three general adhesive types: chemical curing, physical hardening and pressure sensitive adhesives (see Figure 2).

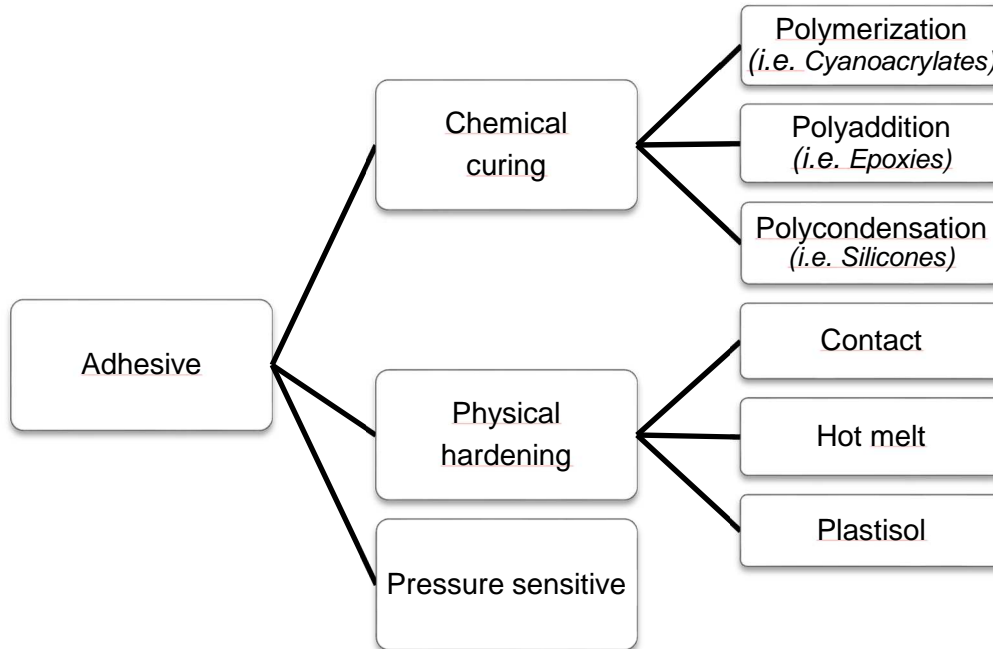


Figure 2. Classification of adhesive types.

Chemical curing

Chemically cured adhesives are known as reactive adhesives; they require a reaction from a liquid to a solid state. The process can be chain or step-growth polymerization, vulcanization or mild cross-linking. Once reacted, they offer high strength and resistance towards humidity, high temperature as well as chemicals. Examples include single component cyanoacrylates or two component epoxies.^[12]

Physical hardening

The type of physical hardening describes adhesives that are already in their final chemical state, such as hot melts. Mostly thermoplastics, elastomers (often based on polyesters or polyamides) and tackifiers resin mixtures, combined with stabilizers and fillers, which can be melted and liquefied, provide good bond flexibility with a wide

2. Fundamentals and state of the art

range of applications. Plastisol's are suspensions of a thermoplastic polymer distributed in a tackifiers phase (liquid plasticizer) without any additional solvent. Heating starts to dissolve the polymer in the plasticizer and the plastisol finally transform into a gel. This process is not reversible and cooling will result in a flexible, permanently plasticized solid.^[13] Contact adhesives are solution polymers which are applied to each surfaces and allowed some time to dry before the two surfaces are pushed together. Once they are dried to a certain degree the bond can be formed immediately and permanently under light pressure.^[14]

Pressure sensitive

Pressure sensitive adhesives bear a special feature. They do not show any phase change from liquid to solid, but remain highly viscous. As a consequence, they are permanently tacky. Bonding is achieved by the ability to wet the surface directly in contact with a substrate and an applied pressure. The required contact time is quite short, around 1 second, and the required pressure is low (e.g. finger pressure). Since these adhesives are soft materials, the strength decreases with increasing temperature. A disadvantage is their tendency to creep, which increases with loads. Creep is defined as the time-dependent deformation of a material that is subjected to a constant load. Typically, within a bonded joint, it will be the adhesive that will suffer creep deformation. Detachment can occur easily, but this behavior is often considered desirable for certain applications.^[8]

2.1.2 Pressure sensitive adhesives

As PSAs are designed to be continuously sticky or tacky adhesives, they can be removable or permanent, depending on the application. As mentioned before, these design possibilities make PSAs very important in many industrial applications. They are intensively used for labels, sticky notes, masking tapes and –foils, as adhesive stripes of any type, one sided, double sided or reinforced. As previously mentioned, pressure sensitive adhesives are typically formulated from low performance natural rubber or certain low to high performance synthetic rubbers and polyacrylates.

2. Fundamentals and state of the art

Table 1. Comparison of main PSA such as natural rubber (NR), styrene-butadiene-rubber (SBR), styrene-block-copolymer (SBC), Acrylics and ethylene-vinyl acetate (EVAc) and their processing.^[15]

Raw material	NR	SBR	SBC	Acrylic	EVAc
Features	Depolymerization possible	Limited copolymerization	Limited copolymerization	Copolymerizable	Limited copolymerization
Synthesis	-	Limited expensive technology	Limited expensive technology	Off-/In-line, free radical, ionic, etc.	High pressure, offline free radical
Products	Solvent-/water-based	Water-based, limited solvent-based	Hot-melt PSA, limited solvent-based	Solvent-/water-based, limited hot-melt PSA	Water-based, limited solvent-based, hot-melt PSA
Formulability	Compatible with base polymers and tackifiers	Limited compatibility	Limited compatibility	Compatible with base polymers and tackifiers	Limited compatibility

Natural rubber (NR) mainly consists of the chemical compound cis-1,4-polyisoprene with high molecular weights of 1000 kDa (M_w) and a broad molecular weight distribution (\mathcal{D}). Its most important property is the elasticity due to the cis conformation of the double bond in polyisoprene.^[16] SBR (styrene-butadiene-rubber) is a synthetic rubber produced by emulsion or solvent polymerization procedures using styrene and butadiene monomers. SBR is mainly used for tire manufacturing as well as in small consumption for adhesive production.^[17]

SBCs (styrene-block-copolymers) are block copolymers such as the well-known styrene-butadiene-styrene (SBS) and styrene-isoprene-styrene (SIS). SBC's have two glass transition temperatures (T_g), one corresponding to the styrene and one to the isoprene polymer. Whereas the plastic part controls the processing the rubber part stands for elasticity. SBC's are typically used in hot melt adhesives.

Acrylic PSAs are made from statistical or random copolymers of alkyl acrylates, which consist of a base monomer, providing low T_g and at least of a second high T_g monomer. As acrylics, mainly *n*-butyl acrylate (BA), methyl acrylate (MA) and 2-ethylhexyl acrylate (EHA) are used. Along with natural or synthetic rubber they are further copolymerized and formulated to some extent. Due to the high chain mobility they are compatible with various kinds of polymers, tackifiers or resins. Poly(methyl acrylate) for instance is an acrylic resin in form of an emulsion.^[15]

2. Fundamentals and state of the art

Finally, ethylene-vinyl acetate type adhesives (EVAc)s are copolymers used as hot melt adhesives or hot glue sticks. EVAc)s are generally used in packaging, textile and bookbinding industries. The disadvantages of such natural rubber adhesives, as well as block copolymer rubbers, are their low grade-stability and lower resistance towards UV-light or thermal exposure.

Acrylic copolymers were established as the first class of synthetic polymers used for PSA production. Acrylic PSAs offer an exceptional combination of performance advantages in comparison to other adhesive types owing to their very wide-spread monomer basis, ability to be co-polymerized, pressure sensitivity and excellent aging and physiological properties. They are available as solvent-based, water-based, and 100% solid systems. They show excellent water resistance, good resistance towards common chemicals, have an advanced UV and oxidative stability as well as the ability to perform over a large temperature range. Of great interest are their optical qualities (color and clarity), durability, and better adhesion properties due to their viscoelastic properties. The latter is already present, without additional additives. Acrylic PSAs consist of a base monomer, a modifying monomer and may be composed of another monomer bearing desired functionalities. Depending on the end application, the monomer selection is crucial for the T_g , which typically lies in the range of 25-45 °C below a given application temperature (i.e. 25-45 °C below room temperature).^[15]

In a common PSA formulation, the base monomer makes up more than 50 % by weight, usually with low T_g of -50 ± 10 °C, which guarantees wettability due to softness and exhibits the property of reaching excellent contact with the adherent's surface. As an example, BA and EHA are representative base monomers; however, as polymers they do not show enough cohesion to ensure good adhesive performance. For this reason it is essential to copolymerize or to blend a modifying monomer to finally raise the cohesive strength and design viscoelastic properties to sustain loads. This is achieved by increasing the polymer's T_g with a higher T_g comonomer (i.e. MA or MMA) or to blend a polymer with higher glass transition temperature. By incorporating monomers or polymers with functional groups, one can change polarity and create effects on adhesive properties based on interactions with the adherent's surface. For instance, by adding 2-hydroxyethyl acrylate (HEA) or acrylic acid (AA) as comonomer one increases the hydrogen bond formation not only in bulk to create higher cohesion,

2. Fundamentals and state of the art

but also with the surface by orientation of the polar groups towards the interface.^[18] As mentioned above, these adhesives are usually produced as solvent based products as well as aqueous dispersions to fulfill the ecological criteria of being free of volatile organic compounds (VOCs).

2. Fundamentals and state of the art

2.2 Principles of adhesion

In general, the term adhesion is defined as *“the act of sticking together or the state of being stuck together”*.^[19] For scientists intensively studying the phenomena of bonding, adhesion is more than just a state of bonding. Many factors influence adhesion properties. Additionally, the cohesion between similar molecules of the adhesive plays a significant role. A polymer cohesion describes the intermolecular attraction of molecules to each other. While adhesion depends on the adherent with its interfacial parameters as well as on the polymer characteristics, cohesion only depends on the polymer properties (i.e. intramolecular forces as well as elastic or viscoelastic properties). Both are also predominant characteristics in the wetting behavior of an adherent's surface.

Understanding adhesion begins with the relevant bonding and debonding mechanisms. During bond formation, a contact in molecular dimensions is achieved in a limited region of the contact area. With increasing contact time and under deformation by flow processes as well as by wetting behavior of the polymer, the size of this contact area is increased.^[20] The separation of an adhesive tape from a substrate is a process in which both the thermodynamic work of adhesion and dissipation factors are involved. Variation of the polymer characteristics, most importantly the molecular weight, the cross-link density or the density of entanglements, as well as the polarity through functional group containing additional monomer will, as a consequence, influence bonding and debonding processes by changing the cohesive strength and wetting ability.

The important fact to be categorized as a PSA is the criterion of Dahlquist, stating that the upper limit of the elastic modulus at 1 Hz has to be lower than $3.3 \cdot 10^5$ Pa.^[21] It is the case that a proper choice of monomer is the indispensable step to achieve desired adhesion with PSAs. So far, adhesive properties are also influenced by the adherent type, its roughness, the surface tension, -energy or interfacial tension as well, which all can prohibit complete wetting of the polymer on the surface decreasing adhesion strength.

2.2.1 Bond formation

Interfacial aspects

The adhesive bond depends on several interactions between the adhesive and the adherent's surface like hydrogen bonding, dipole interactions and van der Waals interactions. There are intermolecular atom/molecule or atom/atom combinations with increasing attraction and decreasing distance due to dipole-dipole or dipole-induced dipole interactions.^[22,23] In order that the interfacial energies take effect, the surface and the molecules of the polymer have to be very close to each other (<1 nm; length scale of a chemical bond distance sp^3 -C: $\sim 1.54 \text{ \AA}$). As a consequence, the polymer must have a low enough viscosity to flow and wet the surface, even if it is slightly cross-linked. Predictions on the adhesive interfacial strength are usually based on thermodynamics. For a separation of the polymer (liquid) from the substrate (solid) a mechanical force must be applied, which is referred to as the adhesive force.

For the desired performance, PSAs must immediately wet the surface as soon as they are brought into contact with it. The driving force for the ability of the adhesive to spread over the adherent surface is governed by the interfacial properties of the adhesive and the adherent. To do so, the relationship between the surface energy of the polymer and the one of the adherent becomes critical.^[24, 25] The total work of peeling or debonding can be described as:

$$W_T = W_A \cdot (1 + \delta(V, T, \dots)) \quad (1)$$

where W_T is the total, W_A the thermodynamic work of adhesion and δ is an amplifying factor related to the viscoelastic dissipation and depends on temperature, rate of debonding and more generally on parameters affecting the viscoelastic properties. This equation shows that W_T can be up 10^4 times higher than W_A .^[26,27] W_A , so far, is the change in free energy when the materials are bonded and stays the same for a reversible debonding. This thermodynamic work of adhesion is related to the surface tensions and expressed in general by the Dupré equation:^[28]

$$W_A = \gamma_s + \gamma_l - \gamma_{sl} \quad (2)$$

2. Fundamentals and state of the art

By separating the two bodies, this force carries out a required work gaining two “new” surfaces under the disappearance of the interface, meaning a change in energy per unit area as one interface is transformed into two separate surfaces (Figure 3).

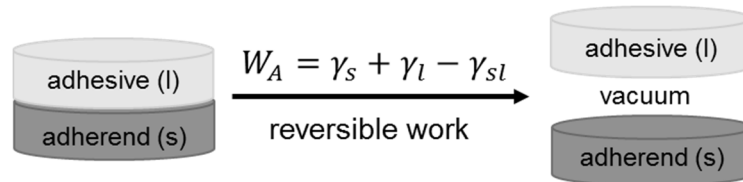


Figure 3. Illustration of the work needed to separate the adhesive from the adherent.

The parameter γ_l expresses the surface or interfacial tension of the adhesive (l), γ_s is the interfacial free energy of the adherend (s), and γ_{sl} is the interfacial free energy of the adhesive/adherent interface.^[29] In order to gain surface energy during the wetting process, the interfacial tension has to predominate over the sum of the respective interfaces. In the case of van der Waals bonds being responsible for W_A , its value can be several orders of magnitude smaller than the viscoelastic dissipation. This was found to be true for peel strength by Zosel,^[30] especially for long contact times, a very weak dependence was observed.^[26] Nevertheless, an external force is needed to achieve complete wetting. However, this required pressure is quite low for acrylic PSAs.

In general, better wetting can be observed with polymers demonstrating low resistance to flow including a substrate promoting the ability of the adhesive material to spread. Not every material can be classified as adhesive only by the ability of wetting a surface properly. Viscoelastic properties of an acrylic PSA are a prominent factor for being an adhesive able to stick to any surface. In high performance PSAs, the viscoelastic properties have to balance each other. This means a perfect balance of an adhesive and a cohesive character to preferentially wet the surface. The thus adjusted material is then able to sustain loads by the extensional deformation of fibrils.^[25] In order to create strong fibril formation, the physical characteristics and the composition of the polymer become a key factor.

Polymer properties

There have been thorough investigations of the influence of molecular weight (weight average M_w), the glass transition temperature, as well as cross-linking density, including the entanglement molecular weight (M_e) on adhesive properties.^[31-42] Additionally, many reports have described the influence of various additional tackifiers, resins, co-monomers owing different polarities and other typical formulating ingredients.^[43-46] These investigations were made in order to reveal the influence on the mechanical behavior of the adhesive in tack-, peel- as well as rheological studies. It is common practice in the industry to use the measurements to describe adhesive performance. Because the values of tack and peel are the result of viscoelastic properties, it is crucial to have an overview of all factors affecting the performance.

Viscoelastic properties are directly related to the polymer's molecular weight and the chain's internal entanglement points as well as the cross-linking density.^[32] Low molecular weight polymers show high viscous flow ability and for that reason improved wetting performance, but vice versa they do not show cohesive strength. By increasing the molecular weight M_n (number average) as well as M_w , one further promotes the amount of entanglements, increase in viscosity, the relaxation time of chain mobility,^[33, 34] the viscoelastic energy dissipation during the debonding process and, finally, the cohesive strength. Regarding the case of a low M_w adhesive, there is sufficient wetting behavior. Whereas with the debonding process, the fracture of fibrils may occur quickly due to the absence of entanglements. In the case of a high M_w adhesive, there is high viscosity. The high viscoelastic energy dissipation resulting from the elongation of fibrils or at high cohesion and adhesive break interfacial aspects, which however can lead to decreasing adhesive performance because of inadequate wetting. For balanced properties, most of the acrylic PSAs exhibit a high dispersity M_w/M_n , in which short chains possess high mobility to wet the adherent and long chains with the ability for entanglements providing elasticity. Here, the critical molecular weight between entanglement points M_e plays a fundamental role. It has an influence on the elastic modulus in the so called rubber plateau region, where G_N^0 is defined as the plateau modulus of the polymer. It's value can be determined by dynamic mechanical analysis (DMA) or through oscillatory measurements. In this concept, Zosel investigated the relationship between debonding energy to the entanglement molecular weight.^[35] The

2. Fundamentals and state of the art

relationship between the characteristic value of G_N^0 and M_e was described by Ferry^[36], Doi and Edwards,^[37] which is true for long, linear and just slightly branched polymer chains:

$$M_e = \frac{K\rho RT}{G_N^0} \quad (3)$$

where R is the universal gas constant, ρ is the density, T is the temperature, and K is a constant with a value of 1 (Ferry) or 4/5 (Doi and Edwards), depending upon convention. To agree with the Dahlquist criteria, the modulus of the adhesive material should not exceed $3.3 \cdot 10^5$ Pa, in other words, the material will not be able to perfectly wet the adherent's surface nor to build up fibril structures. In addition to the physical cross-links by means of entanglement between the long chains, the bulk properties are also related to real cross-links through chemical bonds. The procedure of cross-linking is widely spread in industry in order to improve the adhesive properties in a last step after easy handling and processing of the adhesive material.

Cross-linking is a prominent tool to reduce the maximal elongation for removing the adhesive from the adherent without leaving any residue. The performance of the PSA can be extensively varied. It can be used subsequently in the processing, and therefore it is necessary to have an impact on the cross-link density, which of course influences the adhesion properties significantly. The average molecular weight between two chemical links is defined as M_c . High M_c values imply low cross-linking density, kind of weak, because there is enough space to rearrange the chains and to elongate the network in fibrils till the elasticity comes into play, so the PSA remains tacky. Contrarily, low values, meaning a high density of additional chemical bonds which strengthen the network in a way that there is a direct force, prevent the formation of fibril formation.^[31, 38] UV light technology is commonly used in the industry for easy cross-linking. In acrylic formulations, the cross-linker is present as a photoinitiator additive to react in the final state. By varying the amount of photoinitiator or the UV dose, the degree of cross-linking can be varied. This has been studied in detail and it was shown that high UV light exposure results in significantly reduced tack as well as peel values.^[39, 40] The formation of fibrils and the maximum elongation (ϵ_{max}) are expressed by the ratio $\frac{M_c}{M_e}$. A decrease in this ratio results in decreasing ϵ_{max} . Nevertheless, a slight cross-linking is convenient for fibril stability. It was shown that the work of adhesion reaches a

maximum for a degree of cross-linking just around the gel point, where the storage modulus is almost equal to the loss modulus.^[41] By increasing the density the strain decreases while stress peak height and the height of the plateau will remain constant.^[42]

Changing the end properties by molecular weight or cross-link density is not the only way of creating desirable adhesion performance. The starting material also plays an important role. The glass transition temperature is a common characteristic which should be highlighted. Glass transition temperature is an index for molecular mobility and pressure sensitivity used in PSA polymer technology. Its value can be determined from DMA measurements, defined as the temperature at the maximum of G'' , or by differential scanning calorimetry (DSC) as a step in the calorigram characterizing a second order transition of molecular mobility. The T_g of a PSA has to be well below its service temperature, namely room temperature. Thus, usually, it is in a range of -20 to -50 °C not only for acrylates.^[43, 44] In general, hardness or stiffness increases by T_g . A PSA polymer with a low T_g has improved chain mobility at the test temperature but the viscoelastic deformation may suffer, whereas a high value prevents the polymer from advanced wetting and contact to the adherent. To reach an enhanced performance one can use several empiric equations to describe the T_g of a polymer blend composition or reacted copolymer. Below, the Fox equation stating that the T_g is related to the components as follows, while assuming random miscibility:

$$\frac{1}{T_g} = \frac{w_1}{T_{g1}} + \frac{w_2}{T_{g2}} \quad (4)$$

where w_1 and w_2 are the weight fraction and T_{g1} and T_{g2} are the glass transition temperatures of the mixed components. The T_g strongly depends on the chain mobility or flexibility which is affected by the tacticity and the steric hindrance of side chains, e.g. methyl groups in acrylates. Maximum softness is obtained for poly(octyl acrylate) with a T_g of -80 °C, whereas poly(methyl acrylate) has a T_g of +6 °C and the strong poly(methyl methacrylate) a T_g of ~ +105 °C. In the end, it is possible to vary the glass transition temperature by changing the copolymer composition through various monomer mixtures.

2. Fundamentals and state of the art

A change in the monomer composition not only affects the bulk properties but also contributes to the interfacial interactions. So do monomers with polar groups. Polar groups orientate themselves in bulk direction when exposed to air. But as they are brought in contact with a polar surface, they are able to re-orientate towards this surface and build up a better adhesion with time. In this concept, acrylic acid is a highly investigated and widely used monomer, which tends also to H-bonding as a donor with its carboxylic acid group, contributing to stronger van der Waals attraction at the interface. As previously mentioned, additional polar groups can also lead to an increase in cohesive strength by intermolecular hydrogen bridge bonding (physical bonds). And one has to be careful with the fact that adding a monomer such as acrylic acid (AA) increases the T_g , thereby changing the viscoelastic properties as well, which might cover the interfacial application aspect. Taking these facts into account, the investigation of adhesive properties with respect to tack and peel measurements of compositions bearing polar functionalities have been performed. For example, an increase of 10 wt% of acrylic acid in a copolymer increases the thermodynamic work of adhesion by a factor of 1.5.^[45] In this study, the objective was to separate the interfacial and bulk effects both based on hydrogen bonding. It was concluded that, despite the increase in W_{adh} , the change in viscoelastic properties is the major factor. In fact, by adding AA, the cohesion increases and this can be observed by the transition of the debonding process from a cohesive towards an adhesive failure, without leaving residue on the surface of the adherent.^[46]

Wetting behavior

Considering the mentioned background, the wetting of the substrate, adherent or surface, however, is still the fundamental act in terms of bond formation and adhesive bonding. Proper wetting is considerable important as well as the critical surface tension.^[47] The dominating market tends toward the use of lighter weight materials, lower cost and ever more alternatives in form of new plastics. These trends have pushed PSA performance towards increasing their ability to adhere to those new, lower surface energy, substrates. Generally, adhesives adhere better to materials with higher surface energy. Reasonable background is the fact, that common adhesives show

better adhesion to substrates with higher surface energy than the corresponding adhesive.^[48]

The adherent's surfaces can be divided into two categories: substrates of high surface energy and substrates of low surface energy.^[49] High-energy materials are, for instance, metals and inorganic materials with surface tensions above 500 dynes/cm or mN/m. Low-energy materials by comparison include organic materials such as polymers with surface tension below 100 mN/m. Polymers themselves are classified as high, medium and low energy materials. Low-energy materials wet high-energy surfaces easily and spontaneously due to the reduction of the surface free energy.^[50] Wettability in general depends on several factors:^[51]

- The wetting angle θ , depending on the nature of adhesive and adherent, is described using the Young's equation (5) and illustrated within Figure 4:

$$\gamma_{lv} \cos \theta = \gamma_{sv} - \gamma_{sl} \quad (5)$$

where γ_{lv} , γ_{sv} and γ_{sl} are the surface tensions of fluid in equilibrium with its vapor, of solid in equilibrium with its vapor and between solid and liquid. Therefore, wetting is observed at an angle of 0° or if the surface tension of solid in equilibrium with its vapor is equal or higher than the sum of the other two. This is the reason for good wettability in case of high surface energy and low energy of the liquid.

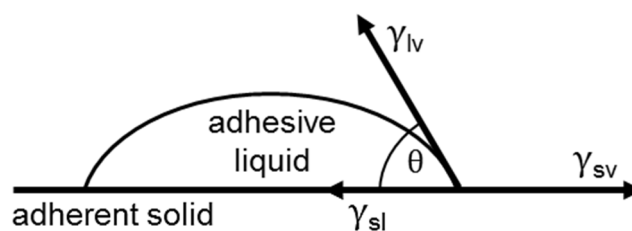


Figure 4. Schematic of the contact angle between adhesive and adherent.

- Viscosity, as described before, also influences the wetting process. It should be low enough to let the adhesive polymer spread on the surface to a certain extent, without being too weak to offer cohesive strength.

2. Fundamentals and state of the art

- Contact pressure is a key factor to force the adhesive to wet the material and to bring it into pores or roughness of the adherent's surface. The more pressure, the better the wetting in almost any case.

Substrate type

Low surface energy plastics (LSE plastics) remain a difficult class of adherents caused due to the lack of polar groups. Common LSE plastics are for example polyethylene, polystyrene or Teflon. Energy values of these really low-energy materials are listed in Table 2 and are generally lower than 50 mN/m.^[50, 20]

Table 2. List of surface tension of different Substrates.

Adherent		Surface tension
		[mN/m]
PC	Polycarbonate	46
PET	Polyethylene terephthalate	43
PE	Polyethylene	31
PS	Polystyrene	33
PP	Polypropylene	30
PVC	Polyvinyl chloride	39
PTFE	Polytetrafluoroethylene	18
Common acrylic PSA		35-45

The adhesion to LSE materials is not been fully investigated yet. Many attempts have been made to find reasonable ways to improve the wetting behavior of this class of surfaces. In the majority of cases, these surfaces have to be pretreated and specially formulated adhesives are required. Usually rubber-based adhesives provide better adhesion to LSE surfaces than acrylates. Substrate pretreatment by surface modification, such as corona and flame treatment^[52, 53] or chemical treatment by the use of primers and adhesion promoters,^[50] is used to increase the surface energy and thereby achieve better adhesion performance.

Another approach is to add tackifiers to the adhesive polymer^[54-59] or at least the introduction of a hydrophobic comonomer such as stearyl acrylate (SA). SA is a mono-functional monomer with low viscosity, toxicity, as well as high reactivity even though they consist of long aliphatic chains. The addition of a hydrophobic monomer actually leads to more hydrophobicity in the side chain of the polymers backbone. Determining how to improve the wetting of LSE surfaces has been examined by Asua as well as Creton and coworkers.^[60; 61] The effect of emulsifier on the wetting ability and introduction of a hydrophobic monomer (SA) into the polymer chain on the adhesion properties on low energy surfaces were investigated. Tack and peel strength are higher for the latex with the lowest gel content. At higher SA concentrations, significantly better tack results were obtained and the peel strength was slightly improved at an optimum SA content.

Substrate roughness

The adhesion significantly depends on the probe surface roughness as described by Zosel in an early study.^[62] Complete contact between the adhesive material and the rough substrate is limited due to its unevenness. The roughness is the factor responsible for the appearance of an inhomogeneous strain field around the heights. As a consequence, residual tensile stress is observed. This concept is illustrated by Figure 5. The full wetting of the adherent surface under low applied pressure is highly reduced with the addition of higher roughness.

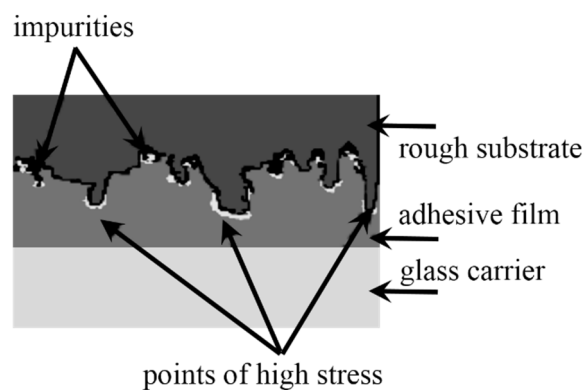


Figure 5. Schematic of a rough surface in contact with an adhesive.^[63]

2. Fundamentals and state of the art

On a smooth surface, cavities occur sequentially and their growth rates increases with the increasing stress level at which they are formed. In contrast, on a rough surface cavity growth starts from existing defects and they grow simultaneously. The cavity formation and their growth is described in detail in section 2.2.3.

2.2.2 Bond separation

Once a bond is formed between a chosen adhesive and an appropriate substrate this bond is, at least in the case of a pressure sensitive adhesives, usually not permanent. In most instances one would like to achieve a clean separation of the adhesive by debonding processes (especially for adhesive tape or sticky notes). But, as already discussed in section 2.2.1, also the debonding process is influenced by the type of adhesive as well as adherent. In addition, testing methods of adhesion properties are mainly focused on the parameters that cause rupture. While in the stage of bond formation, PSAs experience mainly shear deformation, but the debonding stage is dominated by tensile strain and involves the deformation of the adhesive under stress (in extension), finally followed by separation from the substrate. Assuming high adhesion, for instance gained through high contact pressure, viscoelastic properties will play the leading role in this debonding process. Hence, it is essential to obtain a detailed insight into the mechanism of the debonding process, especially in tack- and peel-adhesion tests.

Under an applied force, a homogeneous tensile deformation of the adhesive polymer is observed together with a strong increase in the stress, which is exceeding a maximum in the probe tack curve. The probe tack curve is typically plotted as stress vs. strain or displacement in a common tack-test. This initial deformation, in case of an elastic polymer film, can be expressed by a geometrical parameter (a confinement ratio), an interfacial parameter (the critical energy release rate), and a material depending bulk parameter (the elastic modulus).^[66]

If the bond is formed under the applied force F_a between the surface of a flat cylindrical punch and an elastic polymer film (on rigid substrate), the stored elastic energy U_E , equal to the work of debonding, shown in Figure 6, can be written as:^[64]

$$U_E = \int F_d d\vartheta \quad (6)$$

where F_d is the detaching force and ϑ is the movement of the probe in normal direction.^[11]

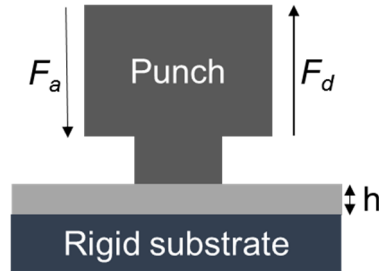


Figure 6. Schematic of a punch surface in contact with an adhesive film.

In case of a crack, the periphery of the circular contact area increases in size and the contact area will decrease simultaneously (from A to $A-dA$). The load required to maintain a fixed displacement as well as the strain energy decrease, respectively. The applied energy release rate G contains the change in stored elastic energy and the change in contact area:

$$G \equiv \left. \frac{dU_E}{dA} \right|_{\vartheta} \quad (7)$$

The energy release rate G is described in the same way as the total work of adhesion W_T , and thus it can be written according to equation (1). It is the fracture energy required to create a unit area of fracture, also seen as crack propagation criterion when G reaches the critical value of G_c (critical energy release rate).

Initial homogeneous deformation of an adhesive has a key parameter, the so called confinement ratio r_c/h , the ratio of the contact radius and thickness of the adhesive film. Assuming that an elastomer is incompressible between two rigid surfaces and further assuming a thin layer that provides a uniform pressure throughout the thickness of the elastic polymer film and for large values of r_c/h , the pressure distribution under the probe surface can be described as parabolic.^[65] Small values in r_c/h lead to a decreasing contact radius by external crack propagation, whereas for high values the detachment is forced by internal growing cracks.^[66]

2. Fundamentals and state of the art

In the case of low viscosity materials, the pressure distribution remains parabolic. Hence, crack propagation occurs by cavitation, which is localized in the center under the attached probe surface.^[67] In solid materials, the pressure distribution is more uniform than the given parabolic assumption. Crack propagation by cavitation can be observed throughout the entire contact area defined by the probe.^[68] It is found that the driving force to increase cavity size is caused by a negative hydrostatic pressure.^[69, 70] For low elasticity and highly flowing adhesive polymer this is the pressure needed to overcome the internal Laplace pressure. Assuming the presence of trapped ideal gas as defect within the bonding process, also defined by the surface roughness, the mechanic equilibrium states that the applied pressure p is equal to the sum of Laplace pressure and the internal pressure:^[71, 72]

$$p = \frac{p_0}{\lambda_r^3} - \frac{2\gamma}{\lambda_r R_0} \quad (8)$$

where p_0 is the initial cavity pressure. The extension ratio $\lambda_r = R_c/R_0$ with the initial radius R_0 and the assumption that there is no change in the shape of the cavity, so that $V \propto \lambda_r^3$. It is to notice that equation (8) does not take elasticity into account. It can be taken into account if the equation is extended by another term including the E or Young's modulus and if the neo-Hookean model is considered.^[73] However, equation (8) fails for very small defect sizes. Most importantly and in summary, an energy is needed to deform the bulk to create a new surface.

Pressure sensitive adhesives are usually characterized by the parameters of tack, peel adhesion, shear resistance and viscoelastic properties through rheological experiments. Unlike peel or shear resistance, it is much more complicated to define tack, also known as quick stick, finger tack or quick adhesion. While difficult to define, it is definitely one of the most important properties of PSAs. Tack is defined by Zosel as the ability of a PSA to allow the formation of a bond of measurable strength to a given substrate under the conditions of light contact pressure in a short contact time.^[20] Typically, 1 s and finger pressure will be enough to achieve good adhesion by a PSA with a given substrate. The tack can also be defined as the work needed to separate the adhesive from the substrate.^[74] Rolling ball and loop tack tests are well known to be simple, but the theoretical aspects for interpretation involve rather complex flow mechanics. However, a probe tack test has the advantage that the process of bonding

and debonding can be separated and the deformation itself is at least in the initial stage quite simple to analyze experimentally.

The first developments in the detailed understanding of the debonding mechanism in a tack-test were based on the PSA's physical properties and the visualization technique of their debonding behavior from a flat cylindrical substrate. Creton, Lakrout and Zosel focused on the experimental examination of this detachment process especially by soft adhesives.^[75-77] Zosel implemented the tack test as a versatile tool to gain information on the adhesive debonding process very easily.

Cavitation, as one of the first stages of debonding, has been studied and described in detail previously by various authors.^[75] Creton *et al.* investigated the cavitation occurring at the beginning of debonding and described different stages of this process. The very first stage is the deformation of the film, directly followed by nucleation of cavities forced to be formed at the interface between adherent and adhesive. The next step comprises cavity growth in lateral dimension and as a consequence of steady tensile force in direction of their growth normal to the polymer film, also described literally as fibril formation or fibrillation. Zosel first studied the morphological change and observed the formation of a fibrillary structure by using an *in situ* optical microscope and stated its importance in adhesive performance.^[20] Finally bonding fracture is observed, either by internal fracture of the fibrils as cohesive failure, or by total detachment from the adherent's surface as adhesive break.

2.2.3 The stages of debonding by cavity nucleation

Cavity growth starts from impurities or defects and trapped air at the interface adhesive/adherent and continues growing into the bulk of the polymer. This behavior was confirmed by tack experiments using optical observation methods to visualize the debonding process.^[68, 81] Model acrylic PSAs were investigated by tack tests using stainless steel probes and by simultaneous observation of cavity growth from underneath the bonding area by Lakrout, Sergot and Creton in 1998. They showed that the maximum tensile stress can be directly related to existing cavities and their growth. Additionally, a good correlation with the shear modulus of the PSA model, but

2. Fundamentals and state of the art

the adhesion energy was found to be mainly related to the elongation properties of the adhesive.^[68]

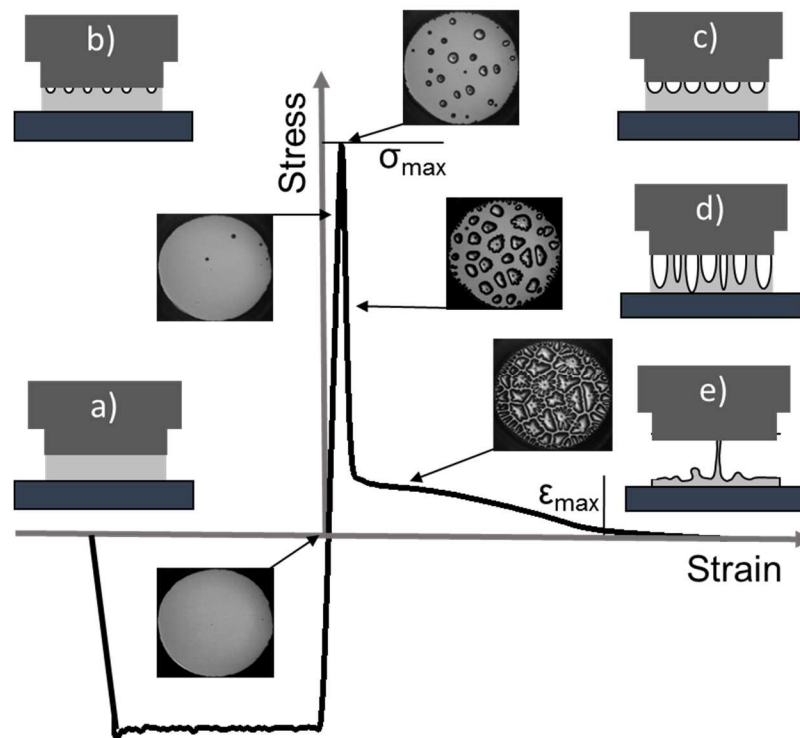


Figure 7. Stages of debonding by cavity nucleation: b), cavity growth in lateral direction. c), growth in the direction of the elongation with change towards a fibril structure. d), fibril growth. e), bond failure in two ways as adhesive or cohesive break.^[85]

Figure 7 shows a detailed schematic illustration of the entire debonding mechanism in a thin film geometry synchronized to the simultaneous observed video optical cavitation process. The process can be observed from beneath a glass plate coated with the colorless PSA polymer film by a video camera. (Such a device is shown by Figure 33 in chapter 4.5 of the experimental part of this work).

Stage a) corresponds to the state where the adhesive is already in contact with the probe surface. This is achieved by a given contact force and contact time (usually 1 s for PSA). These parameters can vary and will thus influence the quality of bond formation as well as the resulting tack value. Stage a) is directly followed by the start of the debonding under release of the probe in the upper direction under a given velocity (in 90° angle). The debonding velocity is also a factor influencing the stress vs. strain curve progression and the tack value, respectively.

Stage b) is characterized by an increase in the stress and the formation of small cavities nucleating from existing defects between the adhesive and the adherent's surface. Since the hydrostatic pressure has to be minimized in the polymer bulk, the nucleation turns towards cavity growth (above a critical stress), a heterogeneous process as mentioned before. First, cavities are expected to appear at a stress level before the maximum value is reached. In this initial stage of cavitation the voids do not "see" each other or are in contact to each other and will grow independently. There are two cases of the mechanism depending on the critical energy release rate (G_c). For low values of G_c , cavities occurred from defects can easily propagate at the interface till they get in touch to each other. At the opposite end for large values of G_c , cavitation will occur by the formation of new smaller cavities in the bulk between those first appeared. There is a qualitative explanation:^[76, 83] For a high molecular polymer, cavity growth is hindered by its high bulk viscosity, so in this case many small cavities will appear. Vice versa in a low viscosity polymer, the growth of voids is easily achieved and larger but less cavities can be expected.^[78]

Generally, the energy release rate (G) increases with the displacement of the probe. The elastic energy is then released by a reduction of the confinement, which can either occur by cavitation in the bulk of the adhesive if the negative hydrostatic pressure is in the order of magnitude of the elastic, or by crack propagation if G is equal or at least higher than the critical energy release rate G_c .^[86, 78] Furthermore, Shull and Creton focused on the contact radius between a growing cavity and the substrate to additionally gain information about the mechanism of failure.^[79] Another study by Nase and coworkers investigated cavitation in three dimensions and observed that a contact angle larger than 90° belongs to viscoelastic solids. Nearly 90° seemed to be typical for highly cross-linked polymers, whereas no contact angle between cavity and the substrates surface was observed for very soft adhesives, leading to cohesive failure.^[87, 88]

Hence, the surface properties play an important role in cavity appearance. Their number as well as their form and cavity size were recently investigated and correlated to the surface roughness.^[71, 85, 89-94.] Zosel emphasized in his work that the work of adhesion significantly depends on the probe surface roughness in a tack test, especially for low contact forces, short contact time and high polymer modulus. In more

2. Fundamentals and state of the art

theoretically studies it is noted that the adhesion on rough surface is limited due to the absence of full contact area. Creton and Leibler describe a model that predicts that the work of adhesion is proportional to the inverse of the shear modulus $G(t)$ of the polymer. An experimental study on SIS block-copolymers illustrated that the number of cavities formed during debonding strongly increases with increase in surface roughness. The characteristics of cavitation as well as cavity growth on smooth and rough surfaces was pointed out in detail. Moreover, Peykova *et. al.* investigated BA/MA copolymers as model PSAs, addressed the influence of surface roughness on the debonding process during a tack experiment.^[85] It was found that increasing roughness significantly influences the cavitation process. Tack values were found to decrease with increasing roughness. The existence of small impurities, usually dust or air bubbles, influence the detachment process. The polymer/voids and polymer/dust areas reduce the adhesive bond strength. A significant difference between cavitation and cavity growth on smooth as well as on rough surfaces was pointed out by Chiche.^[71, 94]

Whereas *stage b)* (Figure 7) starts in the area of the peak stress on the stress-strain curve, *stage c)* describes the decrease in the load bearing area, which is the driving force for cavitation growth. *Stage c)* is accompanied by bulk instabilities indicated by the growth of the preformed cavities along the interface substrate/PSA. Radial flow of the surrounding polymer is required to increase the cavities in size, recently to reduce the pressure during bulk deformation in elongation process. For polymers of significantly low viscosity, a finger-like elongation is observed, which is defined as a Saffman-Taylor instability.^[95] This type of structure is caused by penetration of surrounding air from the outside into the bulk of the adhesive. For typical PSAs, the radial expansion of cavities will continue until a maximum expansion is achieved, or at least when the neighboring cavities are attached. The film thickness is a main parameter for controlling the final size of the cavities.^[67] If the growing cavities finally achieve their maximum size in the radial direction, formation of a fibril structure will take place by vertical elongation.

Stage d) covers the formation of a fibrillated structure and causes failure or debonding from the probes surface. Under a constant debonding, the lateral growth of cavities is in competition with the vertical extension of the polymer in-between. The stretching of

these fibrils is controlled by the debonding rate and leads to storage and dissipation of energy.^[70, 96] Any adhesion of a PSA refers not only to the attached area of the interfacial bond, but also to the strength of the fibrils formed. This strength strongly depends on the polymer type. If the polymer has a significantly too low viscosity, the cohesion is too weak and the adhesive flows rather than resisting the loads. If the polymer is extremely elastic, crack propagation is observed. In this case, coalescence of the cavities appears, resulting in rapid and complete detachment of the adhesive from the surface and low tack energy.

Stage e), the final stage, is the total detachment of the adhesive from the adherent. For polymers exhibiting high cohesive strength detachment occurs at the end of the fibrils and is known as adhesive failure. As mentioned above, for high elasticity polymers the detachment is observed without any fibrillation, directly by edge crack propagation. Common PSAs show adhesive failure depending on their application to be reused without leaving residues on the adherent's surface. Another possible failure mechanism is the cohesive break, where the fibrils are stretched causing instability followed by thinning and finally fibril fracture. This failure process suffers from the residue of polymer leaving on the adherent.

2. Fundamentals and state of the art

2.3 Evaluation methods of adhesive performance

The ability of a PSA to adhere to any kind of surface under an applied low pressure is called initial adhesion or “tack”. It is measured in the unit J/m^2 during a so called probe-tack test. As there are differences in the quantification of the adhesion itself, a variety of proper testing methods has been developed. These methods have one thing in common: the test of a release or detachment of an adhesive polymer being in contact with a surface. The most common and widely used methods in the industry to evaluate the adhesive performance of a PSA are shear resistance, peel at 90° or 180° as well as the mentioned probe tack test.

2.3.1 Shear resistance

Shear resistance is the property of a PSA to sustain loads or shearing force. It is also known as the holding power. A shear resistance test determines the maximum shear stress that is sustained before an adhesive will rupture. In an experiment, the adhesive is brought between the ends of two plates, which are afterwards exposed to a load for short or long periods of time at elevated temperature in the vertical direction parallel to the contact area. The static force is applied by simply using a weight on the free end of one plate or by applying load on both free ends mechanically. Shear resistance of a PSA is directly related to its cohesive strength and creep behavior. It is typically reported in MPa (psi) based on the sheared area. In a classic shear test, simply the time to fail is determined. The time required to fail a shear test decreases with lower viscosity η . Similarly, an increase of the adhesive thickness h decreases the time to fail a shear test, but increases the peel strength. Often exceptionally strong PSAs will prove to be weak against shear when peel tested.

2.3.2 Peel test

A peel test is the most common technique for measuring the adhesion of a thin polymer film. It is used to assess the bond quality since the predominant stress is

tension or peel strength. The peel test provides reliable results for the determination of the total energy G_t required to break an adhesive bond with a given substrate, representing the sum of the fracture energy G_0 and the dissipated viscoelastic energy ψ .^[97]

$$G_t = G_0 + \psi \quad (9)$$

The dissipated viscoelastic energy is connected to the formation and growth of fibril structures. This is the dominant contribution to the peel resistance force, and shows a strong dependence on test conditions.^[27]

With respect to the real break-off area, the fracture energy G_0 can be described by the adhesion energy P , the peel-off angle ω and the width b as:^[98]

$$G_0 = \frac{P}{b} (1 - \cos \omega) \quad (10)$$

Furthermore, the adhesive bond strength can be described by the work of fracture W , which contain the unrecoverable work of translation W_T as well as the work of deformation W_D .^[99]

$$W = W_T + W_D \quad (11)$$

The recorded peel strength is an average constant load per unit width gained during the separation process of a thin flexible strip bonded to a rigid substrate. A test requires at least one flexible strip. The term flexible refers to the ability to bend and detach without breaking. The accuracy of the results depends on the conditions under which the bonding process is carried out. Variables related to the test method are the thickness of the substrate and of the adhesive, the rate of testing speed, geometric arrangement in the test, the temperature and the used of sample preparation. Generally, these variables will change the effective rheological properties of the substrate or the adhesive and may also influence the effective interfacial bond strength. The main difference between the methods is the angle of peel and if it remains constant during the test. Several test methods are used to assess the bonding of a flexible adherent to a rigid substrate. Usually 90° or 180° peel tests are used to

2. Fundamentals and state of the art

conduct a standard test as shown in Figure 8 (known as FINAT 1 and 2, ASTM D3330/D3330M, PSTC 101).^[100, 101, 102]

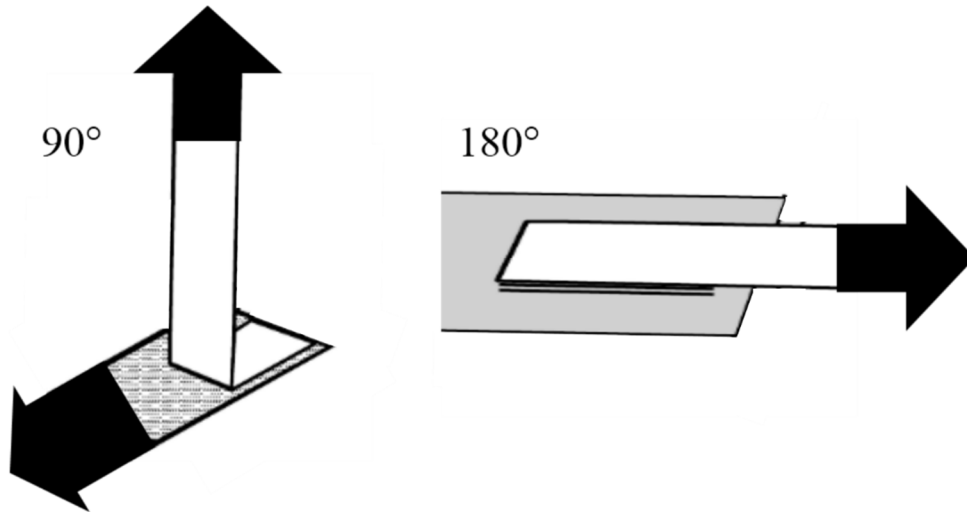


Figure 8. Illustration of a 90° and a 180° peel test.^[27]

Pressure sensitive adhesives can also be classified by their peel strength being either permanent or easily removable in case of a 180° peel test method.^[103] The values ranges from >14 N/25 mm to <1 N/25 mm. With a peel strength of 10 N/25 mm, a PSA shows permanent adhesion whereas 2 – 4 N/25 mm is the usual value observed for repositionable and removable PSAs.

Failure modes in peel test

Due to the diversity of application for PSAs and their varying characteristics they show different kinds of failure mechanisms comparative to the above mentioned failure types within a probe tack test (section 2.2.3). Depending on the substrate as well as the viscoelastic properties of the adhesive bulk polymer, cohesive as well as adhesive failure can be observed.



Figure 9. Failure mode explanation in a 90° peel test.^[27]

For highly viscous adhesives as well as slow debonding rates, cohesive failure is observed which is illustrated in Figure 9 (left). At higher rates or intermediate viscous materials, the mode of failure is stick-slip, where the observed peel force oscillates between well-defined limits. In the latter mode, the adhesive as well as glassy failure is observed alternatingly. Glassy failure is the debonding of the adhesive from the carrier strip, which is often undesirable. In case of adhesive failure, the total detachment of adhesive from the substrates surface without left residue is observed after peel-off.

The failure modes mentioned are mainly controlled by the viscoelastic properties of the polymer as well as by the surface polarity and pre-treatment. A lot of research regarding the formulation of acrylates influencing the PSA performance exists.^[104, 105, 106] Peel resistance of a PSA is low at a low separation rate (same is true for tack tests) and it gradually increases and decreases again as the separation rate increased.^[107] The addition of acrylic acid (AA) leads to better adhesion to substrates, enhancement of cohesion due to an increased T_g and slightly better peel performance with increasing AA content.^[108] The relationship between debonding rate and peel resistance has been examined using poly(BA) homopolymers with varying molecular weights.^[109] The results show an increasing peel strength with molecular weight in the slow peeling region, due to the viscous flow controlling the resistance to peel-off. Furthermore, the relationship between cross-linking density and peel strength was investigated using UV cross-linkable PSAs. As expected, the higher the cross-link density the lower the peel resistance.^[110]

2. Fundamentals and state of the art

2.3.3 Probe tack

A variety of adhesion tests have been developed in the PSA industry. Loop tack, rolling ball and probe tack tests are all used to measure tack for a variety of purposes. Since tack is not a fundamental material property, it depends on a wide range of factors including the method of testing. Measured tack values also depend on the initial conditions.

Probe tack tests, or flat-punch tests, are commonly employed to characterize the pressure sensitive tack of adhesives. A probe tack test has the advantage of applying a uniform strain rate and stress field to the adhesive film over the whole surface of the probe. In practice, a flat-ended cylindrical probe is used to compress the PSA with a given force for very short time (1 s). Hammond was the first to develop an apparatus to represent the adhesion as the maximum force recorded during one duration.^[111] Zosel, as already mentioned, investigated the debonding mechanism in a tack test.^[20, 31, 33 - 35] Typically, the tack is measured as the force required to separate the adhesive from a substrate shortly after having been brought into contact. A defined load of known intensity, a constant temperature and a specific holding time is usually preassigned prior each test. As a result, the maximum nominal stress σ_{max} , the maximum nominal strain ε_{max} , and the adhesion energy, W_{adh} , defined as the integral under the recorded stress-strain curves, are the relevant parameters obtained. The stress-strain curve gives the exact information about fibril formation of the debonding process. The mechanism of debonding can be separated into different stages, allowing a better understanding of the influence of molecular features and the correlation between the rheological properties of the adhesive and the surface properties of the substrate. Here, the investigations concentrate only on the characterization of the debonding mechanism. However, the importance of wetting behavior and surface properties also need to be considered.

Work of adhesion

As described in section 2.2.1, tack is a product of two phenomena, namely the thermodynamic work of adhesion and the viscoelastic function including the temperature and debonding rate dependence of the adhesive during a measurement.

The definition of tack in a probe tack test is considered to be the dissipated energy [J] with separation of unit area [m²] written as:

$$W_{adh} = \frac{1}{A} \int F v_{deb} dt \quad (12)$$

with A [m²] as the contact area wetted by the adhesive, the tensile force F [N] during debonding and the rate of debonding v_{deb} [mm/s].

Stress and strain

The nominal stress is defined as the ratio of applied force and the contact area. The elongation is normalized to the initial film thickness. Both are described as follows, respectively:

$$\sigma = \frac{F}{A} \quad (13)$$

$$\varepsilon = \frac{h - h_0}{h_0} \quad (14)$$

A typical stress-strain curve is illustrated by Figure 7. By separating the two surfaces the force increases rapidly to a maximum and for strong adhesion it tends to decrease to a nearly constant value until final detachment under drop to zero. For a weak adhesion, the force increases and decreases rapidly to zero without the formation of a plateau. The W_{adh} can be very different between both cases. It is known to be strongly influenced by the viscoelastic properties of the adhesive polymer composition and it is greatest with high molecular weight and slightly cross-linked polymers as already explained in detail in the sections above.

2. Fundamentals and state of the art

2.3.4 Rheology of PSAs

Rheology is defined as the science of deformation and flow of matter. All materials and more importantly those whose behavior are intermediate between liquid and solid have one in common, if one applies a stress they will deform or strain. There are defined models specifying the relationship between stress and strain, so called equations of state, starting in the theory of ideally viscous fluids (Newtonian fluids), ideal elasticity (Hookean body) and ideally plastic materials. Nevertheless, real bodies show a combination of the mentioned idealized models.

Basics

The above mentioned properties shear resistance, peel strength as well as tack are directly related to the polymer's response to an applied stress. Most PSAs or more precise the polymeric material exhibit viscoelastic behavior. The viscoelastic properties have been exhaustively investigated,^[112-117] since they show a significant influence on both bond formation (compression, wetting) and deformation in the debonding process of a PSA.

In general, time dependence is observed for mechanical as well as rheological properties. The polymeric material is characterized by the Deborah number De is defined by the ratio of the stress relaxation time and the observation time.^[118] For PSAs it is defined as follows:

$$De = \frac{\tau_r \cdot \frac{\partial_{deb}}{h_0}}{h_0} \quad (15)$$

where τ_r is the relaxation time and $\frac{\partial_{deb}}{h_0}$ is the initial macroscopic strain rate, which is represented by the debonding velocity over the initial film thickness. If De has high values it indicates the elastic behavior of the PSA, whereas at low values of De stress relaxation occurs and the material offers more fluid properties.^[119]

By performing rheological measurements using small amplitude oscillatory shear one is able to test the adhesive performance. In case of small amplitudes the shear stress is proportional to the strain necessary for linear viscoelasticity. Hence, the dynamic modulus $G(\omega)$ is defined by the ratio of shear stress (τ) to shear strain (γ) and is independent of the amplitude. Furthermore $G(\omega)$ can be separated into an elastic part, described by the storage modulus (G'), and a viscous part known as loss modulus (G''). The ratio of G'' over G' is equal to the tangents of the phase angle:

$$\tan \delta = G''/G' \quad (16)$$

In the linear viscoelastic regime, the storage and loss modulus depend on both relaxation and observation time. Shorter relaxation times results in an increase in the values of the viscoelastic moduli.

Table 3. PSA characteristics described by dynamic mechanical properties.

Property	Characteristics	G', G''
High shear resistance	High viscosity at low shear rates	High G' modulus at low frequencies <0.1 Hz
High peel strength	-	High G'' at high frequencies >100 Hz
High tack	Low cross-links	($G' > G''$) at ~ 1 Hz low G' , low $\tan \delta$ peak

For characterizing the adhesive performance quality of a PSA, oscillatory frequency sweeps are well established. In an oscillatory frequency sweep, a constant amplitude (sinusoidal) is applied, while the frequency is varied in a given range. In general, low frequencies (low rates of deformation) characterize the bond formation whereas high frequencies (high rates of deformation) are used to characterize the bond failure. The former relates to tack and peel strength and the latter belongs to the PSAs shear resistance (see also Table 3).^[120]

2. Fundamentals and state of the art

Oscillatory tests

Oscillatory measurements are performed on a rotational rheometer using cone-plate or plate-plate geometries (in the case of viscoelastic polymers). The fixtures can vary in their cone angle as well as diameter. A schematic representation of a common plate-plate geometry is shown in Figure 10.

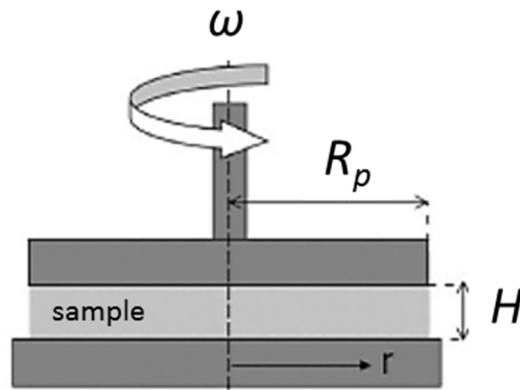


Figure 10. Schematic of a plate-plate fixture used in a rheometer. Ω = angular velocity [rad/s] R_p = plate radius, H = gap height, r = distance.^[121]

Considering the plate radius R_p to be equal to r , the shear rate $\dot{\gamma}$ is given by:

$$\dot{\gamma} = \frac{\omega \cdot R_p}{H} \quad (17)$$

Shear stress is described by following equation:

$$\tau = \frac{T}{2\pi R_p^3} \left(3 + \frac{d \ln T}{d \ln \omega} \right) \quad (18)$$

In order to evaluate the shear stress, sufficient torque (T) as well as rotational velocity (ω) data points are needed.

By applying sinusoidal strain to a sample, it will respond in the same way as sinusoidal stress and with the same frequency as long as the deformation is in the linear viscoelastic region:

$$\gamma = \gamma_0 \sin(\omega t) \quad (19)$$

where γ_0 is the deformation amplitude or the maximal deformation and ω is the angular frequency. The measured response of deformation in an oscillatory test at same frequency f ($\omega = 2\pi f$) is shifted in its phase by the phase shift δ . With the stress amplitude τ_0 the stress is defined by:

$$\tau = \tau_0 \sin(\omega t + \delta) \quad (20)$$

The phase angle δ varies between 90° for ideal viscous materials and 0° for ideal elastic behavior. As already mentioned the tangent of the phase angle is the ratio of the loss over the storage modulus.

In case of oscillatory shear the storage modulus can be described as:

$$G' = \frac{\tau_0}{\gamma_0} \cos \delta \quad (21)$$

The viscous property represented by the loss modulus is proportional to the irreversible dissipated energy during one load cycle, and is described as:

$$G'' = \frac{\tau_0}{\gamma_0} \sin \delta \quad (22)$$

Amplitude sweep

Prior to a standard frequency sweep (variation of the frequency) one has to conduct an amplitude sweep in order to determine the linear viscoelastic regime (LVE) of the material. During the amplitude sweep, the strain amplitude is varied while frequency is kept constant. The common frequency used is 1 Hz ($\omega = 6.28$ rad/s).^[122] The recorded G' and G'' data is plotted versus deformation and in the region of deformation where the moduli both have constant values the LVE regime is found (see Figure 11). It is characterized by no change of the materials structure.

2. Fundamentals and state of the art

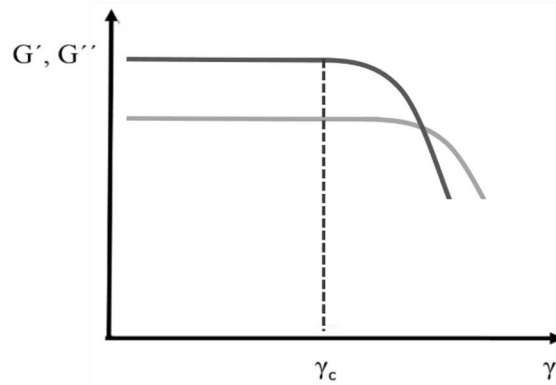


Figure 11. Illustration of G' and G'' as a function of deformation to determine the LVE in an amplitude sweep (log-scale).

Frequency sweep

Frequency sweeps are used to investigate the time-dependent shear behavior, since the frequency is the inverse value of time.^[123] As previously addressed, high frequencies belong to short-term behavior, and low frequencies to long-term behavior. Short time response is dominated by the elastic parts, whereas the viscous part is prominent in long-term response of the material. During such a frequency sweep test the frequency itself is varied and the amplitude is fixed, as is the temperature. The dynamic moduli are determined over a range of frequencies (typically 10^{-3} Hz – 10^2 Hz). The accessible frequency range of a conventional rotational rheometer is somewhat limited. Very high and very low frequencies are not accessible by only a variation of the frequency. For many polymeric materials the expanding of the range is achievable using the time-temperature superposition principle (TTS, also frequency-temperature superposition or the method of reduced variables).

Temperature sweep

Temperature sweeps, in which G' and G'' are determined as a function of temperature at fixed frequency, are a useful tool to determine phase transitions, such as melting or the molecular interactions in networks taking place during heating.

Time-temperature superposition

In many cases, rheology (in particular dynamic spectra at various temperatures) can be used as an indicator of molecular structure. TTS is a well-known procedure and applied either to determine the temperature dependence of the rheological behavior of a polymeric sample or to expand the frequency (time) regime at a given temperature at which the material behavior is studied. The principle is based on the assumption that all relaxation times belonging to a given process have the same temperature dependence. Simultaneously, all contributions to the moduli should be proportional to ρT (density-temperature-correlation). It can be used not only in linear rheology, but also within the probe tack test, addressing large deformations.^[124]

In order to characterize the complete mechanical behavior in a large frequency range covering up to 10 decades, one can measure the polymer sample at different temperatures (from minus degrees to above the melting point). Subsequently, one can shift the recorded G' and G'' data points (curves) along the frequency axis (x-axis) to one fixed reference temperature.

The shift factor a_T for each data set is given by the universal equation of William, Landel and Ferry (WLF equation).^[124]

$$\log a_T = \frac{-C_1(T - T_{Ref})}{C_2 + T - T_{Ref}} \quad (23)$$

where T is the temperature during the experiment, T_{Ref} is the reference temperature and C_1 , C_2 are material constants. Usually, T_{Ref} is chosen to be about 50 °C above the T_g of the sample. Generally, TTS can be applied as long as no structural change or phase transition occurs within the investigated temperature range.

The temperature strongly influences the chain mobility. With increasing temperature the mobility of the polymer chains increases and vice versa. The influence of the temperature variation on the molecules motion is identical with the effect of time variation, which is true for linear, or just slightly cross-linked polymers. The shift of the data points measured at different temperatures horizontally along the time axis results

2. Fundamentals and state of the art

in a so-called master curve, which covers the linear viscoelastic properties of a polymeric material in a large decade range (example see Figure 12).

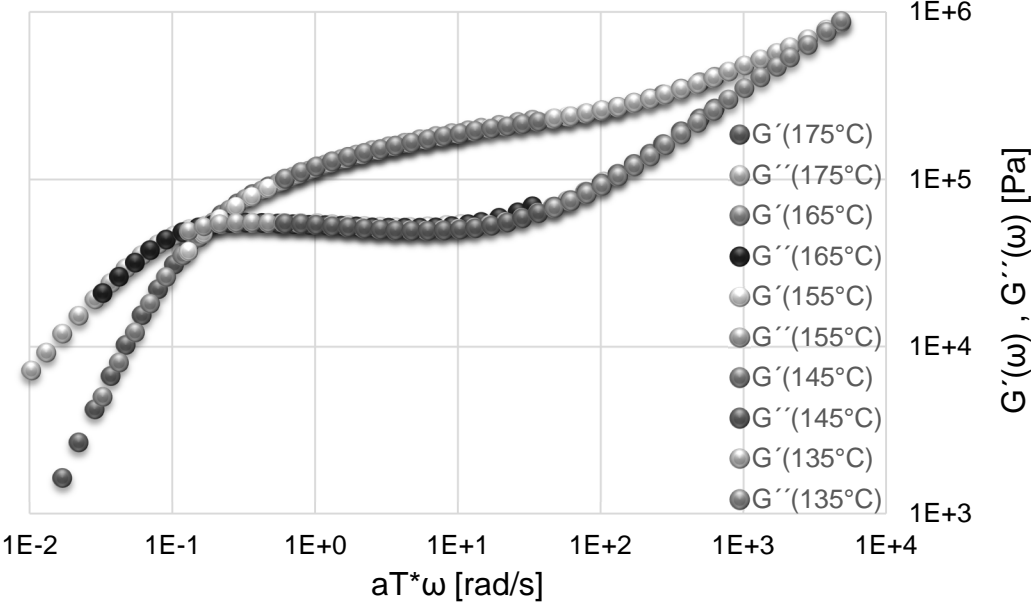


Figure 12: Dynamic mechanical data of a polystyrene (220 kDa M_n). Original master curve at a reference temperature of 175°C.^[125]

2.4 Principles of polymer synthesis

The basic characteristic of a polymer is the generation of its entire structure through the repetition of one or many elementary units (polymer i.e. “many member”).^[126] The elementary units, i.e. monomers, are connected in any conceivable pattern like linear, non-linear, cross-linked or branched, and the simplest is the linear structure to obtain linear polymers. In this context, the degree of polymerization is defined as the number of repeating units in a molecule. In a polymer material not every macromolecule has the same degree of polymerization, hence there is an average molecular weight distribution and an average degree of polymerization. For classification of polymers, two broad classes were defined by Carothers as there are step growth polymers (polyaddition and polycondensation products) as well as chain growth polymers (radical, anionic, cationic and living/controlled products).^[127] The major contrast between both is the process by which the polymers are formed.

2.4.1 Step growth polymerization

Condensation polymerization as well as polyaddition polymerization proceeds by a stepwise intermolecular condensation of functional groups, such as ester or amides and under elimination of small molecules as by-product, like water or methanol. The process is either a homopolymerization of one single AB-type monomers owing two different functionalities or a copolymerization of two monomers of type AA and BB. The polymer backbone includes the reacting functional groups, often polar in nature and hence with different chemical and physical properties. Common condensation polymers are polyesters like polyethylene terephthalate (PET) or Nylon6.6 *via* common condensation polymerization under elimination of water.

In general, condensation products are lower in molecular weight than addition polymers and are formed in slower reaction. A high conversion is needed to gain a high molecular weight. The reacting monomers are consumed in the early stages to form oligomers, which are able to combine and form longer chains. Bi-functional monomers yield linear polymers, whereas multifunctional monomers lead to branched polymers.

2. Fundamentals and state of the art

The Carothers equation defines the degree of polymerization (X_n), for an extent of reaction (p), where p is defined as:

$$p = \frac{\text{number of groups reacted}}{\text{number of groups initially}} = \frac{N_0 - N}{N_0} = 1 - \frac{N}{N_0} \quad (24)$$

with N as the number of groups at time t and finally:

$$X_n = \frac{N_0}{N} = \frac{1}{1-p} \quad (25)$$

2.4.2 Chain growth polymers

Chain growth polymerization usually proceeds *via* an active species, e.g. radicals. Free radical polymerizations are of particular importance to the industrial sector for a variety of reasons. Many monomers capable of undergoing chain reactions are available in large quantities. The free radical mechanism is well understood and any extension of the concepts to new monomers is generally straightforward. And finally polymerization proceeds in a relatively facile manner since exhaustive removal of moisture is generally unnecessary while polymerization can be carried out in either bulk or solution.^[128]

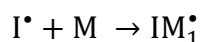
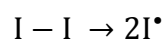
The initiation starts *via* specially designed initiators. The reactive species propagates until termination or side reactions occur. Each growth step consists of a reaction with a monomer. A combination of two propagating chains results in deactivation unlike in condensation polymerization. Compared to a step-growth polymer chain the chain-growth polymer commonly exists exclusively of carbon atoms due to the usually involved unsaturated monomers. In general, chain-growth polymerization yields high molecular weight polymers. In case of free radicals participating, a so called free radical polymerization mechanism takes place.

The reaction mechanism can be described by three general steps: the initiation, the propagation and the termination. Chain transfer has a very significant contribution and

can also occur in various ways (i.e. to monomer, to solvent, to polymer, to transfer-agent, ...).

Initiation via radicals

An initiator (I) form radicals in a controlled way either by heat or electromagnetic radiation (e.g. light). A radical is a highly reactive species with an unpaired electron (R^\bullet). These free radicals can be formed by two methods, either homolytic scission (i.e. homolysis) or *via* a single-electron transfer processes. Most common initiators are peroxy and azo components and decompose *via* homolytic scission at temperatures ranging from 60-90°, since they contain week bonds. Multifunctional initiators form different radicals, containing more than one unstable group.^[129, 130] Examples of such compounds include benzoyl peroxide, *t*-butyl hydroperoxide and AIBN (Azobisisobutyronitrile). The second step within the initiation process involves the attack of one free radical to the π -bond of a monomer molecule to produce the chain initiating radical. The first step is described as follows:



Propagation step

The growth of the polymer chain by propagation is the addition of large numbers of monomer to the active end of a chain. A new radical is formed very rapidly (1 – 10 ms) during each addition step similar to previous one, but larger by one monomer unit in a head to tail or head to head conformation:



2. Fundamentals and state of the art

Termination step

The termination step comprises the reaction of propagating active chains by either a recombination or a disproportionation reaction. *Via* combination two radicals couple, whereas in disproportionation reaction a saturated as well as an unsaturated product is obtained.^[131]

Chain Transfer

Free radical chains can also stop propagation in the linear direction and form polymer by chain transfer reactions. The transfer does not eliminate the reactive center but transfers the radical functionality to another molecule in the reaction medium. Chain transfer is observed for molecules of initiator, monomer and solvent, and deliberately added transfer agents.

Commonly, such agents are added to limit the molecular weight of the polymer chain.^[132]

Kinetic equations

The kinetic of the three different processes can be analyzed and lead to following expressions:

Assuming a quasi-steady-state approximation of a constant free radical concentration during the polymerization, one can define the rate of polymerization (R_p) as follows:

$$R_p = k_p [M] \left(\frac{fk_d[I]}{k_t} \right)^{\frac{1}{2}} \quad (26)$$

where k_x describes the rate constants for propagation, depolymerization and termination, respectively. $[M]$ and $[I]$ define the monomer and initiator concentrations and f is the fraction of initiator free radicals successful in initiating chains and has a typical value in the range 0.2 to 0.7. The latter term of equation (26) denotes the radical concentration. As it can be taken from the equation the rate of polymerization is

proportional to the monomer as well as the Initiator concentration.

The kinetic chain length ν results from the average number of monomer units reacted with an active center during its lifetime. It is also related to the molecular weight by the mechanism of termination. The kinetic chain length is written as following equation:^[133]

$$\nu = \frac{k_p[M]}{2(fk_dk_t[I])^{\frac{1}{2}}} \quad (27)$$

Further assuming no chain transfer, the rate of polymerization can be correlated to above described equation of the kinetic chain length. This results in a simple correlation of molecular weight and the monomer as well as Initiator concentration. The equation shows that by attempting to increase the degree of polymerization rate by decreasing the initiator concentration, thus results in a polymer with shorter chain length, since the value of ν is inversely proportional to the initiator. It is evident that the molecular weight strongly depends on the monomer concentration.

In conclusion the molecular weight is affected as follows:

- The more initiator radicals, the more chains, the lower M_n
- The more monomer at constant $[I]$, the higher M_n
- Increase in temperature causes faster reaction and lower M_n
- Higher pressure increases propagation, simultaneously inhibits the termination. The consequence is a higher M_n
- Additional chain transfer agent lowers M_n but narrows the distribution

At low monomer conversions (in the beginning), the reaction rate can be easily predicted by using this equation. The conversion first increases rapidly and finally declines gradually with further progression of the reaction. However, once a certain conversion has been reached, the termination rate constant (k_t) becomes dependent. In that case, the polymer gets less mobile and the solution (bulk) becomes more viscous; thereby the diffusion of the active centers or remaining polymer-radicals is hindered. Hence, the value of k_t decreases significantly. With increasing conversion the radical concentration increases, leading to the gel effect, also known as Trommsdorff-Norrish Effect.

2. Fundamentals and state of the art

Molecular weights and polydispersity

The degree of polymerization has a dramatic effect on the mechanical properties of a polymer. As chain length increases, mechanical properties such as ductility, tensile strength, and hardness rise significantly. Besides this, the individual polymer chains rarely have the same degree of polymerization and hence the molar mass shows a distribution described by an average value. Since the specific distribution has a big effect on the final properties of a polymer it necessarily needs a definition. The molecular weight distribution or dispersity (\mathfrak{D}) is defined as the relationship between the weight average (M_w) and the number average molecular weight (M_n) and indicates how narrow the distribution is. An individual definition of each molecular weight (unit is usually kDa or g/mol) is described as follows:^[134]

$$\overline{M}_n = \frac{\sum M_i N_i}{\sum N_i} \quad (28)$$

$$\overline{M}_w = \frac{\sum M_i^2 N_i}{\sum N_i M_i} \quad (29)$$

where N_i is the number of molecules of molar mass M_i .

The M_n is the simple average of the molecular masses of individual chains (asking every polymer chain for its molecular mass), whereas for the M_w a larger molecule has a larger contribution than a smaller molecule (asking every unit for the molecular mass of its polymer chain). Finally, the dispersity is defined as the ration:^[135]

$$\mathfrak{D} = \frac{\overline{M}_w}{\overline{M}_n} \quad (30)$$

There are several techniques to determine the molecular weights such as gel permeation chromatography for both, especially for the M_n colligative methods such as vapor pressure osmometry and end-group determination *via* IR or ¹H-NMR (if the molecular weight is reasonable low and the type of end group is known) are used. M_w can be determined by diverse scattering methods as well as sedimentation velocity. Depending on the method, two more average molecular masses found. Next to the number average and the weight average one can determine the z-average (M_z) by

ultra-centrifugation as well as the viscosity average molar mass (M_v) obtained from viscosimetry.^[136]

2.4.3 Homogeneous bulk-/solution polymerization

Bulk polymerization is the simplest form of free radical polymerization method since it involves only the pure monomer in combination with a monomer-soluble initiator. The advantages of bulk polymerization include high molecular weights in high conversion and usually a high purity of the products. As the free radical kinetics apply, however, bulk polymerization is difficult to control. Disadvantages arise due to the high reaction rate and rate of propagation as conversion increases and thereby broaden the molecular weight distribution. Difficulties in from of heat transfer are very well known, since these reactions are exothermic with high activation energies involved, and have a tendency towards the above mentioned gel effect. Usually the reaction progress is kept at low conversion and the unreacted monomer is recycled and polymerized stage-wise. Efficient stirring is required, since the viscosity of the reaction medium increases rapidly with conversion.^[133] This procedure is commonly used for ethylene, styrene and methyl methacrylate monomers.

Solution polymerization is a homogeneous method if the polymer remains soluble and an excellent method to overcome the heat transfer problem successfully. In case of an insoluble polymer precipitation occurs during the reaction, making it a heterogeneous procedure, and the product is obtained as e.g. powder. Again, the free radical kinetics can be applied. Dilution of the monomer with a suitable solvent allows even more efficient stirring and facilitates the heat transfer since the viscosity is decreased significantly. However, additional solvent results in other difficulties, as chain transfer to solvent comes into account under reduction of the molecular weight. Furthermore, the rate and degree of polymerization is decreased to a great extent. Another aspect is the use of solvent itself, even if the excess is removed afterwards by specific methods, impurities may remain in the polymer bulk or indeed it is difficult to remove the solvent from a final form causing degradation of the bulk performance. Finally, one should take the environmental impact on the pollution by the use of organic solvents into account.

2. Fundamentals and state of the art

Nevertheless, the use of solution polymerization is an employed industrial process with focus to the preparation of polymers where the presence of a solvent is required, such as in paints, varnishes and adhesives.

2.4.4 Heterogeneous Polymerization

Heterogeneous polymerization methods are of great industrial importance, due to the prevalent use under control of the thermal issues and viscosity. Common types include: dispersion, suspension, and emulsion polymerization.^[137]

Dispersion polymerization

Dispersion polymerization is a type of precipitation polymerization. As the reaction proceeds, polymer particles form, become unstable and start coagulation until stable particles are formed, creating the heterogeneous medium.^[138] Polymer molecules act as stabilizer in this case. The mechanism is equal to that of the emulsion polymerization, which will be explained hereafter.^[132] In dispersion polymerization nearly monodisperse polymer particles can be formed reaching 0.1 to 15 μm which range in-between the size of emulsion and suspension ones. Instrumental calibration standards as well as chromatography column packing materials are therefore a main product resulting from this technique.

Suspension polymerization

A general description of a suspension polymerization is made by the definition of the procedure as a heterogeneous polymerization using a monomer in the presence of an inorganic stabilizer, an oil-soluble initiator and usually water as the continuous phase. The reaction is carried out by mechanically suspending the reactants in the continuous phase, whilst the monomers undergo polymerization by forming beads or pearls of polymer in the range of 50 to 1000 μm .^[139] The main advantage is the formation of a defined stable latex which can be directly used in coatings or paints. The kinetics are

similar to bulk reactions, but the physical state of the medium allows better heat transfer. Industrial importance belongs to the production of PS, PMMA, PVC as well as PVAc. Disadvantage is an unfavorable restriction in the choice of monomer, since the glass transition of the resulting polymer should be higher than the polymerization temperature otherwise aggregation will occur.

Emulsion polymerization

The unique characteristic of emulsion polymerization technique is being a free radical polymerization proceeded in a multiple-phase colloidal system.^[140] It involves the dispersion of a monomer in a continuous aqueous phase with an emulsifier/surfactant (oil-in-water) followed by the polymerization using a water-soluble initiator. Surfactants can aggregate at the hydrocarbon/water interface and stay in equilibrium with free surfactant molecules in the aqueous phase. The initial emulsion contains surfactant-stabilized monomer droplets, having diameters greater than 50,000 Å (5 µm) and serving in the later reaction as reservoir.^[141] Since the reaction takes place in the formed particles, it has a significant influence on the reaction kinetics. First, the growing free radicals are isolated so it cannot participate in a termination reaction with a radical of another particle, and second, the highly reactive radicals confined in the domains tend to terminate rapidly. As a result, the total number of radicals in the whole reaction medium is usually within the dimension of the number of particles. Thus, emulsion polymerization does not involve simply the conversion of monomer drops to polymer particles, as is the case with suspension or miniemulsion polymerization. The final reaction product is a polymer latex with particle diameters in the range of 100 to 500 nm (0.1 to 0.5 µm).^[142] The first theory successfully explain the distinct features of emulsion polymerization was developed by Smith and Ewart,^[143] and Harkins^[144] in the 1940s, based on their studies of polystyrene. Smith and Ewart divided the mechanism of emulsion polymerization into three intervals.

Interval I

In the beginning most of the monomer is dispersed in droplets as mentioned before. The continuous aqueous phase contains the water-soluble initiator, emulsifier/surfactant (free dissolved or aggregated as small micelles), optional buffers,

2. Fundamentals and state of the art

as well as a small content of free monomer molecules and small monomer swollen micelles above the critical micelle concentration (cmc, diameter $\sim 100 \text{ \AA}$). Interval I is the particle nucleation with a growing number of polymer particles including monomer molecules. It ends commonly early in the reaction.

Interval II

During interval II, monomer (from the reservoir) and radical oligomers (built up from free monomer particle in the continuous phase) diffuse into the monomer-swollen polymer particles where the propagation takes place. Usually all micellar surfactant dissipated and there is a constant number of polymer particles.

Interval III

Starts, if the transport of monomer from the droplets into the particles stops (when the monomer to polymer ratio is equal to that in the particles and the thermodynamic driving force for transport becomes zero). This is true as long as the number of particles formed from the droplets is orders-of-magnitude smaller than the number formed by nucleation. All monomer droplets are consumed. Remaining monomer is in the polymer latex particle and still a constant number of particles is retained.

Advanced control of thermal and viscosity matters are attained using emulsion polymerization technique. Analyzing the kinetics results in the relationship between molecular weight, the rate and degree of polymerization described as follows:

$$R_p \sim [M][I]^{2/5}[S]^{3/5} \quad (31)$$

$$\bar{X}_n \sim [M][I]^{-3/5}[S]^{3/5} \quad (32)$$

The proportionalities show that the molecular weight may be increased without decreasing the rate of polymerization. Nevertheless, surfactant molecules and other polymerization auxiliaries remain in the polymer or are difficult to remove. Furthermore, water removal is an energy-consuming process. Emulsion polymerizations are usually

designed to operate at high conversion of monomer to polymer. This can finally result in significant chain transfer to polymer.

Miniemulsion polymerization

Miniemulsions have some peculiar and desirable properties compared to conventional emulsions.^[145] Ugelstad et al. were the first to demonstrate that nucleation of monomer droplets could be observed for a major part of particles if the droplet size is small enough using long chain fatty alcohols such as cetyl alcohol as well as surfactant.^[146] Emulsions can degrade principally by both, coalescence and diffusional degradation (Ostwald ripening). Coalescence can be suppressed by the addition of a sufficient level of surfactant. Ostwald ripening may be slowed or even prevented by adding an oil-soluble co-surfactant such as long-chain alkanes and alcohols. Co-surfactants lower the Gibbs free energy of the droplets whilst decreasing the driving force for diffusion.^[147, 148]

Starting with a pre-emulsion obtained using high shear force *via* sonification methods, the monomer droplets break up into smaller droplets typically in the range of 100 to 500 nm in diameter. As a consequence, a large droplet surface area is gained which results in most of the surfactant being adsorbed to the droplets surface. Hence, just a negligible amount of free surfactant is available to form micelles. The monomer droplets itself become the primary locus of particle nucleation and serve as mini-reactors. In miniemulsion polymerization, radicals enter directly the monomer droplets and initiate polymerization inside of them.^[149 -154]

2. Fundamentals and state of the art

2.5 Appropriate polymers from renewable resources

Sustainable and bio-based products with manufacturing processes that combine chemical, thermal, or mechanical methods forward to protect nature and environment, enable greater independence from fossil raw materials. These products make a significant contribution to the structural change from a petroleum based to a more bio-based industry

A change from fossil feedstock to renewable resources offers a great opportunity for industrial applications, as renewables are believed to be capable of fulfilling highly challenging tasks.^[2, 155, 156] The use of vegetable oils and fats as renewable raw materials is well established and a subject of continued investigation.^[157] The structural diversity of fatty acids depends on the oil source. It enables the design of a multitude of monomers, fine chemicals, and polymers, which can be derived in a straightforward fashion.

In addition, plant oils have been used for decades as surfactants, in paint formulations, for coating and resin applications and as flooring materials. The latter may be highlighted by the probably best known example Linoleum, which was developed by Frederik Walton (UK) and already industrially produced in 1864.^[158] Its main component is linseed oil, providing an environmentally friendly alternative to common PVC floorings.

2.5.1 Plant oils as renewable raw material

Nowadays, plant oils are the most important renewable raw material for the chemical industry, at least in Germany (30% of the 2.7 million tons of renewable raw materials 2005 in Germany were plant oils). Plant oils are heavily used as raw materials for surfactants, cosmetic products, and lubricants.^[3] Moreover, it is to mention that in the European Union more than 19.4 and 7.9 millions of tonnes rapeseed and sunflower is produced (2011), respectively.^[159, 160]

The predominant fatty acids present in plant oils in form of triglycerides (tri-esters of glycerol) are a diversity of saturated and unsaturated compounds with long and straight aliphatic chains. The structure of the triglycerides are highly dependent on the plant, the crop, the growing conditions, and the season.^[161, 162] Coconut and palm kernel oil

(laurics) contain a high percentage of saturated C12 and C14 fatty acids and are most important for the production of surfactants. Sunflower oil, for example, is composed of mainly four long chain fatty acids in a varying amount as shown in Figure 13.

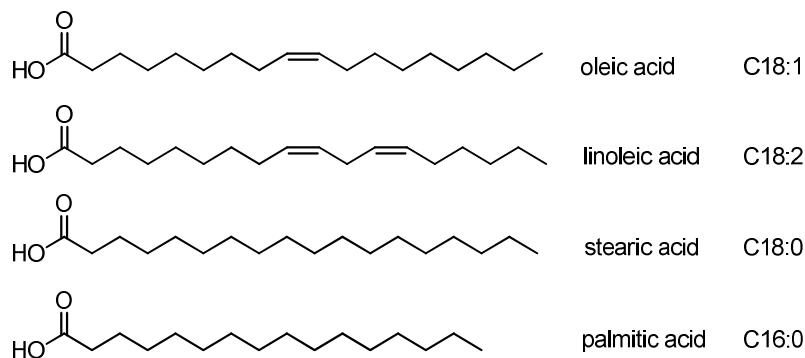


Figure 13. Structure of fatty acids (e.g. sunflower oil).^[163]

Defined as omega-9 (C18:1), omega-6 (C18:2), and omega-3 (C18:3), these fatty acids remain common (poly-) unsaturated structures, especially in the domestic vegetable oil compositions. Natural rapeseed oil contains up to 50 % of erucic acid (C22:1, omega-9),^[164] a compound which significantly lowers the nutritional value of for example rapeseed press cake as animal feed. On this account, so called canola oil was produced as an edible oil and is, except to only a very small amount, free of erucic acid.^[165] Next to human edible and animal feed both are produced as well for use as biodiesel fuel. Of capital importance are oils with high content of only one fatty acid, such as high oleic oils with a content of oleic acid (C18:1) exceeding 90%, have large potential for the substitution of petrochemicals currently in use.^[166,167]

Triglycerides have been highlighted to play main role as sources for polymers from renewable resources in the 21st century.^[168] The characterization and introduction of triglycerides in polymer application was highly reviewed, focusing mainly on cross-linked systems for coating and resin applications. Besides their direct polymerization they are increasingly used for the production of monomers. Moreover, the unsaturation is well suited for olefin metathesis reactions.^[169]

Especially epoxy resin formation using the epoxidized plant oils and fatty acids remain the most frequently studied polymerization. The epoxidation of unsaturated

2. Fundamentals and state of the art

compounds can be achieved in a straightforward fashion by commonly conducted reactions using molecular oxygen, hydrogen peroxide or enzymes.^[5]

In particular, enzymes have been intensely studied, whereby the reaction proceeds via an in situ formation of peroxy acids for the chemical epoxidation of the double bond.^[170 - 172] Such a procedure has the general advantage of suppressing undesired ring opening reactions of the obtained epoxides.

2.5.2 PSAs from renewable feedstock

Efforts to utilize renewable materials in PSA products are already discussed in the literature. Starting with an early study of also patented gluten-based PSA in 1971 using a partially hydrolyzed gluten polypeptide, obtained as a byproduct of the starch extraction, as starting material. As dried product with molecular weights up to 20 kDa (M_w) is was described as having PSA properties.^[173] Moreover a dispersion of wheat gluten and soy protein isolate was described as wood adhesive. The adhesive properties of the soy protein isolate particularly with regard to water resistance was showed to be superior.^[174] Also biodegradable species were taken into account.^[175] Compositions of cross-linked poly(hydroxyalkanoate) (PHA) were also evaluated as PSA.^[176] A biodegradable PSA using NR with an acrylic polymer and tackifiers (e.g. terpene, rosin) was patented in 1998.^[177]

Further investigations focused primarily on triglycerides and polyols (derived from vegetable and/or animal fats and oils) along with lactides and lactones (derived from carbohydrates).^[178, 179] For instance, acrylated macro-monomers were synthesized through the ring-opening copolymerization of L-lactide and ϵ -caprolactone with 2-hydroxyethyl methacrylate and were used for copolymerization reactions with acrylic co-monomers to produce polymers of high biomass content for PSA applications.^[180, 181] Furthermore, an approach to incorporate significant amounts of lactic acid macromonomers in the backbones of typical acrylic PSA polymers by miniemulsion polymerization was described.^[182] Moreover, a new PSA system composed of a ABA triblock copolymer was prepared by sequential ring-opening polymerizations using the renewable monomers menthide and lactide. The triblock copolymer was processed with up to 60 wt% of a renewable rosin ester tackifiers.^[183]

As mentioned above, different synthesis procedures for the functionalization of triglycerides have been studied, including enzymatic epoxidation, hydroxymethylation, esterification, or acrylation.^[168, 184 - 187] The range of properties enables many different applications, which make fatty acids superior candidates for use as composite, engineering thermoplastic materials, or pressure-sensitive adhesives.^[188, 190] For example, the synthesis of renewable PSAs *via* photo-catalyzed cationic polymerization of epoxidized soybean oil (ESO) has been reported in a patent application.^[191] Sun *et al.* explored a concept for novel bio-based PSAs derived from soybean oil with the aim to raise thermal stability and transparency as well as peel strength, for use in the optical electronic applications.^[192] A solvent-free PSA based on acrylated ESO was prepared *via* UV initiated free-radical polymerization, resulting in a high-shear performing product.^[193] Moreover, copolymer networks of ESO with lactic acid oligomers for pressure-sensitive adhesive have been discussed recently.^[194] It is known that epoxidized soybean oil (ESO) can be acrylated on industrial scale using acrylic acid. Hydroquinone is used as inhibitor to reduce polymerization side-reactions. Different catalysts based on amines or metal organic chromium catalysts are of great interest in the direct acrylation process.^[195,184]

In particular rapeseed oil was used as a base material for PSAs. Included triglycerides underwent a three-step reaction. The double bond in the oleic methyl ester was epoxidized by peroxy acid. Hydroxyl-containing polyesters could be obtained *via* step-growth polymerization of epoxidized oleic acid and showed adequate adhesion but low molecular weights.^[196] The mentioned epoxidized fatty acid methyl ester was also acrylated using acrylic acid. The acrylate groups were free-radically polymerized.^[10] Wool *et al.* endeavored also the design of PSA copolymers based on fatty acid methyl ester. In their work, acrylated methyl oleate (AMO) was first synthesized and subsequently polymerized using emulsion and miniemulsion polymerization techniques.^[197, 190] They copolymerized the AMO monomer with both, methyl methacrylate (MMA) and ethylene glycol dimethacrylate (EGDMA) to improve PSA performance and described the product as a new class of bio-based adhesive materials with potential for applications in tissue engineering, wound healing, and transdermal drug delivery.^[198] For the monomer synthesis, a chromium catalyst was used to open the epoxide with acrylic acid to obtain the acrylated derivatives. However, the use of chromium poses additional complications due to harmful effects of Cr(VI) as

2. Fundamentals and state of the art

well as Cr(III) on human health, which involves the respiratory tract and cancer issues.^[199] Therefore, either the development of chromium-free catalytic systems is necessary or the disuse of such systems is to prefer.

3. RESULTS AND DISCUSSION

In the early stages of each adhesive development, one has to consider basic conditions. In order to use fatty acid methyl esters as monomer and due to the inherent reactivity, the double bonds of unsaturated fatty acids are commonly preferred for functionalization, leading to formation of very attractive raw materials to be used in for instance for step-growth polymerizations. Considering the adhesive aspects, especially acrylates are of great interest due to their facile accessibility as well as their similar chemical structure to the mentioned petroleum based monomers. The performed polymerization procedures results in polymeric materials with adhesive performance and can be divided into two types: solvent borne polymers and water based dispersions, depending on the polymerization technique. Solvent born or bulk polymers formed by radical processes show, in general, improved performance compared to water based dispersions. Nevertheless, the environmentally friendlier technique finally has a high impact on an industrial scale.

3.1 Synthesis of the acrylated fatty acid methyl esters

In this work, the focus was on native vegetable oils providing oleic acid as well as erucic acids in high amounts and being commercially available. The required methyl ester starting materials were synthesized in large scales prior use in purities above 90 % according to standard laboratory procedures.^[237] As already mentioned, the fatty acid methyl esters have to undergo a synthesis pathway towards the respective acrylate since the internal double bond of the fatty acid is relatively unreactive to proceed directly in common free radical polymerization procedures. Different pathways could be found in literature as already described and were adopted or transferred and optimized towards the fatty acid methyl esters. With respect to environmentally friendly synthesis procedures and industrial concerns, the described reaction pathways do not require the use of chromium catalysts.

3. Results and discussion

The mainly investigated routes to successfully convert the internal double bonds into a more reactive acrylate functionalized monomer ready for polymerization, are subdivided in three procedures and illustrated within Figure 14.

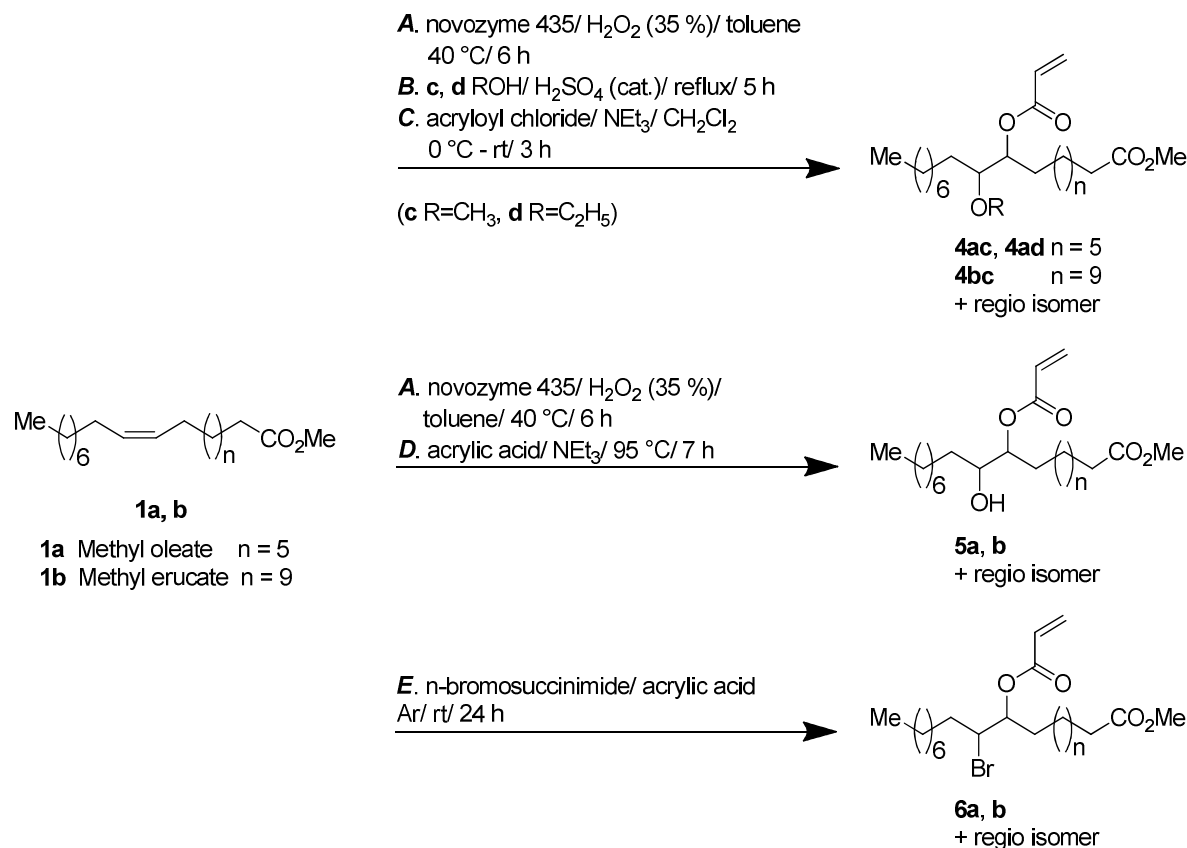


Figure 14. Synthesis pathways to oleate and erucate derivatives **4ac** (AMO), **4ad**, **4bc**, **5a,b** and **6a,b**.

3.1.1 Three-step procedure

To avoid the use of transition metal containing catalyst, an investigation of a three step synthesis pathway as an alternative route to previously reported procedures was investigated.^[190, 195] The involved reaction steps (epoxidation, ring-opening and acrylation) make this procedure favorable from both an economic and ecologic viewpoint, regardless of the additional reaction step.

Illustrated by the first reaction pathway in Figure 14, procedure **A** comprises the enzymatic epoxidation of methyl oleate as well as methyl erucate.^[185, 171, 200] More precisely, the enzymatic epoxidation was performed using a specific *Candida antarctica* lipase B named Novozym[®] 435. This commercial product, expressed in

Aspergillus niger and immobilized on macroporous acrylic resin, has been described for the methanolysis for biodiesel fuel production as well as for the epoxidation reaction by demonstrating an selective and environmentally benign alternative to traditional industrial processes.^[201, 202] The enzymatic epoxidation is a method of choice, resulting in the respective epoxidized fatty acid methyl ester as a colorless wax (**2a** and **2b**) in quantitative yields.

Without further purification, the ring opening was then performed either with methanol or ethanol (procedure **B**).^[203, 204] A hydroxy- in combination with a methoxy- or ethoxy-group was thus obtained as a mixture of regio isomers. Yields of ~70 % were obtained in this step to receive structure **3ac**, **3ad** and **3bc**. The introduction of other groups instead of methoxy- and ethoxy- functionalities may generally affect the polymers end-properties and finally the adhesive performance. A further try to introduce 4-vinyl benzene sulfonic acid according to literature^[205] was not successful and yielded no monomer for polymerization and was therefore neglected.

After purification of the received substances, further esterification/acrylation by adding acryloyl chloride and trimethylamine led to the formation of methoxyacrylate (or ethoxyacrylate) fatty acid derivatives in yields of 72 %.^[206] Procedure **C** required carefully proceeding as well as extensive purification due to the formation of the triethylammonium chloride salt, which was removable on the one hand, but within time consuming filtration especially at large scales on the other hand. Noteworthy, purification by silica column chromatography with a mixture of hexane/ethyl acetate was absolutely necessary, because it is well known that free radical polymerization is very sensitive towards impurities. Most importantly, a formed di-acrylate byproduct was reduced to a minor content (<2 %). Adversely, preconditioning towards high purity causes a lack of yield and needed at best five days. Usually larger scales had to be fractionated before purification resulting in increased effort. Nevertheless, an overall yield of 49 % could be achieved *via* reactions **A**, **B** and **C** (compare Figure 14) to finally receive pure monomers **4ac**, **4ad** as well as **4bc**.

3. Results and discussion

3.1.2 Two-step procedure

To further simplify the monomer synthesis, to reduce the reaction time and to obtain higher yields by reducing the necessary reaction steps, a direct ring opening of the epoxide with acrylic acid (AA) was investigated using triethylamine as catalyst to obtain the hydroxyacrylate derivative (procedure **D**), inspired by literature focusing on triglyceride modification.^[207, 208] The procedure was adopted and transferred to methyl oleate- (and erucate-) based epoxides synthesized prior using procedure **A**. The synthesis of the methyl oleate based monomer was further optimized towards an equal molar ratio of the epoxide to AA. These reaction conditions are also favorable for the erucate based epoxide. Table 4 summarizes the results of conversion in the ring opening reaction of the oleate based epoxide at 95 °C in 7 h of reaction time and confirms that two equivalents of AA lead to high conversions of up to 88 %.

*Table 4. Conversion in the ring opening of the oleate based epoxide, EMO (procedure **D**).*

EMO : AA : cat.^{a)}	Conversion^{b)}
eq.	[%]
1 . 4 : 1	77
1 . 3 : 1	80
1 . 2 : 1	88
1 . 1 : 1	78

^{a)}Epoxide : acrylic acid : trimethyl-amine; reaction 7 h/ 95 °C; ^{b)}¹H-NMR results.

However, the described synthesis pathway was somewhat troublesome due to the high temperature. These difficulties comprise mainly the homopolymerization of the acrylic acid in combination with co- as well as homo-polymerization of synthesized fatty acid based monomers. Furthermore, the epoxide is also able to undergo homopolymerization or copolymerization, however the conversion and final yields.

In general, the following observations were made:

Increasing the amount of AA caused polymerization to polyacrylic acid (PAA, or copolymer) at a temperature of 95 °C decreasing the conversion, as a matter of course which is confirmed by Table 4. Polymerization, however, was also observed at longer reaction times as well as in up-scaled reactions, which is attributed to a probably less efficient heat transfer in the reaction mixture. Similar results were obtained by varying the amount of catalyst, concomitantly lowering the conversion for both higher and lower concentrations. Hydroquinone was thus added as inhibitor according to a literature report (0.3 wt%).^[209] However, by using a ratio of reactants of 1 : 2 : 1 (compare Table 4), additional hydroquinone became redundant since no polymerization product was observed after 7 h reaction time. Purification of the crude mixture by silica column chromatography with a mixture of hexane/ethyl acetate was again mandatory to obtain the pure and colorless monomer. Better overall yields of about 64 % were achieved after purification.

3.1.3 One-step procedures

In view of a technical upscale, alternative one-pot procedures were then considered. The mainly investigated one-pot procedure **E** yield bromoacrylated monomers **6a** and **6b** by using *n*-bromosuccinimide to finally receive acrylate monomers ready for polymerization. The reaction pathway is shown in Figure 14. Reaction conditions were adopted from procedures described elsewhere.^[187, 206] A significant excess of AA used in previous reports was proven to be unnecessary. The amount of AA could be reduced to 10 equivalents, leading to conversions of 81 %. The synthesis was performed for 24 h at room temperature without observing polymerization side-reactions. Increasing the reaction time to 48 h showed only a slight influence on the conversion (89 %), as Table 5 illustrates. Yields of 66 % were obtained after purification by silica column chromatography in this one step procedure.

3. Results and discussion

Table 5. Conversion of the one-pot bromoacrylation (procedure E).

FAME : AA : cat.^{a)}	Conversion^{b)}	FAME : AA : cat.^{a)}	Conversion^{b)}
eq.	[%]	eq.	[%]
1 : 250 : 2	91	-	-
1 : 125 : 2	79	1 : 125 : 1	62
1 : 75 : 2	60	1 : 75 : 1	65
1 : 10 : 2	74	1 : 10 : 1	81
1 : 10 : 2 ^{c)}	89	1 : 10 : 1 ^{c)}	89

^{a)}Fatty acid methyl ester : acrylic acid : N-bromosuccinimide per eq. double bond. Reaction 24 h/ rt; ^{b)}¹H-NMR; ^{c)}per eq. double bond. Reaction 48 h/ rt.

Continuous research concerning one-pot reaction was performed, because direct addition reactions are more attractive in terms of atom efficiency, energy saving and cost effectiveness. According to literature, a one-step acrylation of the fatty acid methyl ester was thus performed by reacting methyl oleate and acrylic acid directly under the catalysis of boron trifluoride etherate (BF₃·Et₂O).^[210] Using this reaction pathway, one obtains only the acrylate functionality by direct introduction to the double bond of the methyl oleate (reaction pathway shown in the experimental section in Scheme 4). The synthesis was performed using methyl oleate at 75 °C for selected reaction times varying from 6 h to 4 days. The conversion was determined *via* ¹H-NMR. An increase in reaction time increases the conversion up to 90 %, which is clearly illustrated in Table 6.

Table 6. Conversion of the one-pot acrylation of methyl oleate catalyzed by $\text{BF}_3 \cdot \text{Et}_2\text{O}$.

MO : AA : cat.^{a)}	reaction time	Conversion^{b)}
eq.	[h]	[%]
1 : 5 : 0.35	6	57
1 : 5 : 0.35	24	55
1 : 5 : 0.35	96	80
1 : 4 : 0.35	6	45
1 : 4 : 0.35	24	56
1 : 4 : 0.35	96	90

^{a)}methyl oleate : acrylic acid : boron trifluoride diethyl etherate; reaction 75 °C; ^{b)}¹H-NMR results.

Decreasing the amount of acrylic acid caused lower conversion at same conditions. The same was observed for lower catalyst concentrations. Due to the high reaction temperature of 75 °C, polymerization to polyacrylic acid was observed at higher amounts of acrylic acid. This may be suppressed by the addition of hydroquinone as described above, but moreover difficulties occurred within the column purification step making the synthesis unfavorable and time consuming. The crude product was highly colored and furthermore not addressable towards free radical polymerization. Concerning the toxicity of the $\text{BF}_3 \cdot \text{Et}_2\text{O}$ end the long reaction times of four days, this monomer synthesis strategy was not further investigated due to its poor polymerization performance.

Nevertheless, further conditions and approaches were described by Mr. David Peter during his bachelor thesis, focusing on one pot reaction pathways based on the direct introduction of functionalities to the double bond of the oleic-based methyl ester.^[211] Varying reaction pathways were addressed, such as the introduction of acrylonitrile in acidic conditions using sulfuric acid in a Ritter reaction according to literature.^[212, 213] This reaction was performed by cooling and stirring at room temperature for one day. Similar reaction conditions could have been transferred to the acidic introduction of acrylic acid.^[214] Longer reaction times were established to yield high conversion, but forced polymerization as a side reaction.

3. Results and discussion

As described above, the reduction of the synthesis steps from three to only one came along with a reduction in time consumption and with an increase in yield for selected monomers, as hoped for. The yields increased from 48 % to 66 %. Side reactions like polymerization only occurred for the ring-opening reaction using AA at high temperatures of 95 °C. Polymerization was not observed in the three- or one-step (at room temperature) reaction procedure. Side reactions as well as incomplete conversion were obtained within the three step synthesis, thereby reducing the overall yields.

Representative $^1\text{H-NMR}$ spectra of the synthesized and further investigated monomers are shown below in Figure 15. (Please note that the spectra of monomer 5a contains remaining epoxide at a chemical shift of 2.81 – 2.93 (m, 2 H, 2 CH)).

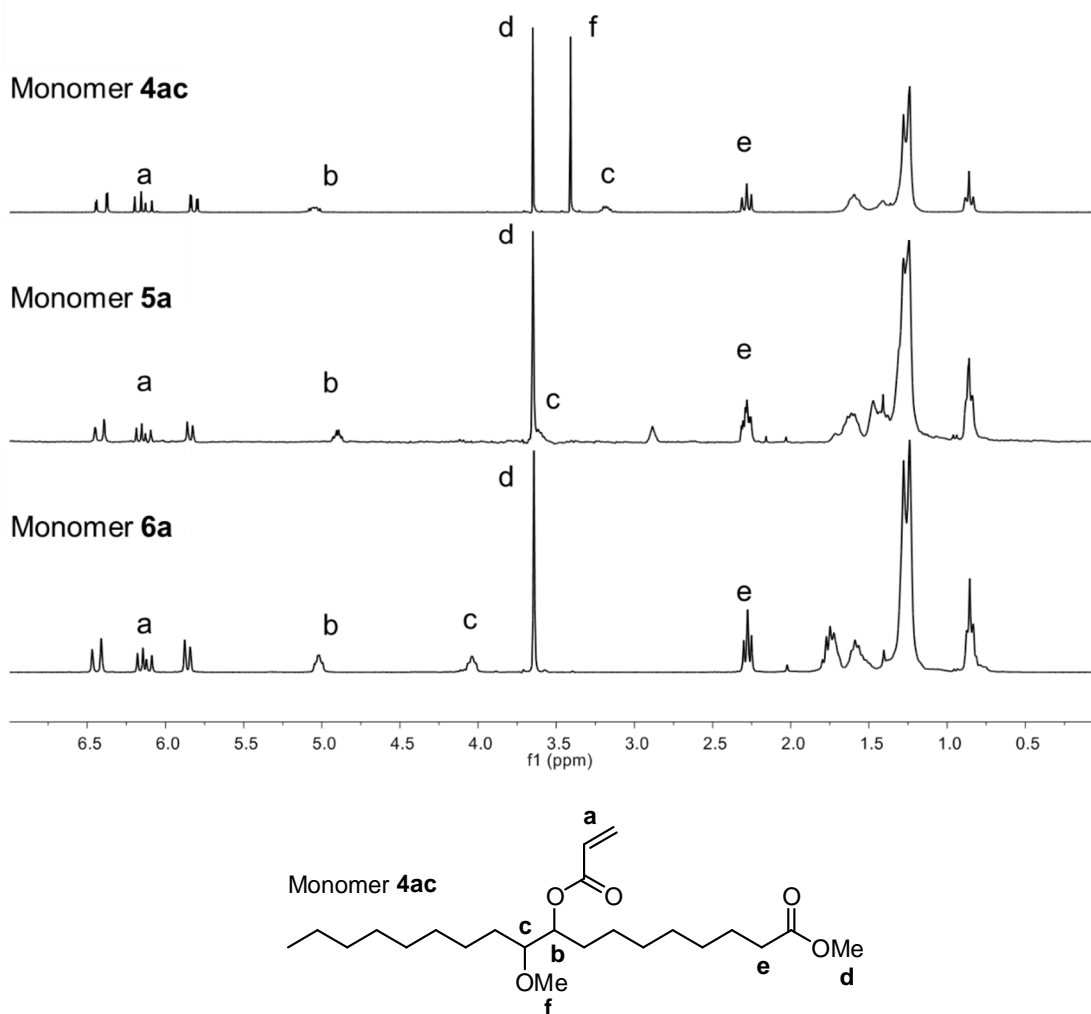


Figure 15. $^1\text{H-NMR}$ spectra of oleate based monomers synthesized in three-, two- and one-step procedures, measured in *d*-chloroform and showing respective chemical shifts of functional groups additionally illustrated by the chemical structure of monomer 4ac (bottom).

The NMR spectra of the acrylic monomers **4ac**, **5a** and **6a** show clearly the appearance of the terminal double bond of the acrylate group (a). The respective chemical shifts of b, d and e protons reflect the positions at the backbone near to the acrylic functionality (b), of the methyl group of the ester (d), as well as next to the ester function at the end of the backbone (e). Due to the structural variation of monomer **5a** (-OH) and **6a** (-Br), the chemical shift for f disappear, whereas the signal of the proton c shifts towards higher ppm, respectively.

Another important fact is the efficiency by reducing the steps in the reaction pathway, considering the amount of waste produced described by the E-factor (kg product/kg waste).^[215] The one step procedure showed the lowest value for the E-factor, indicating its improved sustainability. The E-factor was calculated without considering the purification steps leading to E-factors of 25.0, 6.00 and 1.60 for the three-, two-, and one-step procedure, respectively. Further consideration of purification methods such as column chromatography will lead to a significant increase of the calculated E-factors, and even more pronounced for the three step procedure, where the second and third step have been purified using this purification method.

Due to the somewhat limited equipment in lab scale reaction, one was limited to a synthesis volume of about 100 mL of the starting material. Furthermore, large scale production was limited due to the purification steps *via* column chromatography. In general, 40 g of monomer (**4ac**) could be obtained at the most. The three step synthesis was proceeded batch wise up to ~15 times in terms of lab residence.

Finally, each of mentioned acrylates was able to participate in a free radical polymerization because of the high reactivity of the introduced acrylic double bond.^[216] Most importantly for this study, all polymers derived from the described monomers showed good adhesive properties, despite of their small structural variations.

3. Results and discussion

3.2. Synthesis of poly(fatty acid methyl esters)

3.2.1 Polymer synthesis in solution/bulk

With the mentioned monomers in hand, polymerization was performed batchwise using 1 - 2 g of monomer for each trial. AIBN (2,2'-azobis(2-methylpropanitrile)) served as thermal initiator (0.60 mol%, Figure 16).

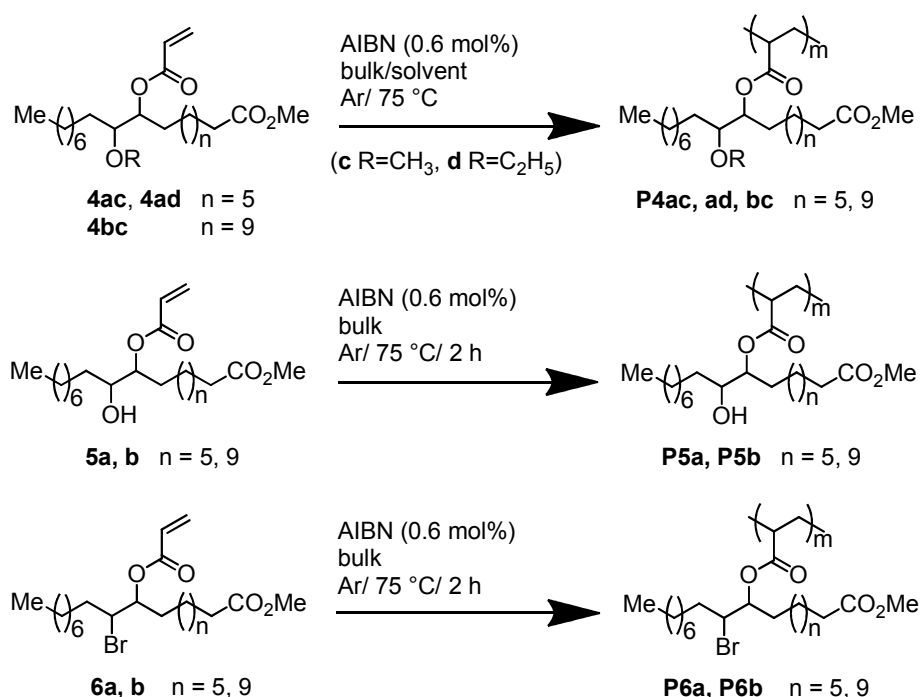


Figure 16. Homopolymerization to obtain polymers **P4ac**, **P4ad**, **P4bc**, **P5a**, **P5b**, **P6a**, **P6b**.

The synthesis pathways are shown in Figure 16. First test reactions were performed using monomer **4ac** in toluene as solvent in varying monomer to solvent ratios. Gas chromatographic measurements (GC) using hexadecane as internal standard were then performed to follow the reaction kinetics by determining the conversion. As expected, the more toluene (solvent) was used, the slower the reaction takes place and the lower the conversion. Other solvents showed similar performance on reaction kinetics. Furthermore, a solvent mixture of acetone/petrol ether in a 24 h synthesis (adopted from an industrial procedure), led to molecular weights of 300 kDa with excellent reproducibility. More or less, these molecular weights seemed to be too low for pressure sensitive adhesive performance.

Thus, the reactions were carried out in bulk to obtain highly viscous polymeric material. Precipitation in ice-cold methanol yielded about 78 % of highly viscous, colorless to yellowish (mainly **P6** derivatives) and most importantly tacky polymers. Molecular weights of up to 2 000 kDa (M_w) were observed by this bulk polymerization procedure, as illustrated in Table 7.

Table 7. Average number (M_n) and weight (M_w) average molecular weight as well as dispersity (\mathcal{D}) of synthesized polymers according to GPC.

Polymer	M_n [kDa]	M_w [kDa]	\mathcal{D}
P4ac	160	900	6
P4ad	120	1 500	13
P4bc	130	1 900	15
P5a	70	200	3
P5b	120	300	3
P6a	70	250	3
P6b	85	140	2

Higher M_w was obtained for **P4** derivatives, compared to **P5** and **P6** derivatives, which is desirable according to further PSA application. The latter reached molecular weights of about 300 kDa (M_w), which is at the lower end of typical PSA formulations.^[217] Additionally, **P4** polymers showed a high dispersity (\mathcal{D}), probably due to the formation of short- and long-chain branches through intra- and intermolecular chain transfer to polymer. Such side reactions are well known in free radical polymerization of acrylic monomers.^[218-220] For **P5** and **P6** derivatives, a lower dispersity of 2 was obtained. Increasing the reaction time forced gel formation in almost all cases, which made a rigorous time-control necessary in order to obtain soluble materials.

The respective NMR spectra of synthesized polymers are shown in Figure 17. The disappearance of the acrylate signals show clearly the formation of a polymer, as well

3. Results and discussion

as the shift of the protons at position b towards lower ppm. In general, broad signals are obtained for the polymer compared to the respective monomer. As mentioned for the monomer NMR spectra, the proton c shifts towards higher ppm in the same way.

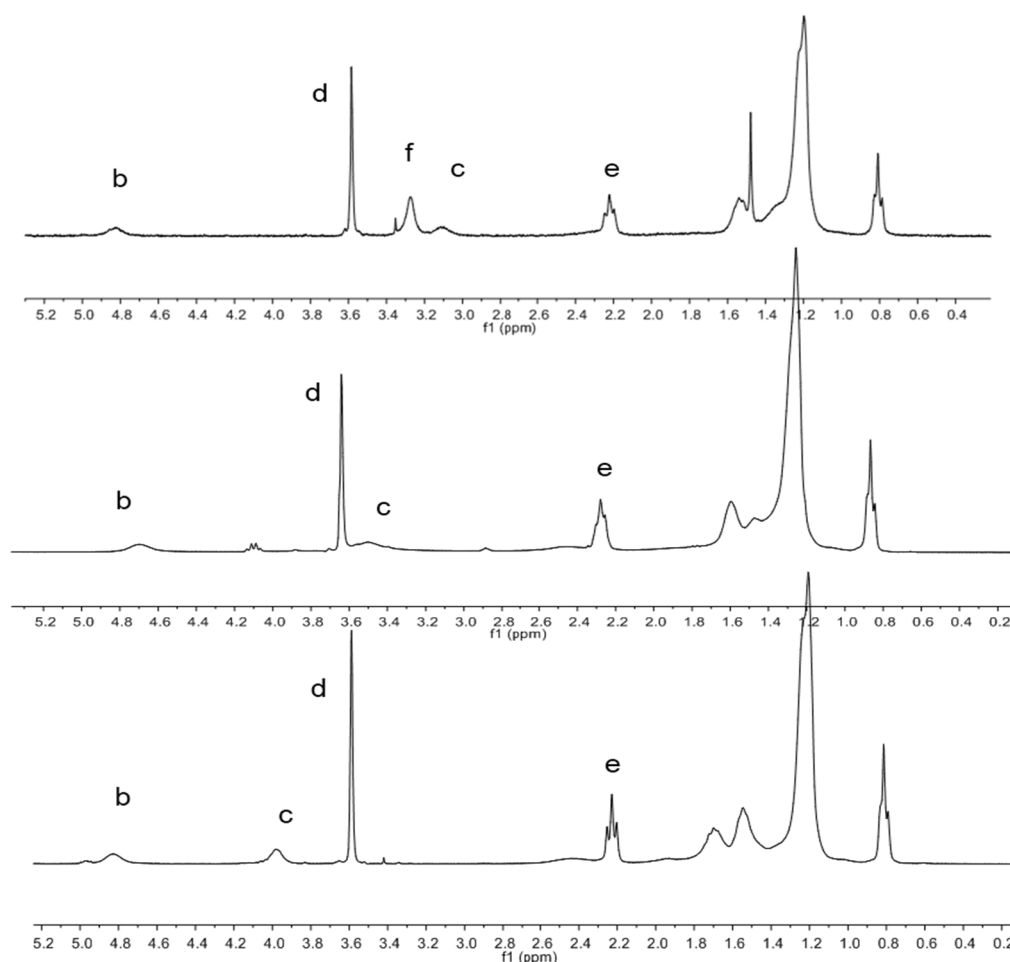


Figure 17. Respective NMR spectra (CDCl_3) of **P4ac**, **P5a**, **P6a**..

Complementary, different methods of controlled radical polymerization were employed in order to gain kinetic data and ultimately obtain multiple polymers with low dispersity ($\mathcal{D} = 1.1\text{--}1.3$). Based on first screenings covering the atom transfer radical polymerization (ATRP) process on monomer **4ac**, the potential of monomer **4ac** to react in a controlled radical polymerization process was investigated in detail within a supervised bachelor thesis.^[221] The methods employed to achieve these goals were free radical polymerization (FRP), reversible addition-fragmentation chain transfer (RAFT) polymerization, nitroxide-mediated polymerization (NMP), and single-electron transfer living radical polymerization (SET-LRP). These polymerization methods were more or less successful. However, expected degrees of polymerization were never

reached. Due to the high sterical hindrance and the obviously low diffusion rate of the macromonomer, only low molecular weight polymers (~8 kDa) could be obtained.

Consequently, high molecular weight, which is essential for the tackiness and cohesive strength of pressure sensitive adhesive polymers, remained challenging. Difficulties arised within conditions using small amounts of solvent or at least in cases of solvent free (or bulk) reactions, especially near high conversions. The well-known gelation was frequently observed. These high gel content polymers (65-80 %) where highly swellable, elastic and tacky materials, as well as insoluble in organic solvents. The gel content was determined gravimetrically. The gel-like materials could not be filtered and clogged the pores of the filter syringe just before GPC measurements. Very broad molecular weight distributions were observed for low gel content polymers when partly dissolved (< 10 %), or with higher crosslink-density no GPC data could be taken. In general, gel-like polymers observed during polymerization were unfeasible for any mechanical and adhesive tests. On this account, the following mechanical data shown within section 3.3 is represented by polymer samples with gel contents of << 10 %. However, all obtained polymers showed typical characteristics of PSAs. All samples were characterized by GPC, shown within Table 7 as well as Table 8 (chapter 3.3.1). Therefore, polymers were dissolved in tetrahydrofuran (THF) and solutions were purified through a filter syringe.

3. Results and discussion

3.2.2 Modification of the polymer

Besides the desired high molecular weight, another approach to gain cohesive performance was explored by introducing hydrogen bonding between existing polymer chains. For this purpose, the methyl ester functionality at the side chain of the polymer **P4ac** was cleaved to obtain the carboxylic acid. The saponification reaction involved a soft base (lithium hydroxide, LiOH) and was performed in a THF/water mixture (1:1) at 4 °C in 24 h reaction time (see also Figure 18). The resulting polymer **P7ac** was precipitated in ice-cold methanol. Using hydrochloric acid in order to lower the pH (< 7) led to the desired polymer performance. Problems occurred at basic conditions at the end of the reaction, where a hard, brittle as well as cloudy and insoluble material was obtained.

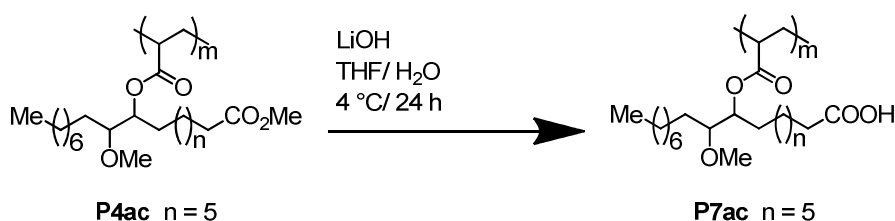


Figure 18. Deprotection of the methyl ester functionality in the side chains of polymer **P4ac**.

GPC data of the desired polymer sample after and before the saponification procedure is shown in Table 8. The molecular weight seems to increase after the synthesis procedure. The increase in molecular weight can be attributed to the additional reversible chemical cross-links, build up by the hydrogen bonds. **P7ac** was dissolved in HFIP (Hexafluoro-2-propanol) to break the hydrogen bonds and to ensure the existence of a physical cross-linked system. GPC measurements of the latter solution finally leads to similar GPC values as **P4ac** using THF-GPC.

Table 8. Number (M_n) and weight (M_w) average molecular weight as well as dispersity (\mathcal{D}) of saponified polymer according to GPC.

	M_n [kDa]	M_w [kDa]	\mathcal{D}
P4ac	113	651	5.7
P7ac^{a)}	339	1 820	5.4
P7ac^{b)}	105	359	3.4

^{a)}solvent THF. ^{b)}solvent HFIP (Hexafluoro-2-propanol).

Oscillatory shear measurements of the polymer **P7ac** showed only a slight increase in elastic performance (G' as well as G'') in comparison to the original **P4ac**. Due to the additional operating expenditure and the additional synthesis step, one decided to find more efficient ways to increase the cohesion of described polymers. Nevertheless, it is to mention that there are different and interesting ways to change the performance of adhesive-like materials (polymeric materials).

3.2.3 Copolymer synthesis

As mentioned in chapter 2, mainly copolymers are used for acrylic formulations to ensure a proper adhesive performance. Thereby, cohesion is gained only by copolymerizing the starting monomer in an appropriate ratio to raise the T_g and to strive for a given application. Copolymerization is defined as the process in which two or more different monomers react through means of polymerization.^[222] Since copolymers are composed of at least two different structural units, there are different classifications as to how these constituents are sequenced along the chain.^[223] Determining the monomer reactivity ratio is essential, as its value helps to predict the composition of the copolymer (such as the distribution of the monomer units on the chain), and to understand the kinetics as well as the mechanical properties of the copolymer.

First studies on the monomer reactivity of **4ac** was investigated within a supervised bachelor thesis. The comonomers used for the copolymerization studies on monomer **4ac** were butylacrylate (BA), 2-ethylhexylacrylate (EHA) and methyl methacrylate

3. Results and discussion

(MMA). Monomer reactivity ratios were evaluated by custom linearization methods, such as Finemann-Ross and Kelen-Tüdös methods.^[224, 225] Different feed ratios of the monomer **4ac** and the comonomer were used for this calculation. A detailed illustration of the results made, are shown in the respective reference.^[226] In the study, it was found that **4ac** showed a higher reactivity ratio value than EHA and MMA in bulk, and a lower reactivity ratio value than EHA and BA in solution. This study also demonstrates that the monomer reactivity ratios depend on the solvent. In general, the copolymerization was performed similar to bulk (homo-) polymerization, using AIBN as thermal initiator (0.6 mol% per 1 g **4ac**) at 75 °C and varying feed ratio.

3.2.4 Polymer synthesis in miniemulsion

The methyl oleate based monomer **4ac** was used to study the miniemulsion polymerization of acrylated fatty acid derivatives. The miniemulsion was prepared as described in the experimental section (4.3.2). Different surfactant concentrations were used to vary the particle diameter. Moreover, the initiator concentration was varied to change the molecular weight. Table 9 lists the variation of molecular weight with initiator concentration as well as the particle size variation with surfactant concentration. The molecular weight increased with decreasing initiator concentration and the particle size decreased with increasing surfactant concentration, as expected.^[151, 154]

Table 9. Results of miniemulsion polymerization. Left: Variation of molecular weight with initiator concentration. Right: Variation of particle size with surfactant concentration.

Entry ^{a)}	AIBN [mol%]	M_n [kDa]	M_w [kDa]	\bar{D}	d_{DLS} [nm] ^{b)}	Entry ^{c)}	SDS eq.	d_{DLS} [nm] ^{b)}	PD_{DLS} ^{d)}
A	1.50	43	230	5	370	D	0.01	374	0.03
B	1.00	66	190	3	374	E	0.10	276	0.03
C	0.50	91	760	8	392	F	1.00	70	0.04
						G	2.00	46	0.03

^{a)}Variation of initiator concentration using 0.01 eq SDS/ 75 °C/ 1.5 h. ^{b)}particle diameter. ^{c)}Variation of SDS concentration using 1.00 mol% AIBN/ 75 °C/ 1.5 h. ^{d)}polydispersity index values (PD_{DLS}) are those referred to as Malvern polydispersity. A value closer to 0.01 indicates a narrower distribution.

An oil-soluble initiator (AIBN) was used for the miniemulsion polymerization instead of common water soluble alternatives, since this leads to increased polymerization rates. In this respect, Thomas and coworkers have shown that it is possible to achieve high molecular weights if low initiator concentrations are used.^[227] Using the miniemulsion technique, it was possible to create polymer molecular weights up to about 800kDa. The dispersions showed long-term stability (>2 years) and were synthesized without co-stabilizer. The reaction time determined whether a soluble polymer (~1.5 h) or a non-soluble cross-linked latex (~3 h) was obtained. Soluble polymers obtained within 1.5 h were chosen for comparison with solution polymerization products.

3. Results and discussion

3.3 Adhesive performance

The adhesive properties of a pressure sensitive adhesive are determined by various intrinsic bulk parameters, such as polymer composition, average molecular weight (M_w), dispersity (\mathcal{D}), and crosslink density. Furthermore, substrate properties such as surface energy or roughness (R_a , defined as the average deviation from the mean surface plane: $R_a = \frac{1}{N} \sum_{n=1}^{n=N} |Z_n - Z|$), as well as external parameters, such as humidity or temperature, play an important role. The degree of crosslinking was varied upon storage of the ready-to-test films for different periods of time at 120 °C. Furthermore, first results regarding adhesion to low energy substrates and resistance to water uptake will be presented.

3.3.1 Viscoelastic properties

Characterization of linear viscoelastic properties was performed by means of temperature sweeps in oscillatory shear mode at fixed frequency. Figure 19 illustrates the performance of different polymers prepared in this study. Their molecular weights are shown in Table 10.

Table 10. Number (M_n) and weight (M_w) average molecular weight as well as dispersity (\mathcal{D}) of tested samples according to GPC.

Polymer	M_n [kDa]	M_w [kDa]	\mathcal{D}
P4ac_miniemulsion	80	300	4
P4ac/high	120	650	5
P4ac/low	90	270	3
P5a	130	280	2
P6a	110	270	2

The storage modulus (G') is plotted versus temperature (see Figure 19).^[190, 197] The data for all products synthesized here are in a similar range, but the storage modulus, characterizing the elastic material response, especially at high temperatures, is significantly lower than that of the commercial petroleum-based co-polymer Acronal V212 (BASF SE) used here as a reference for typical PSA polymers (see Figure 19).

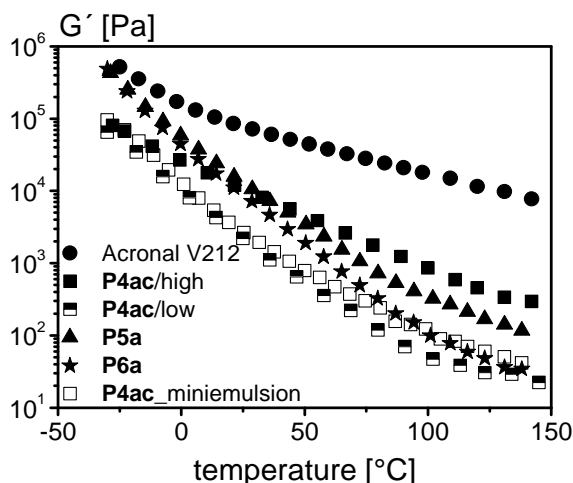


Figure 19. Storage modulus vs. temperature of bulk and miniemulsion homopolymers (molecular weights see Table 10) compared to a commercial acrylate co-polymer Acronal V212 provided as aqueous dispersion.

The first important fact to be highlighted is the criterion of Dahlquist for PSAs, stating that the upper limit of the elastic modulus at room temperature has to be lower than $3.3 \cdot 10^5$ Pa, which is fulfilled for polymers **P4ac**, **P5a** and **P6a** including the derivatives and miniemulsion product.^[21] Secondly, the low elasticity at high temperatures indicates a weak cohesion and shear strength especially in comparison to the commercial co-polymer. But this can be further improved by, e.g., introducing appropriate co-monomers resulting in a lower molecular weight between entanglements. Especially a broad molecular weight distribution including a fraction of ultra-high molecular weight, long-chain branched or cross-linked molecules will lead to the required increase of elasticity at high temperatures. This is confirmed by sample **P4ac/high**. Its higher M_w and polydispersity compared to **P4ac/low** obviously results in the expected increase in elasticity required for good cohesive properties.

3. Results and discussion

3.3.2 Tack and peel performance

Tack tests were performed at room temperature using a cylindrical flat steel probe. Detachment of the polymer due to cohesive failure was observed for all polymers synthesized here, but not for the Acronal V212. The corresponding tack data are shown in Figure 20. As expected, Acronal V212 exhibits the highest tack value, whereas the values for the synthesized homopolymers seem to be very similar and are in a reasonable range for PSA applications. This can be attributed to the viscoelastic influence, which is dominant in cohesive failure detachment. Noteworthy, the commercial petroleum-based co-polymer Acronal V212 is a well behaved dispersion with defined polymer microstructure including a special composition of comonomer as well as specific additives, resulting in an improved T_g and improved adhesive performance. In contrast, the here synthesized polymers are pure bulk homopolymer with very low T_g s in the range of $-60\text{ }^\circ\text{C}$. As outlined above, an appropriate degree of cross-linking or long-chain branching thus has to be introduced to achieve adhesive failure and higher tack. The polymer from miniemulsion polymerization shows the lowest tack, reaching only one third of the value found for the other materials. Since its storage modulus and molecular weight are similar to those of the other products, we attribute this to a contamination of the sample with residual monomer and/or surfactant, disturbing the wetting of the substrate as well as the bulk performance as it can act as a plasticizer.

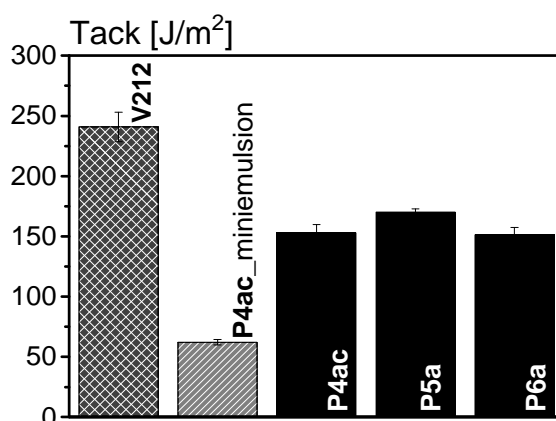


Figure 20. Tack of AMO-homopolymers compared to that of the commercial acrylate co-polymer Acronal V212. Debonding rate: $1\text{ mm}\times\text{s}^{-1}$; probe diameter: 5 mm.

Peel strength is a key parameter for the performance of PSAs. Figure 21 shows the results of the 90° peel tests performed as described in section 4.6.

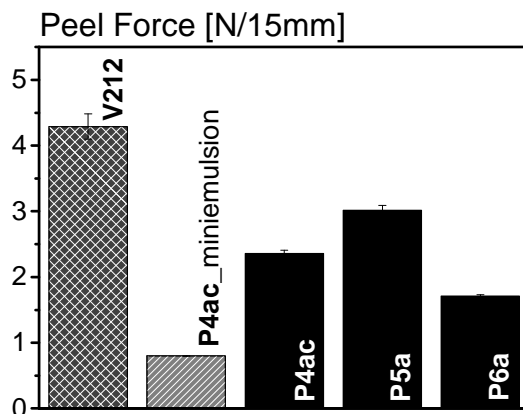


Figure 21. Peel force in 90° at 4 mm/s per 15 mm width.

The carrier foils coated with bio-homopolymer were peeled-off by cohesive failure, leaving residue on the glass substrate. Adhesive break was observed for Acronal V212. The peel value obtained for the Acronal V212 is 4.3 N/15mm. The synthesized bio-homopolymers exhibit lower values around 2.0 - 3.0 N/15mm, which are still in a reasonable range for typical PSA applications. Peel measurements seemed to be more sensitive towards molecular weight (M_n), since the values vary in the order: **P5a** > **P4ac_high** > **P6a** > **P4ac_miniemulsion**. Hydrogen bonding may explain the exceeding value of **P5a**. The overall lower values compared to the Acronal V212 are again attributed to the low viscoelastic performance of bulk homopolymers as mentioned within the results for tack tests. The low value found for the polymers obtained from miniemulsion polymerization can again be attributed to the presence of non-reacted monomer. For applications requiring a clean removal of polymer foils/stripes (adhesive failure), the molecular weight has to be further increased. Alternatively, long-chain branching or chemical cross-links may be introduced as already mentioned above. Comparable results to the above mentioned overall adhesive performance was also obtained with the polymer of the erucate derivatives. In general, now significant difference was observed comparing oleate and erucate based polymers.

3. Results and discussion

3.3.3 Influence of molecular weight on tack and peel

Tack and 90° peel tests were performed on **P4ac** homopolymers of different molecular weight. The obtained results are shown in Figure 22. Note that, due to limited synthesis capacity, tack and peel experiments could not be performed with the same samples, instead different batches had to be used. The M_w values of the samples used in tack experiments varied between 66 kDa and 690 kDa, those for the peel test samples between 370 kDa and 1180 kDa. Figure 22 also includes the respective dispersity values \mathcal{D} , indicating that all samples had a broad molecular weight distribution, as typical for free radical polymerization.

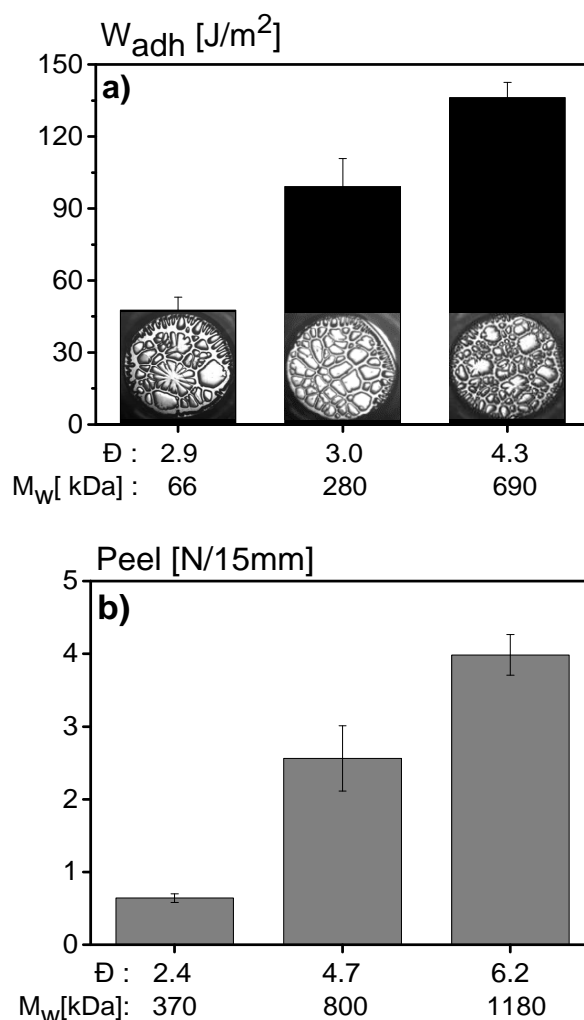


Figure 22. Work of adhesion a) and peel strength b) of **P4ac** homopolymers with different average molecular weight M_w and dispersity \mathcal{D} . Tack experiments were performed using a steel probe with $Ra = 3$ nm, 1 mm/s debonding velocity and 1 s bonding time. Peel tests were performed on glass plates at a debonding velocity of 4 mm/s.

As expected, the work of adhesion W_{adh} as well as the peel strength strongly increase with increasing M_w . Similar results have been observed for various petro-chemical PSA polymers and this phenomenon is attributed to the increasing number of entanglements per chain.^[46, 228, 229]

Cavitation is a phenomenon well known to occur during the debonding step in tack experiments. The images of the polymer layer, taken at the maximum point of stress during debonding, clearly show that the number of cavities strongly increases from 34 to 51 and 93 with increasing M_w (Figure 22a). This is in line with earlier findings for conventional polyacrylates^[85] and a consequence of an increasing fraction of the substrate surface not wetted by the polymer during contact formation due to increased viscosity. In all these experiments, cohesive failure occurred indicating that these polymers exhibit a low degree of crosslinking or long-chain branching (gel content determined to <2 %).^[230]

3. Results and discussion

3.4 Tailoring adhesion behavior via curing

The synthesized polymers are not crosslinked and almost completely soluble. Thus, they can be easily applied via solvent casting or slot-die coating. Curing of the already coated thin polymer layers results in crosslinking reactions and, depending on curing time, this can result in a non-soluble gel-like, but highly swellable material. This processing step can be used to tune the viscoelastic and adhesive properties of the polymer in a wide range according to the demanded specifications in different applications. The effect of curing on linear viscoelastic and adhesive behavior has been investigated for different homopolymers synthesized using monomers deduced from fatty acid methyl ester based on native sunflower oil.

3.4.1 Effect of curing on shear modulus

The effect of curing on shear modulus $G^* = G' + iG''$ of **P4ac** is shown in Figure 23. In Figure 23a, the storage modulus G' determined after different times of curing is plotted as a function of the temperature, data were taken at a fixed frequency of $f = 1$ Hz.

The modulus G' increases with increasing curing time and in the high temperature range ($T > 100$ °C), it reaches more than 1000-fold its initial value after 28 h of heat treatment. The modulus of the samples with short curing time steadily decreases with increasing temperature. After 5 h of curing, G' levels off at a constant value at temperatures $T > 100$ °C indicating the formation of a sample spanning network of crosslinks. Further curing then results in an increasing crosslink density as indicated by the higher level of G' in the high temperature range.

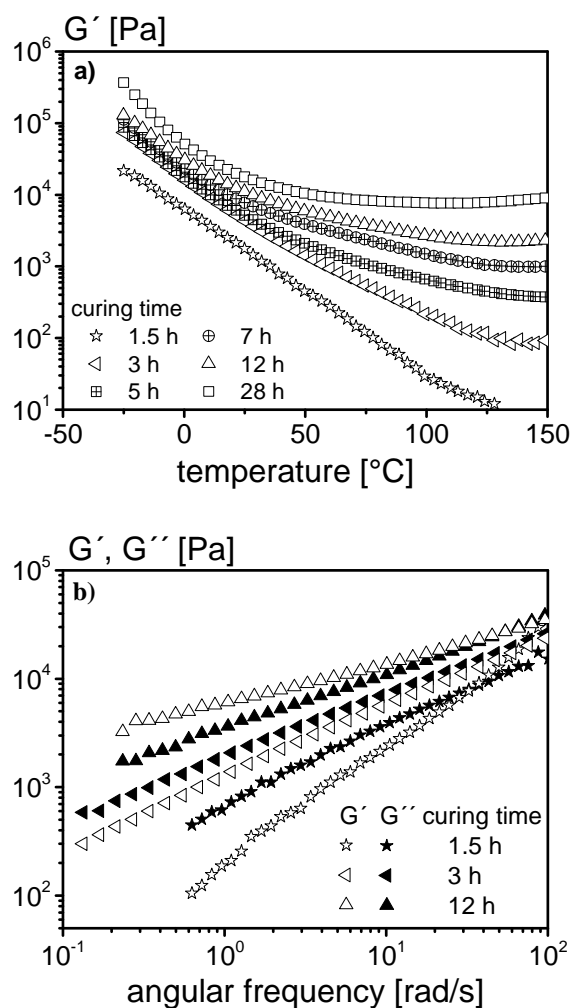


Figure 23. Storage and loss modulus data of cured **P4ac** ($M_w = 280$ kDa, $\bar{D} = 3$) by means of oscillatory shear measurements. a) G' as function of temperature at different curing times measured at 1 Hz frequency and 0.01 strain. b) G' and G'' as function of angular frequency measured at 20 °C.

Figure 23b displays the dependence of G' and G'' on the frequency for three different curing times. After 1.5 hours of heat treatment, G'' is still much higher than G' in the low frequency regime ($2\pi f = \omega < 10$ rad/s) and a crossover of G' and G'' occurs around $\omega \approx 40$ rad/s. This behavior is typical for flexible, non-crosslinked polymers. After 3 hours of curing, G' and G'' are almost equal in their absolute values and exhibit a similar frequency dependence over an extended frequency range of more than three orders of magnitude. This is typical for the so-called sol-gel transition, when the formation of a sample spanning network sets in.^[231] For curing times longer than this critical value, G' exceeds G'' and reaches a constant level at frequencies below $\omega = 0.1$ rad/s corresponding to the high temperature plateau value shown in Figure 23a as expected for crosslinked, gel-like or rubbery materials.

3. Results and discussion

3.4.2 Effect of curing on tack and peel

The effect of curing time on adhesion properties has been investigated for **P4ac**, **P5a** and **P6a** homopolymers.

Tack and peel strength data for **P4ac** obtained after different curing times are shown in Figure 24. The work of adhesion, W_{adh} , in tack experiments was determined using different steel and PE probes. Peel tests were performed on a glass substrate.

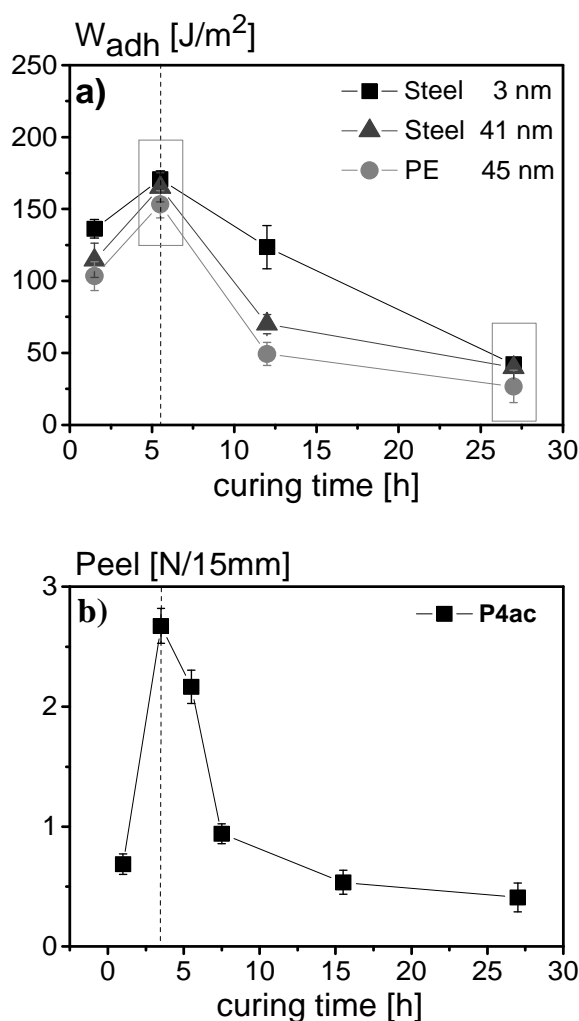


Figure 24. Tack performance and peel strength of cured **P4ac** ($M_w = 690$ kDa, $\bar{D} = 4.3$) on varying substrate types.

Both tack and peel strength exhibit a pronounced maximum at a curing time of about 5 hours, just above the sol-gel transition, after a sample spanning network is formed, and decrease monotonically for longer periods of heat treatment. Moreover, this maximum marks the transition from cohesive to adhesive failure.

Representative images of the respective substrate surface visualizing the different debonding characteristics in tack as well as peel experiments are shown in Figure 25.

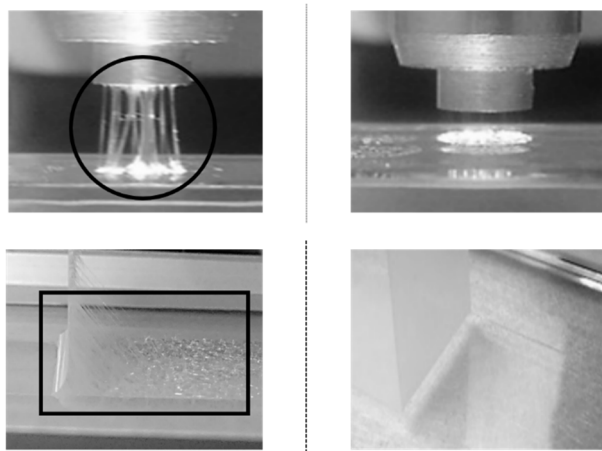


Figure 25. Cohesive (left) and adhesive failure (right) in tack and peel measurements of **P4ac** ($M_w = 690$ kDa, $\bar{D} = 4.3$) cured for 1.5 h (left) and 27.5 h (right).

Figure 26 visualizes the dependence of adhesive failure in tack as well as peel measurements on viscoelastic properties of cured **P4ac** samples shown within Figure 23a. With increasing crosslink density, the modulus G' as well as the tack and peel values increase until the maximum pronounces an elastic network. Beyond the maximum, the wettability and contact area towards the substrates surface is reduced due to the high elastic parts and simultaneously, with further increase of the network density, the adhesive performance decreases.

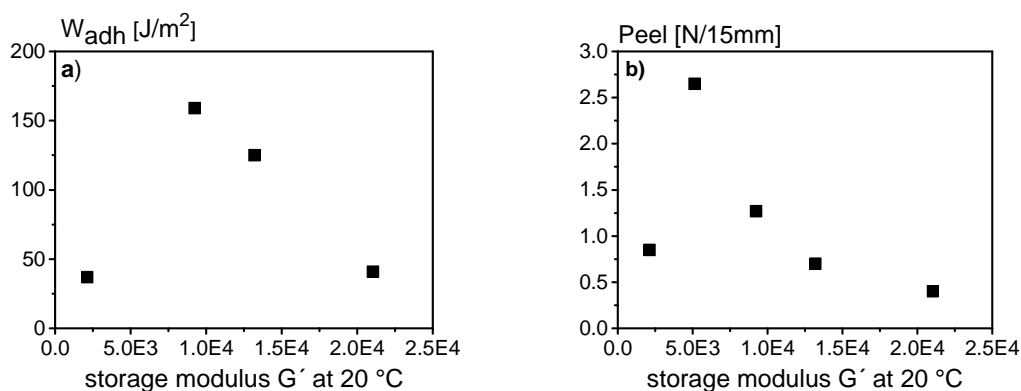


Figure 26. Tack and Peel data vs. G' at 20 °C to visualize the dependence of adhesive performance on viscoelastic properties.

3. Results and discussion

In addition, curing under exposure to UV light resulted in similar observations. The increase in crosslink density due to the formation of a network by a side reaction is also initiated using UV light, underlining the suggestion of a radical mechanism taking place.^[238]

Tack and peel strength data for **P5a** and **P6a** homopolymers are shown in Figure 27. The **P5a** exhibits similar behavior as **P4ac** and a maximum in W_{adh} and peel strength is observed for a curing time of about 5 hours, which again is accompanied by the transition from cohesive to adhesive failure. In contrast, W_{adh} as well as peel strength remain constant within the experimental error irrespective of curing time for **P6a**.

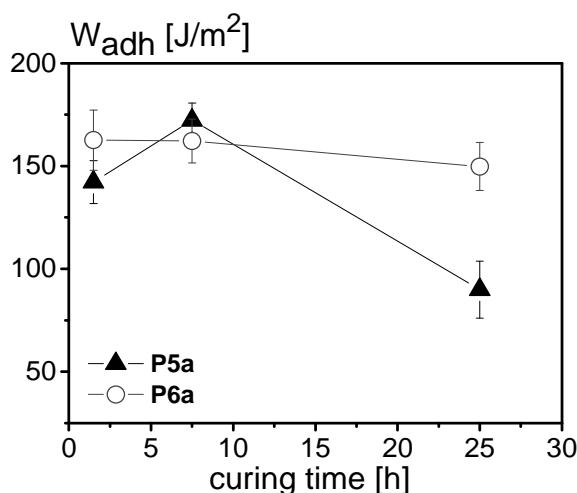


Figure 27. Tack values of cured **P5a** ($M_w = 290$ kDa, $\bar{D} = 2.2$) and cured **P6a** ($M_w = 250$ kDa, $\bar{D} = 3.5$). Tack tests were done using a steel probe with $R_a = 41$ nm.

Moreover, cohesive failure is observed for all **P6a** samples in tack as well as in peel experiments. Obviously, no or only little crosslinking takes place during curing. We attribute this to the bromo functionality of this polymer, which can act as retarder reducing the number of free radicals and thus suppressing gel formation.

This hypothesis is further supported by the peel results obtained for **P4ac** with added hydroquinone (HQ 1 wt%) as radical quencher shown in Figure 28 together with data for **P5a** and **P6a**. These results indicate that the curing follows a radical reaction. The radicals may be formed by residual initiator or thermally. HQ is known to serve as polymerization inhibitor, able to prevent occurring radical crosslinking reactions.^[232, 233]

The results thus strongly suggest that the observed curing proceeds via a radical mechanism.

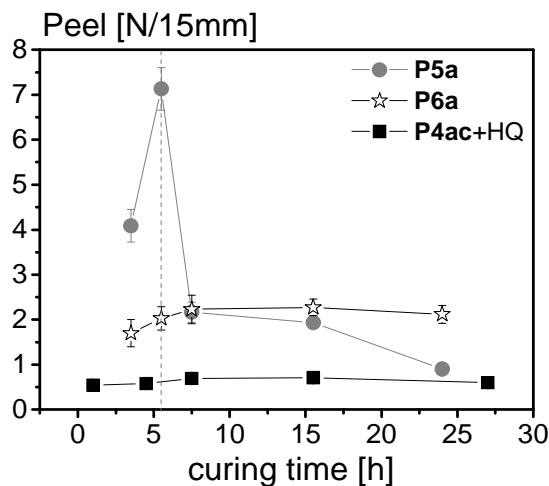


Figure 28. Peel strength of cured **P5a** ($M_w = 290$ kDa, $\bar{D} = 2.2$), cured **P6a** ($M_w = 250$ kDa, $\bar{D} = 3.5$) and a mixture of **P4ac+HQ** ($M_w = 550$ kDa, $\bar{D} = 5.1$).

While **P5a** exhibits a pronounced maximum similar to the one observed in tack experiments, the peel strength of **P6a** and **P4ac+HQ** remains on a low level independent of curing time and failure is always cohesive, indicating that crosslinking is suppressed.

3. Results and discussion

3.5 Adhesion to low energy substrates

Early studies on the adhesion of model PSAs to low energy surfaces date back to the 1970s.^[47] Recently, the interest in this topic reoccurred and in the majority of cases two types of substrates were investigated, namely stainless steel and polyolefins, such as PE.^[60, 234] Accordingly, the tack of the highly hydrophobic homopolymer **P4ac** as well as the copolymer p(**4ac**/MMA) on steel (surface energy $\gamma = 43 \text{ mJ/m}^2$) and PE ($\gamma = 30 \text{ mJ/m}^2$) substrates of similar roughness was investigated and compared to conventional petroleum-based PSAs. First, the linear viscoelastic properties of the investigated polymers are discussed. Figure 29 displays the storage modulus G' as a function of temperature for the investigated samples, namely a commercial acrylate copolymer from emulsion polymerization (Acronal V212) widely used in PSA applications, a linear p(BA/MA) copolymer synthesized in solution polymerization ($M_w = 192 \text{ kDa}$, $\bar{D} = 6.4$)^[60] and two homopolymers **P4ac** with $M_w = 280 \text{ kDa}$ and $\bar{D} = 3$ differing in curing time as well as a non-cured copolymer composed of **4ac** and methyl methacrylate (MMA) with a molar ratio of 80:20 ($M_w = 341 \text{ kDa}$, $\bar{D} = 2.0$).

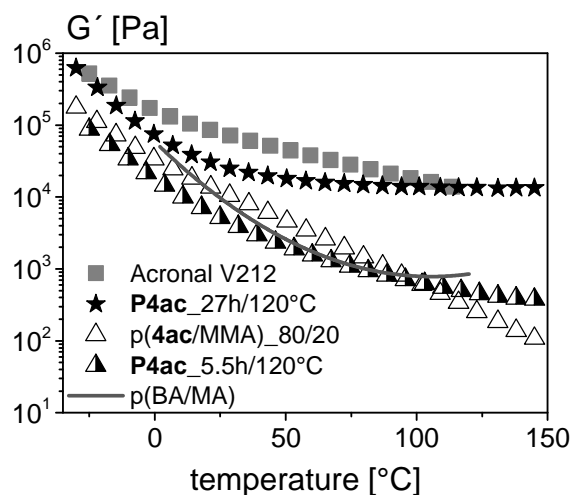


Figure 29. Storage modulus as a function of temperature at 1 Hz and 0.01 strain for a model copolymer dispersion Acronal V212 compared to a synthesized cured homopolymer **P4ac** ($M_w = 280 \text{ kDa}$, $\bar{D} = 3$) and a non-cured copolymer p(**4ac**-MMA) in a molar ratio of 80/20 ($M_w = 341 \text{ kDa}$, $\bar{D} = 2.0$). Values for p(BA/MA) calculated from $G'(\omega)$ data shown in Peykova et. al.^[85]

The cured **P4ac** polymers clearly exhibit a plateau in G' at temperatures $T > 100 \text{ }^\circ\text{C}$ as already mentioned. The sample cured for 27 hours shows absolute modulus values

close to that of Acronal V212 throughout the investigated temperature range. In contrast, the modulus of the non-crosslinked p(**4ac**/MMA) copolymer decreases monotonically with increasing temperature, but the absolute values are similar to that of **P4ac** homopolymer cured for 5.5 hours and are about two orders of magnitude lower than that of the Acronal V212 and the long cured **P4ac** in the high temperature range ($T > 100^\circ\text{C}$). The solution polymerized p(BA/MA) exhibits a temperature dependence similar to that of the non-cured p(**4ac**/MMA).

In order to get a first insight into the adhesive performance of hydrophobic plant-oil based PSAs on low energy substrates, the adhesion to a PE probe with a surface roughness of $R_a \approx 45$ nm and to a steel probe with similar roughness of $R_a = 41$ nm were compared. Figure 30 shows the ratio of the resulting work of adhesion W_{adh} values obtained on PE and steel for the samples described above. Tack data for the solution-based copolymer were taken from Peykova *et. al.*^[235] obtained at a debonding velocity of only 0.1 mm/s but otherwise similar test conditions. Adhesive failure was observed in all cases, except for the p(BA/MA).

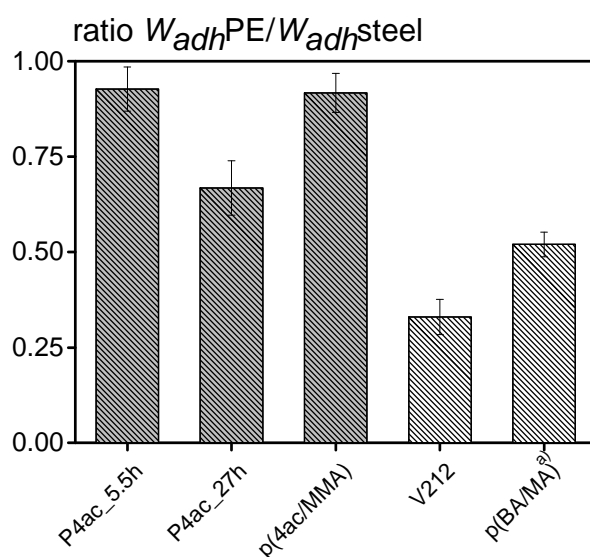


Figure 30. Ratio of W_{adh} measured on PE ($R_a \approx 45$ nm) and on steel ($R_a = 41$ nm) of a cured homopolymer **P4ac**_5.5h and **P4ac**_27h ($M_w = 690$ kDa, $\bar{D} = 4$) and a non-cured copolymer p(**4ac**/MMA) in a molar ratio of 80/20 ($M_w = 341$ kDa, $\bar{D} = 2.0$) compared to acrylate copolymer dispersion Acronal V212 and model solution-based copolymer p(BA/MA) ($M_w = 192$ kDa, $\bar{D} = 6.4$) at a debonding velocity of 1 mm/s. ^{a)}Tack data of copolymer p(BA/MA) taken from Peykova *et. al.*^[235] Note that respective measurements were performed at a debonding velocity of only 0.1 mm/s.

3. Results and discussion

Figure 30 clearly demonstrates that the reduction in W_{adh} on the surface PE compared to the steel probe is much less pronounced for the **P4ac** polymers than for the commercial acrylate adhesives from emulsion and solution polymerization. The p(BA/MA) exhibits at tack ratio of about 0.5 and for the Acronal V212 it is close to 0.3. The latter very low ratio may be attributed to the surfactants included in this emulsion polymer generally known to deteriorate adhesion. The weakly or not crosslinked hydrophobic **P4ac** and p(**4ac**/MMA) show tack ratios between 0.9 and 1.0, demonstrating their high potential for adhesion applications on low energy substrates. A tack ratio of about 2/3 is found for the densely crosslinked **P4ac**. This may be attributed to the poor wetting of the rough low energy substrate.

3.6 Water resistance

Performance of PSAs under conditions of high humidity or in an aqueous environment is another feature of significant technical relevance. In general, the adhesive properties of dispersion-based PSAs suffer from contact with water due to the presence of hydrophilic components, such as co-monomers or surfactants needed in the emulsion polymerization process. In order to get a first insight into the behavior of plant oil based PSAs from solution polymerization we have compared the loss of peel strength after immersion in water for 24 h for a commercial acrylate type office tape (tesa SE), the Acronal V212 from emulsion polymerization and two **P4ac** homopolymers differing in curing time. Corresponding data are shown in Figure 31.

Obviously, the reduction in peel strength is much less pronounced for the **P4ac** polymers than for the commercial acrylate adhesives; the latter lose more than 80 % of their original peel strength, while the **P4ac** retains about 3/4 of their initial strength even after 24 h storage in water. The strong loss in adhesion of the Acronal V212 comes along with a strong moisture-whitening, which itself is an important quality attribute, especially for consumer applications. In contrast, the **P4ac** polymers remain absolutely clear even after this extended immersion in water.

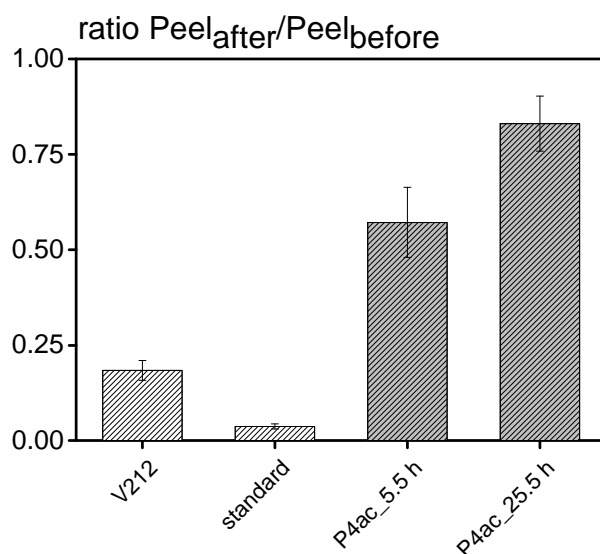


Figure 31. Remaining peel strength after 24 h water immersion of acrylate copolymer Acronal V212, a standard office tape (tesa SE product) and cured **P4ac** after 5.5 h and 25.5 h of curing time ($M_w = 480$ kDa, $\bar{D} = 4$).

3. Results and discussion

We attribute these findings to the pronounced hydrophobicity of the **4ac** monomer (solubility in water $< 10^{-7}$).^[190, 236] This is typical for monomers derived from plant oils and demonstrates the high potential of the thereof obtained PSAs for such generally challenging applications.

4. EXPERIMENTAL PART

4.1 Materials and methods

Methyl oleate (**1a**) as well as methyl erucate (**1b**) were synthesized according to a standard laboratory procedure^[237] (>90 %, respectively), hydrogen peroxide solution (35 %, Aldrich), Novozyme 435 (lipase acrylic resin from *candida antarctica*, Aldrich), methanol (99.9 % , Aldrich), ethanol (\geq 99.8 %, Aldrich), sulfuric acid (96 %, Acros Organics), acryloyl chloride (>97 %, Aldrich), triethylamine (99 %, Aldrich), sodium chloride (>99.5 %, Aldrich), sodium sulfate (99 %, Acros Organics), sodium bicarbonate (>99 %, Fisher Scientific), acrylic acid (99 %, Aldrich), hydroquinone (>99 %, Aldrich), *n*-bromosuccinimide (NBS) (99 %, Aldrich), potassium iodide (99 %, Aldrich), sodium thiosulfate (>99 %, Aldrich), sodium hydroxide (99 %, Aldrich), boron trifluoride diethyl etherate (>46.5 % Aldrich), 2,2'-azobis(2-methylpropionitril) (AIBN, >98 %, Aldrich), lithium hydroxide monohydrate (99.9 %, Aldrich), chloroform-d (99.8 atom-% D, Armar Chemicals). Solvents (technical grade) were used without further purification.

Moreover, unless otherwise noted, all reactions were carried out under argon atmosphere. The analytical techniques employed in the development of this thesis, together with the technical specifications of the equipment used are listed below:

Typical round bottom flasks of varying size were used for monomer synthesis, whereas the polymerization reactions were performed using a Radleys Carousel™ 6 Plus (Radleys Discovery Technologies, UK) equipped with 100 mL round bottom flasks.

Thin layer chromatography

TLC experiments were performed on silica gel coated aluminum foil (silica gel 60 F₂₅₄, Merck). Compounds were visualized by staining with Seebach-solution (mixture of phosphomolybdic acid hydrate, cerium-(IV)-sulfate, sulfuric acid and water).

4. Experimental part

Nuclear magnetic resonance

NMR spectra were recorded on a Bruker AVANCE DPX system at 300 MHz for ^1H NMR and 75 MHz for ^{13}C NMR. Chemical shifts (δ) are reported in parts per million relative to tetramethylsilane (TMS, $\delta = 0.00$ ppm) as internal standard. CDCl_3 was used as solvent and the resonance signal at 7.26 ppm (^1H) and 77.16 ppm (^{13}C) served as reference for δ .

Gas chromatography

GC-MS (EI) chromatograms were recorded using a Varian 431 GC instrument with a capillary column FactorFourTM VF-5ms (30 m \times 0.25 mm \times 0.25 μm) and a Varian 210 ion trap mass detector. Scans were performed from 40 to 650 m/z at rate of 1.0 scans \times s $^{-1}$. The oven temperature program was: initial temperature 95 $^\circ\text{C}$, hold for 1 min, ramp at 15 $^\circ\text{C}\times\text{min}^{-1}$ to 220 $^\circ\text{C}$, hold for 4 min, ramp at 15 $^\circ\text{C}\times\text{min}^{-1}$ to 300 $^\circ\text{C}$, hold for 2 min. The injector transfer line temperature was set to 250 $^\circ\text{C}$. Measurements were performed in the split-split mode (split ratio 50 : 1) using helium as carrier gas (flow rate 1.0 mL $\times\text{min}^{-1}$).

Gel permeation chromatography

Polymers were characterized *via* GPC measurements, using a LC-20AD (Shimadzu) system equipped with a SIL-20A autosampler and a RID-10A refractive index detector in THF (flow rate 1 mL/min) at 50 $^\circ\text{C}$ and with the following column system: main-column PSS SDV analytical (5 μm , 300 \times 8.00 mm, 10,000 Å) with a PSS SDV analytical pre-column (5 μm , 50 \times 8.0 mm). Determination was carried out relative to PMMA standards (Polymer Standards Service) ranging from 1.1 to 981 kDa.

Differential scanning calorimetry

Glass transition temperatures (T_g) were determined *via* differential scanning calorimetry (DSC) using a Mettler Toledo DSC821e calorimeter in the range of -75 $^\circ\text{C}$ to 250 $^\circ\text{C}$ under a nitrogen atmosphere and a heating rate of 10 K $\times\text{min}^{-1}$. Sample mass was in the range of 6-10 mg.

Dynamic light scattering

Particle size (d_{DLS}) was obtained using a dynamic light scattering (DLS) instrument (Malvern Instruments, Zeta Sizer Nano S) with a scattering angle of 176.1° . The reported diameter is an intensity-weighted average particle size (z-average), comprised of 5 measurements analyzed in 10 runs. The reported polydispersity index values (PD_{DLS}) are those given by the instrument and are not conventional PDI values. These PD_{DLS} values are referred to as Malvern polydispersity. A value close to 0.01 indicates a narrow distribution. The latex samples were diluted approximately 1 : 15 with distilled water prior to DLS analysis.

Tack measurement

The experimental set-up used for the tack measurements has been thoroughly described previously.^[85] It was based on a commercial device Texture Analyzer TA.XTplus (Stable Micro Systems, UK) modified with a quartz force sensor (Kistler Instrumente GmbH, Germany) covering a force range of ± 500 N with a threshold of 1 mN. Probe tack tests were performed at 21 °C. The Texture Analyzer TA.XTplus was also equipped with a high-speed camera KL MB-Kit 1M1 (Mikrotron GmbH, Germany) used in combination with a zoom objective 90° KL-Z6 and a cold light source KL3000B. The camera was attached under an adjustable vacuum table, where a transparent glass plate with the coated sample was positioned in order to take images of the contact area during contact formation and debonding. The camera allowed to record 124 frames/s at maximum resolution of 1280x1024 pixels. The true contact area was obtained in each test by analyzing the images using Visiometrics Image Processing System (IPS) software, developed by Prof. Dr. Stephan Naser (University Darmstadt). Tack tests were performed at 21 °C using three different cylindrical punch substrates, steel probes with average roughness $R_a = 3$ nm and 41 nm as well as a polyethylene (PE) probe with $R_a \approx 45$ nm. The probe velocity for bonding was set to 1 mm/s, a contact force of 10 N was selected and a contact time of 1.0 s was chosen. Detachment followed at a release rate of 1.0 mm/s. The work of adhesion W_{adh} , often also termed tack, was calculated using the area under the nominal stress vs. strain curve as described by Peykova et. al..^[85]

4. Experimental part

Peel measurement

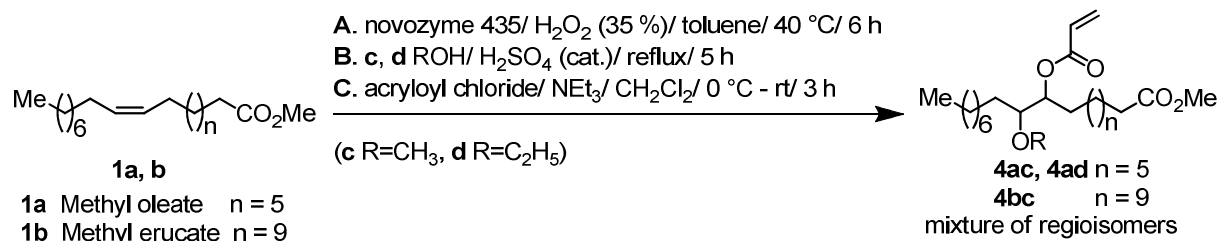
For peel tests a 90° peel device (FINAT No. 2) was used in combination with the TA.XTplus Analyzer. In each test, a 15 mm wide carrier foil (coated with the given polymer) was peeled at a constant speed of 4.0 mm·s⁻¹ from a fixed glass plate at an angle of 90°. The peel force was determined as the average force value obtained during a debonding length of 80 mm.

Oscillatory measurements

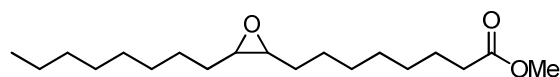
Storage and loss moduli (G' , G'') were determined using a Physica MCR-501 (Anton Paar, Austria, Graz) equipped with a plate/plate fixture (diameter $d = 8.0$ mm, gap height $h = 1$ mm). Moduli were measured at a given frequency of 1.0 Hz and a deformation of $\gamma = 0.01$ at temperatures ranging from -30 °C to 150 °C with a heating rate of 5 K/min.

4.2 Monomer synthesis

4.2.1 Monomer synthesis in a three-step procedure (A, B, C)

Scheme 1. Synthesis pathway in three steps towards monomer **4ac**, **4ad** and **4bc**.

Synthesis of methyl 9, 10-epoxy octanoate (procedure A)

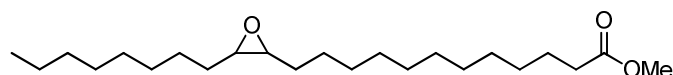


40 g of fatty acid methyl ester **1a** (1.00 eq, 135 mmol) was dissolved in 120 mL toluene, and subsequently 0.80 g Novozyme 435 was added. Then, 40 mL hydrogen peroxide solution (35 %) was added dropwise to the stirred mixture. After two hours reaction time at 40 °C, again 20 mL hydrogen peroxide solution (35 %) was added. The reaction process was monitored by TLC until complete formation of the epoxidized fatty acid methyl ester was indicated. After filtration, the organic layer was separated, washed several times with water and brine, dried over Na_2SO_4 and evaporated to dryness, to obtain the methyl 9, 10-epoxy oleate **2a** as a colorless wax in quantitative yields (41.8 g, 99 %). TLC (*n*-hexane / ethyl acetate 5 : 1) $R_f = 0.54$. ^1H NMR (CDCl_3 , 300 MHz) $\delta = 0.88$ (t, $J = 6.7$ Hz, 3 H, CH_3), 1.22 – 1.50 (m, 24 H, 12 CH_2), 1.50 – 1.62 (m, 2 H, CH_2), 2.21 – 2.31 (m, 2 H, CH_2CO), 2.81 – 2.93 (m, 2 H, 2 CH), 3.62 (s, 3 H, COOCH_3) ppm. ^{13}C NMR (CDCl_3 , 75 MHz) $\delta = 14.02$ (CH_3), 22.60 (CH_2), 24.84 (CH_2), 26.50 (CH_2), 26.54 (CH_2), 27.72 (CH_2), 27.76 (CH_2), 28.98 (CH_2), 29.11 (CH_2), 29.16 (CH_2), 29.27 (CH_2), 29.47 (CH_2), 29.49 (CH_2), 31.80 (CH_2), 34.01 (CH_2), 51.37 (OCH_3), 57.17 (CH), 57.22 (CH), 174.22 (CO) ppm. GC-MS of $\text{C}_{19}\text{H}_{36}\text{O}_3$

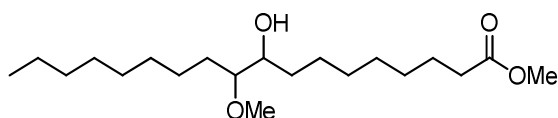
4. Experimental part

($M^+ = 313.3$, $M\text{-MeO}^+ = 280.3$). FAB of $C_{19}H_{36}O_3$ ($M+H^+ = 313.27$). HRMS (FAB) of $C_{19}H_{36}O_3$ $[M+H]^+$ calc. 313.2743 found 313.2722.

Synthesis of methyl 13, 14-epoxy dodecanoate



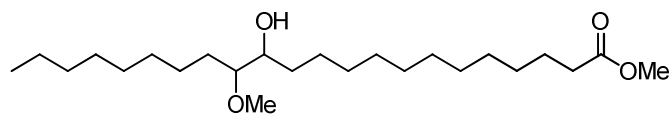
Following procedure **A** 40 g of the fatty acid methyl ester **1b** ($n = 9$) (1 eq, 109 mmol) were used to obtain the epoxide of methyl erucate **2b** as a colorless wax in almost quantitative yields (38.7 g, 96%). TLC (*n*-hexane / ethyl acetate 5 : 1) $R_f = 0.59$. 1H NMR ($CDCl_3$, 300 MHz) $\delta = 0.88$ (t, $J = 6.6$ Hz, 3 H, CH_3), 1.20 – 1.54 (m, 32 H, 16 CH_2), 1.56 – 1.68 (m, 2 H, CH_2), 2.20 – 2.37 (m, 2 H, CH_2), 2.86 – 2.94 (m, 2 H, 2 CH), 3.65 (s, 3 H, CH_3) ppm. ^{13}C NMR ($CDCl_3$, 75 MHz) $\delta = 14.02$ (CH_3), 22.60 (CH_2), 24.59 (CH_2), 24.69 (CH_2), 24.89 (CH_2), 24.92 (CH_2), 26.55 (CH_2), 27.76 (CH_2), 28.89 (CH_2), 29.00 (CH_2), 29.09 (CH_2), 29.17 (CH_2), 29.19 (CH_2), 29.38 (CH_2), 29.45 (CH_2), 29.47 (CH_2), 29.48 (CH_2), 31.80 (CH_2), 34.05 (CH_2), 51.34 (OCH_3), 57.20 (CH), 57.22 (CH), 174.25 ($COOCH_3$) ppm. GC-MS of $C_{23}H_{44}O_3$ ($M\text{-MeO}^+ = 336.3$). FAB of $C_{23}H_{44}O_3$ ($M+H^+ = 369.33$, $M+Na^+ = 391.32$). HRMS (FAB) of $C_{23}H_{44}O_3$ $[M+H]^+$ calc. 369.3369 found 369.3338.

Synthesis of 9(or 10)-hydroxy-10(or 9)-methoxy octadecanoate (procedure B)

40 g of **2a** (1.00 eq, 128 mmol) was dissolved in methanol (~30 eq, 125 mL) and concentrated sulfuric acid was added drop wise (~150 drops 3.75 mL). The reaction mixture was refluxed for five hours and then cooled to room temperature. After neutralization with NaHCO₃ and filtration, the solution was evaporated to dryness. The residue was diluted with 150 mL ethyl acetate and 100 mL distilled water. The organic layer was separated, washed several times with water and brine, dried over Na₂SO₄ and evaporated to dryness, to receive the crude product as a yellowish mixture. After purification by column chromatography (*n*-hexane / ethyl acetate 9 : 1 to 5 : 1), methyl 9(or 10)-hydroxy-10(or 9)-methoxy octadecanoate **3ac** was obtained as a colorless oil (30.9 g, 70%). TLC (*n*-hexane / ethyl acetate 5 : 1) *R*_f = 0.43. ¹H NMR (CDCl₃, 300 MHz, mixture of regioisomers) δ = 0.87 (t, *J* = 6.5 Hz, 3 H, CH₃), 1.19 – 1.71 (m, 27 H, OH, 13 CH₂), 2.30 (t, *J* = 7.5 Hz, 2 H, CH₂CO), 2.98 (q, *J* = 5.5 Hz, 1 H, CH), 3.37 – 3.53 (m, 1 H, CH), 3.40 (s, 3 H, CH₃), 3.66 (s, 3 H, COOCH₃) ppm. ¹³C NMR (CDCl₃, 75 MHz, mixture of regioisomers) δ = 14.17 (CH₃), 22.74 (CH₂), 24.79 (CH₂), 24.94 (CH₂), 24.95 (CH₂), 25.84 (CH₂), 28.99 (CH₂), 29.15 (CH₂), 29.18 (CH₂), 29.27 (CH₂), 29.43 (CH₂), 29.45 (CH₂), 29.49 (CH₂), 29.65 (CH₂), 29.68 (CH₂), 29.79 (CH₂), 29.80 (CH₂), 29.90 (CH₂), 31.79 (CH₂), 31.80 (CH₂), 33.24 (CH₂), 33.39 (CH₂), 34.14 (CH₂), 51.50 (CH₃OO), 58.19 (OCH₃), 72.66 (CHOH), 84.40 (CHOCH₃), 174.36, 174.33 (COOCH₃) ppm. FAB of C₂₀H₄₀O₄ (M+H⁺ = 345.3, M+Na⁺ = 367.3, M-OH⁺ = 327.4). HRMS (FAB) of C₂₀H₄₀O₄ [M+H]⁺ calc. 345.3005 found 345.3003.

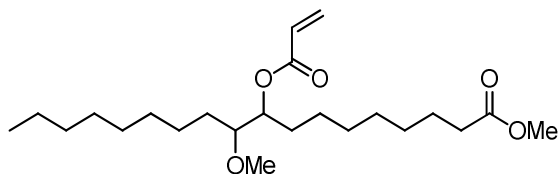
4. Experimental part

Synthesis of methyl 13(or 14)-hydroxy-14(or 13)-methoxy docosanoate



Following procedure **B**, 40 g of **2b** (1 eq, 116 mmol) was used to synthesize the methyl 13(or 14)-hydroxy-14(or 13)-methoxy docosanoate **3bc**, which was obtained after column chromatography as a colorless oil in a yield of 29.8 g (64%). TLC (*n*-hexane / ethyl acetate 5 : 1) $R_f = 0.51$. ^1H NMR (CDCl_3 , 300 MHz, mixture of regioisomers) $\delta = 0.88$ (t, $J = 6.5$ Hz, 3 H, CH_3), 1.19 – 1.70 (m, 34 H, 17 CH_2), 2.30 (t, $J = 7.5$ Hz, 2 H, CH_2), 2.99 (q, $J = 5.5$ Hz, 1 H, CH), 3.38 – 3.53 (m, 1 H, CH), 3.41 (s, 3 H, CH_3), 3.66 (s, 3 H, CH_3) ppm. ^{13}C NMR (CDCl_3 , 75 MHz, mixture of regioisomers) $\delta = 14.02$ (CH_3), 22.58 (CH_2), 22.60 (CH_2), 24.88 (CH_2), 24.97 (CH_2), 25.69 (CH_2), 29.07 (CH_2), 29.18 (CH_2), 29.20 (CH_2), 29.22 (CH_2), 29.35 (CH_2), 29.36 (CH_2), 29.49 (CH_2), 29.50 (CH_2), 29.52 (CH_2), 29.67 (CH_2), 29.82 (CH_2), 29.90 (CH_2), 31.80 (CH_2), 31.82 (CH_2), 33.30 (CH_2), 34.02 (CH_2), 51.33 (CH_3OOC), 58.00, 58.02 (OCH_3), 72.54 (CHOH), 84.24 (CHOCH_3), 174.23 (COOCH_3) ppm. FAB of $\text{C}_{24}\text{H}_{48}\text{O}_4$ ($\text{M}+\text{H}^+ = 401.3$; $\text{M}+\text{Na}^+ = 423.3$, $\text{M}-\text{OH}^+ = 383.3$; $\text{M}-\text{OMe}^+ = 369.3$). HRMS (FAB) of $\text{C}_{24}\text{H}_{48}\text{O}_4$ [$\text{M}+\text{H}$] $^+$ calc. 401.3631 found 401.3633.

Synthesis of methyl 9(or 10)-acryloyloxy-10(or 9)-methoxy octadecanoate (procedure C)

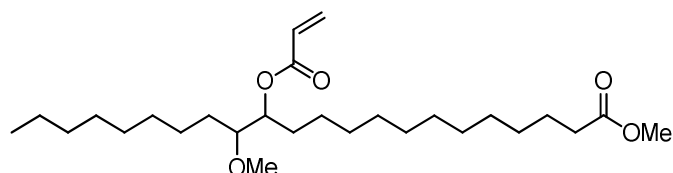


30 g of 9(or 10)-hydroxy-10(or 9)-methoxy octadecanoate **3ac** (1.00 eq, 87.0 mmol) was dissolved in 100 mL dichloromethane and cooled down with an ice bath to 0 °C. Acryloyl chloride (2.00 eq, 174 mmol, 17.5 mL) was added to the stirred solution. Then triethyl amine (6.00 eq, 522 mmol, 72.8 mL) was added slowly and drop wise during one hour. The reaction progress was monitored by TLC. After three to four hours the volatiles were removed under reduced pressure and the residue was dissolved in ethyl acetate and water. The organic layer was separated, washed with water and brine, dried over Na₂SO₄ and evaporated to dryness, which led to a dark orange colored oil. The crude product was purified by silica column chromatography (*n*-hexane / ethyl acetate from 10 : 1 to 5 : 1) to obtain methyl 9(or 10)-acryloyloxy-10(or 9)-methoxy octadecanoate **4ac** as a colorless oil (25 g, 72 %, >48 % in three steps). TLC (*n*-hexane / ethyl acetate 5 : 1) *R*_f = 0.68. ¹H NMR (CDCl₃, 300 MHz, mixture of regioisomers) δ = 0.87 (t, *J* = 6.7 Hz, 3 H, CH₃), 1.18 – 1.52 (m, 22 H, 11 CH₂), 1.54 – 1.69 (m, 4 H, 2 CH₂), 2.29 (t, *J* = 7.5 Hz, 2 H, COCH₂), 3.13 – 3.24 (m, 1 H, CH), 3.42 (s, 3 H, CH₃), 3.66 (s, 3 H, COOCH₃), 5.01 – 5.09 (m, 1 H, CH), 5.82 (dd, *J* = 10.4, 1.5 Hz, 1 H, =CH₂^a), 6.15 (dd, *J* = 17.4, 10.2 Hz, 1 H, COCH), 6.41 (dd, *J* = 17.4, 1.50 Hz, 1 H, =CH₂^b) ppm. ¹³C NMR (CDCl₃, 75 MHz, mixture of regioisomers) δ = 14.01 (CH₃), 24.81 (CH₂), 24.83 (CH₂), 25.53 (CH₂), 25.55 (CH₂), 25.58 (CH₂), 25.60 (CH₂), 28.95 (CH₂), 28.97 (CH₂), 29.00 (CH₂), 29.05 (CH₂), 29.14 (CH₂), 29.16 (CH₂), 29.23 (CH₂), 29.35 (CH₂), 29.41(CH₂), 29.43 (CH₂), 29.45 (CH₂), 29.53 (CH₂), 29.55 (CH₂), 29.66 (CH₂), 29.79 (CH₂), 29.82 (CH₂), 31.76 (CH₂), 31.78 (CH₂), 33.98 (CH₂), 51.34 (OOCH₃), 58.49 (OCH₃), 74.34 (CH_{acrylate}), 81.50, 81.52 (CHOCH₃), 128.56 (CH=CH₂), 130.62 (CH₂=CH), 165.91 (CO_{acrylate}), 174.16, 174.18 (COOCH₃) ppm. GC-MS of C₂₃H₄₂O₅ (M⁺ = 399.2). FAB of C₂₃H₄₂O₅ (M+H⁺ = 399.3,

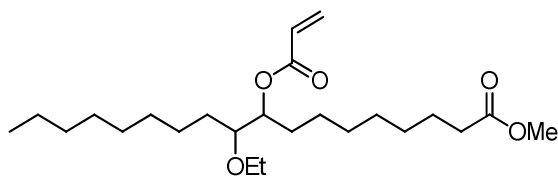
4. Experimental part

M-OMe⁺ = 367.3, M-AcrylCO₂⁺ = 327.3). HRMS (FAB) of C₂₃H₄₂O₅ [M+H]⁺ calc. 399.3105 found 399.3107.

Synthesis of methyl 13(or 14)-acryloyloxy-14(or 13)-methoxy docosanoate



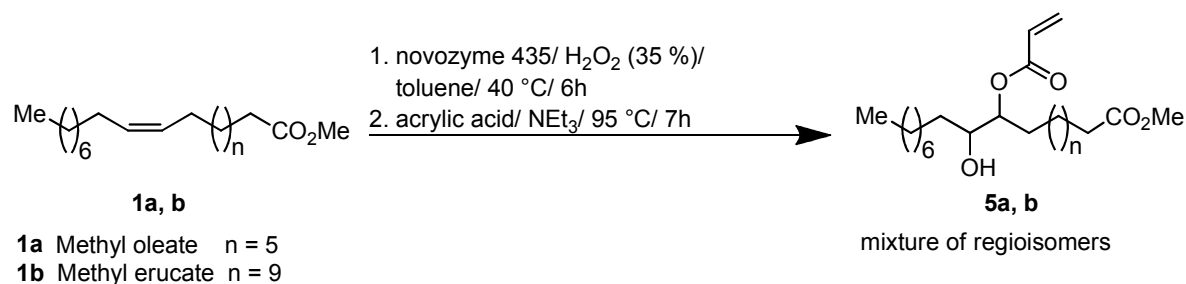
Following procedure **C**, 27 g of **3bc** was used to obtain 21 g of the product **4bc** after column chromatography as a colorless oil (70 %, >44 % in three steps). TLC (*n*-hexane / ethyl acetate 5 : 1) *R*_f = 0.63. ¹H NMR (CDCl₃, 300 MHz, mixture of regioisomers) δ = 0.87 (t, *J* = 6.7 Hz, 3 H, CH₃), 1.16 – 1.51 (m, 30 H, 15 CH₂), 1.54 – 1.70 (m, 4 H, 2 CH₂), 2.29 (t, *J* = 7.5 Hz, 2 H, CH₂), 3.13 – 3.24 (m, 1 H, CH), 3.42 (s, 3 H, CH₃), 3.66 (s, 3 H, CH₃), 5.02 – 5.09 (m, 1 H, CH), 5.82 (dd, *J* = 10.4, 1.5 Hz, 1 H, CH), 6.15 (dd, *J* = 17.4, 10.4 Hz, 1 H, CH), 6.41 (dd, *J* = 17.4, 1.50 Hz, 1 H, CH) ppm. ¹³C NMR (CDCl₃, 100 MHz, mixture of regioisomers) δ = 14.03 (CH₃), 24.88 (CH₂), 25.61 (CH₂), 25.62 (CH₂), 28.89 (CH₂), 29.08 (CH₂), 29.16 (CH₂), 29.18 (CH₂), 29.36 (CH₂), 29.39 (CH₂), 29.42 (CH₂), 29.44 (CH₂), 29.47 (CH₂), 29.58 (CH₂), 29.68 (CH₂), 29.84 (CH₂), 31.78 (CH₂), 31.79 (CH₂), 34.03 (CH₂), 51.34 (COOCH₃), 58.51 (OCH₃), 74.39 (CHAcrylate), 81.53 (CHOCH₃), 128.61 (CHCH₂), 130.55 (CH₂CH), 165.89 (COAcrylate), 174.18 (COOCH₃) ppm. FAB of C₂₇H₅₀O₅ (M+H⁺ = 455.4; M-OMe⁺ = 423.4; M-AcrylCO₂⁺ = 383.4). HRMS (FAB) of C₂₇H₅₀O₅ [M+H]⁺ calc. 455.3731 found 455.3730.

Synthesis of methyl 9(or 10)-acryloyloxy-10(or 9)-ethoxy octadecanoate

With the epoxide **2a** in hand, procedure **B** was performed as described above, using ethanol (30 eq) to finally receive the ethoxy octadecanoate derivative **3ad**. The acrylation was proceeded described within procedure **C**. The crude mixture was purified by column chromatography to obtain the pure product. The methyl 9(or 10)-acryloyloxy-10(or 9)-ethoxy octadecanoate **4ad** was obtained as a colorless oil (>42 % in three steps). TLC (*n*-hexane / ethyl acetate 5 : 1) $R_f = 0.67$. ^1H NMR (CDCl_3 , 300 MHz, mixture of regioisomers) $\delta = 0.85$ (t, $J = 6.5$ Hz, 3 H, CH_3), 1.06 – 1.69 (m, 29 H, 13 CH_2 , 1 CH_3), 2.23 (t, $J = 7.4$ Hz, 2 H, CH_2), 3.13 – 3.24 (m, 1 H, CH), 3.40 – 3.55 (m, 2 H, CH_2), 4.05 (s, 3 H, CH_3), 4.98 – 5.10 (m, 1 H, CH), 5.80 (dd, $J = 10.3, 1.5$ Hz, 1 H, CH), 6.11 (dd, $J = 17.5, 10.3$ Hz, 1 H, CH), 6.34 (dd, $J = 17.5, 1.50$ Hz, 1 H, CH) ppm. ^{13}C NMR (CDCl_3 , 75 MHz, mixture of regioisomers) $\delta = 14.02$ (CH_3), 15.53 ($\text{CH}_3\text{CH}_2\text{O}$), 22.83 (CH_2), 25.53 (CH_2), 25.55 (CH_2), 25.58 (CH_2), 28.95 (CH_2), 28.97 (CH_2), 29.00 (CH_2), 29.45 (CH_2), 29.55 (CH_2), 30.56 (CH_2), 30.69 (CH_2), 31.76 (CH_2), 31.68 (CH_2), 33.59 (CH_2), 51.74 (COOCH_3), 64.32 (OCH_2CH_3), 76.78 (CHacrylate), 81.43 ($\text{CHOCH}_2\text{CH}_3$), 128.73 (CHCH_2), 130.61 (CH_2CH), 165.21 (COacrylate), 174.38 (COOCH_3) ppm. FAB of $\text{C}_{24}\text{H}_{44}\text{O}_5$ ($\text{M}+\text{H}^+ = 413.3$, $\text{M}+\text{Na}^+ = 435.3$, $\text{M}-\text{AcrylCO}_2^+ = 341.3$). HRMS (FAB) of $\text{C}_{24}\text{H}_{44}\text{O}_5$ [$\text{M}+\text{H}$] $^+$ calc. 413.3176 found 413.3180.

4. Experimental part

4.2.2 Monomer synthesis in a two-step procedure (procedure **A**, **D**)

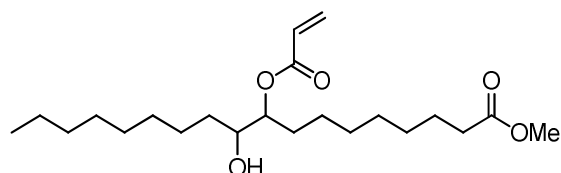


Scheme 2. Synthesis pathway in two steps leading to monomer **5a** and **5b**.

Synthesis of methyl 9, 10-epoxy oleate

Following procedure **A** the epoxide was obtained as described before.

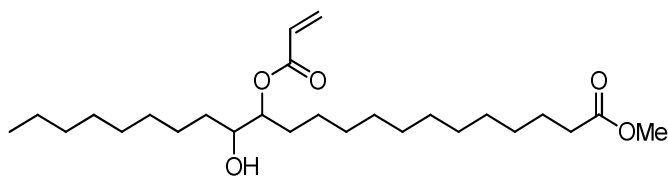
Synthesis of methyl 9(or 10)-acryloyloxy-10(or 9)-hydroxy octadecanoate (procedure **D**)



In the first step, the epoxide **2a** was obtained following procedure **A**. 10 g of epoxide **2a** (1.00 eq, 32.0 mmol) was mixed with 2.00 eq acrylic acid (64.0 mmol, 4.39 mL) and 1.00 eq triethylamine (32.0 mmol, 4.43 mL). Subsequently, the reaction mixture was purged with argon for 10 min. The reaction mixture was heated to 90 °C for seven hours. After cooling to room temperature, the solution was quenched with an excess of a water / ethyl acetate mixture. The organic layer was separated and washed several times with water, NaHCO₃ solution and brine. After drying over Na₂SO₄ the organic layer was evaporated to dryness. The crude mixture was purified by column chromatography (*n*-hexane / ethyl acetate 30 : 1 to 4 : 1) to obtain the pure product methyl 9(or 10)-acryloyloxy-10(or 9)-hydroxy octadecanoate **5a** as a colorless oil (7.80 g, 64 %). TLC (*n*-hexane / ethyl acetate 5 : 1) *R*_f = 0.55; ¹H NMR (CDCl₃, 300 MHz, mixture of regioisomers) δ = 0.86 (t, *J* = 6.1 Hz, 3 H, CH₃), 1.17 – 1.52 (m, 22 H,

11 CH₂), 1.53 – 1.75 (m, 5 H, OH, 2 CH₂), 2.27 (t, $J = 7.5$ Hz, 2 H, CH₂CO), 3.57 – 3.64 (m, 1 H, CH), 3.65 (s, 3 H, COOCH₃), 4.85 – 4.95 (m, 1 H, CH), 5.85 (dd, $J = 10.3$, 1.4 Hz, 1 H, =CH₂^a), 6.12 (dd, $J = 17.3$, 10.4 Hz, 1 H, COCH), 6.40 (dd, $J = 17.3$, 1.4 Hz, 1 H, =CH₂^b) ppm; ¹³C NMR (CDCl₃, 75 MHz, mixture of regioisomers) $\delta = 14.05$ (CH₃), 22.61 (CH₂), 22.63 (CH₂), 24.84 (CH₂), 24.90 (CH₂), 25.49 (CH₂), 25.57 (CH₂), 27.11 (CH₂), 27.17 (CH₂), 29.21 (CH₂), 29.28 (CH₂), 29.39 (CH₂), 29.48 (CH₂), 29.64 (CH₂), 29.72 (CH₂), 30.60 (CH₂), 31.82 (CH₂), 31.86 (CH₂), 34.01 (CH₂), 34.05 (CH₂), 51.39 (OOCH₃), 72.58 (COH), 76.80 (CH_{acrylate}), 128.40 (CH=CH₂), 130.97 (CH₂=CH), 166.13 (CO_{acrylate}), 174.27 (COOCH₃) ppm; FAB of C₂₂H₄₀O₅ (M+H⁺ = 385.3, M+Na⁺ = 407.3, M-AcrylCO₂⁺ = 313.3); HRMS (FAB) of C₂₂H₄₀O₅ [M+H]⁺ calc. 385.2876 found 385.2874.

Synthesis of methyl 13(or 14)-acryloyloxy-14(or 13)-hydroxy docosanoate

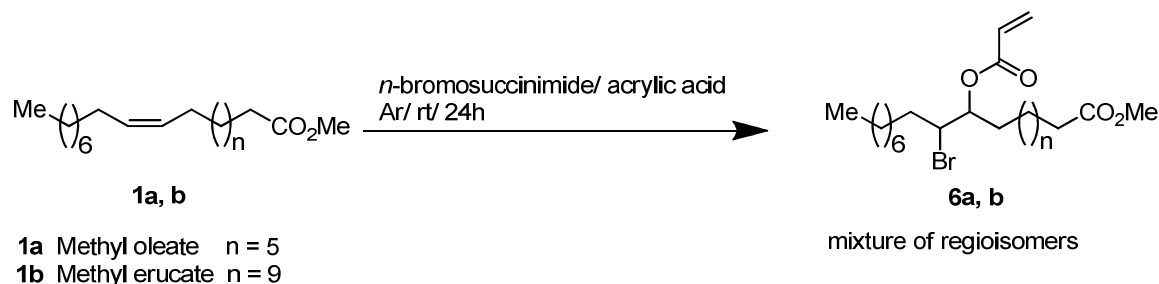


Following procedure **A** and **D** the erucate derivative **5b** was obtained as a light yellowish oil in a yield of 60 %. TLC (*n*-hexane / ethyl acetate 5 : 1) $R_f = 0.56$; ¹H NMR (CDCl₃, 300 MHz, mixture of regioisomers) $\delta = 0.80$ (t, $J = 6.07$ Hz, 3 H, CH₃), 1.14 – 1.49 (m, 30 H, 15 CH₂), 1.50 – 1.71 (m, 5 H, OH, 2 CH₂), 2.21 (t, $J = 7.50$ Hz, 2 H, CH₂), 3.52 – 3.64 (m, 1 H, CH), 3.64 (s, 3 H, CH₃), 4.85 – 4.95 (m, 1 H, CH), 5.83 (dd, $J = 10.30$, 1.40 Hz, 1 H, CH), 6.07 (dd, $J = 17.30$, 10.40 Hz, 1 H, CH), 6.38 (dd, $J = 17.30$, 1.40 Hz, 1 H, CH) ppm. ¹³C NMR (CDCl₃, 75 MHz, mixture of regioisomers) $\delta = 14.05$ (CH₃), 22.61 (CH₂), 22.63 (CH₂), 24.84 (CH₂), 24.90 (CH₂), 25.28 (CH₂), 25.36 (CH₂), 25.49 (CH₂), 25.57 (CH₂), 27.11 (CH₂), 27.17 (CH₂), 29.21 (CH₂), 29.28 (CH₂), 29.39 (CH₂), 29.48 (CH₂), 29.64 (CH₂), 29.72 (CH₂), 30.56 (CH₂), 30.60 (CH₂), 31.82 (CH₂), 31.86 (CH₂), 34.01 (CH₂), 34.05 (CH₂), 51.39 (COOCH₃), 72.48 (COH), 76.80 (CH_{acrylate}), 128.40 (CHCH₂), 130.97 (CH₂CH), 166.13 (CO_{acrylate}), 174.26, 174.30 (COOCH₃) ppm. FAB of

4. Experimental part

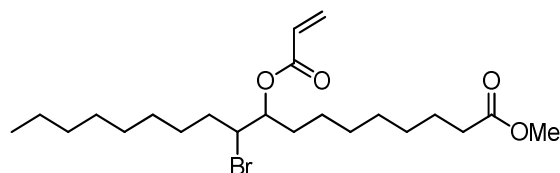
$C_{26}H_{48}O_5$ ($M+H^+ = 441.4$, $M+Na^+ = 463.4$, $M-AcrylCO_2^+ = 369.4$). HRMS (FAB) of $C_{26}H_{48}O_5$ $[M+H]^+$ calc. 441.3502 found 441.3503.

4.2.3 One-step synthesis pathway (procedure E)



Scheme 3. Synthesis pathway in one step towards monomer **6a** and **6b**.

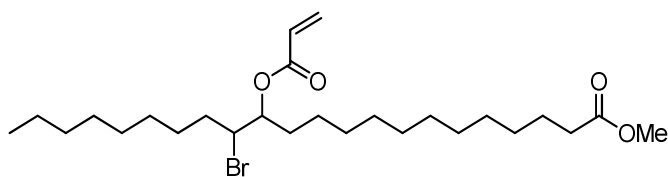
Synthesis of methyl 9(or 10)-acryloyloxy-10(or 9)-bromo octadecanoate (procedure E)



In an argon purged flask, 10 g of the fatty acid methyl ester **1a** (1.00 eq, 34.0 mmol) was mixed with 10.0 eq acrylic acid (340 mmol, 23.3 mL) and 1.80 eq *n*-bromosuccinimide (61.2 mmol, 10.9 mL). The reaction mixture was stirred for two days protected from light at room temperature. The reaction mixture was quenched by an excess amount of diethyl ether and H_2O (1 : 1). The ether layer was separated, washed several times with KI solution, sodium thiosulfate solution, an aqueous NaOH (10 %) solution, and with water and brine before it was dried over Na_2SO_4 and evaporated to dryness. Purification by silica column chromatography provided **6a** as yellowish oil (9.98 g, 66 %). TLC (*n*-hexane / ethyl acetate 5 : 1) $R_f = 0.62$; 1H NMR ($CDCl_3$, 300 MHz, mixture of regioisomers) $\delta = 0.82$ (t, $J = 6.6$ Hz, 3 H, CH_3), 1.17 –

1.52 (m, 22 H, 11 CH₂), 1.53–1.72 (m, 4 H, 2 CH₂), 2.25 (t, $J = 7.5$ Hz, 2 H, CH₂CO), 3.66 (s, 3 H, COOCH₃), 3.98 – 4.05 (m, 1 H, CH), 4.95 – 5.04 (m, 1 H, CH), 5.85 (dd, $J = 10.3, 2.4$ Hz, 1 H, =CH₂^a), 6.09 (dd, $J = 17.3, 10.3$ Hz, 1 H, COCH), 6.37 (dd, $J = 17.3, 1.6$ Hz, 1 H, =CH₂^b) ppm. ¹³C NMR (CDCl₃, 75 MHz, mixture of regioisomers) $\delta = 14.08$ (CH₃), 22.62 (CH₂), 24.84 (CH₂), 25.22 (CH₂), 25.29 (CH₂), 27.60 (CH₂), 27.66 (CH₂), 28.68 (CH₂), 28.96 (CH₂), 29.16 (CH₂), 29.30 (CH₂), 31.79 (CH₂), 32.20 (CH₂), 34.00 (CH₂), 35.01 (CH₂), 51.41 (COOCH₃), 57.54 (CBr), 75.14 (CH_{acrylate}), 128.18 (CHCH₂), 131.36 (CH₂CH), 165.51 (CO_{acrylate}), 174.18 (COOCH₃) ppm. FAB of C₂₂H₃₉BrO₄ (M+H⁺ = 446.3, M-AcrylCO₂⁺ = 375.3). HRMS (FAB) of C₂₂H₃₉BrO₄ [M+H]⁺ calc. 446.2730 found 446.2729.

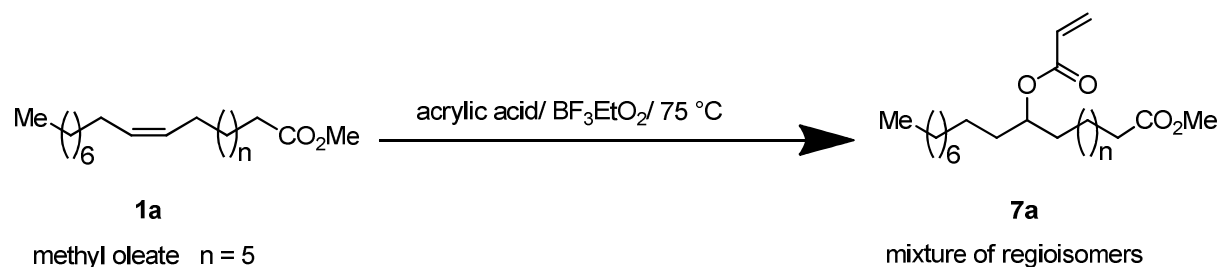
Synthesis of methyl 13(or 14)-acryloyloxy-14(or 13)-bromo docosanoate



Using **1b** and following procedure E the product **6b** was obtained after column chromatography in a yield of 57 % TLC (*n*-hexane / ethyl acetate 5 : 1) $R_f = 0.65$; ¹H NMR (CDCl₃, 300 MHz, mixture of regioisomers) $\delta = 0.85$ (t, $J = 6.60$ Hz, 3 H, CH₃), 1.15 – 1.42 (m, 30 H, 15 CH₂), 1.43–1.67 (m, 2 H, CH₂), 1.68 - 1.81 (m, 2 H, CH₂), 2.28 (t, $J = 7.50$ Hz, 2 H, CH₂), 3.61 (s, 3 H, CH₃), 3.99 – 4.09 (m, 1 H, CH), 4.97 – 5.08 (m, 1 H, CH), 5.85 (dd, $J = 10.3, 2.4$ Hz, 1 H, =CH₂^a), 6.09 (dd, $J = 17.3, 10.3$ Hz, 1 H, COCH), 6.37 (dd, $J = 17.3, 1.6$ Hz, 1 H, =CH₂^b) ppm. ¹³C NMR (CDCl₃, 75 MHz, mixture of regioisomers) $\delta = 14.07$ (CH₃), 22.62 (CH₂), 24.93 (CH₂), 25.29 (CH₂), 26.88 (CH₂), 27.28 (CH₂), 27.64 (CH₂), 27.78 (CH₂), 28.87 (CH₂), 29.10 (CH₂), 29.14 (CH₂), 29.30 (CH₂), 29.36 (CH₂), 29.46 (CH₂), 29.66 (CH₂), 31.78 (CH₂), 32.19 (CH₂), 34.05 (CH₂), 35.03 (CH₂), 51.33 (COOCH₃), 57.62 (CBr), 75.17 (CH_{acrylate}), 128.22 (CHCH₂), 131.30 (CH₂CH), 165.52 (CO_{acrylate}), 174.18 (COOCH₃) ppm. FAB of C₂₆H₄₇BrO₄ (M+H⁺ = 503.3, M-AcrylCO₂⁺ = 431.3). HRMS (FAB) of C₂₆H₄₈BrO₄ [M+H]⁺ calc. 503.2730 found 503.2734.

4. Experimental part

Synthesis of methyl 9(or 10)-acryloyloxy octadecanoate



Scheme 4. Synthesis pathway in one step towards monomer **7a**.

In an argon purged flask, 1 g of the fatty acid methyl ester **1a** (1.00 eq, 3.38 mmol) was mixed with 4.00 eq. acrylic acid (13.5 mmol, 0.97 g) and 0.35 eq. $\text{BF}_3 \cdot \text{Et}_2\text{O}$ (0.12 mmol, 0.17 g). The reaction mixture was stirred for 4 days at 75°C . The reaction mixture was quenched by an excess amount of ethyl acetate and saturated NaHCO_3 solution (1 : 1). The organic layer was separated, washed several times with water and brine before it was dried over Na_2SO_4 and evaporated to dryness. The crude product **7a** was obtained as orange colored oil (0.87 g, 90 % conversion in yield of 70 %). ^1H NMR (CDCl_3 , 300 MHz, mixture of regioisomers) $\delta = 0.86$ (t, $J = 7.0$ Hz, 3 H, CH_3), 1.17 – 1.38 (m, 22 H, CH_2), 1.44 – 1.70 (m, 4 H, CH_2), 1.88 – 2.01 (m, 2 H, CH_2), 2.28 (t, $J = 7.8$ Hz, 2 H, CH_2), 3.64 (s, 3 H, CH_3), 4.92 (m, 1 H, CH), 5.85 (dd, $J = 10.3$, 2.4 Hz, 1 H, $=\text{CH}_2^{\text{a}}$), 6.09 (dd, $J = 17.3$, 10.3 Hz, 1 H, COCH), 6.37 (dd, $J = 17.3$, 1.6 Hz, 1 H, $=\text{CH}_2^{\text{b}}$) ppm. ^{13}C NMR (CDCl_3 , 75 MHz, mixture of regioisomers) $\delta = 14.02$ (CH_3), 22.92 (CH_2), 24.84 (CH_2), 25.22 (CH_2), 25.29 (CH_2), 27.60 (CH_2), 27.66 (CH_2), 28.68 (CH_2), 28.96 (CH_2), 29.16 (CH_2), 29.30 (CH_2), 29.31 (CH_2), 31.65 (CH_2), 32.20 (CH_2), 34.70 (CH_2), 34.91 (CH_2), 51.81 (COOCH_3), 76.24 ($\text{CH}_{\text{acrylate}}$), 128.48 (CHCH_2), 130.36 (CH_2CH), 163.91 ($\text{CO}_{\text{acrylate}}$), 174.28 (COOCH_3) ppm. HRMS (FAB) of $\text{C}_{22}\text{H}_{40}\text{O}_4$ $[\text{M}+\text{H}]^+$ calc. 368.2910 found 368.2912.

4.3 Polymer synthesis

4.3.1 Solvent-/bulk polymerization

All monomers were reacted as described in the representative procedure for **4ac**: 2.00 g of monomer **4ac** (1 eq, 5.00 mmol) was mixed with 0.60 mol% AIBN (4.92 mg). The mixture was purged with argon for several minutes. The polymerization was performed at 75 °C for up to 6 hours. After the reaction, the polymer was dissolved in toluene and precipitated by slowly dropping into ice-cold methanol as colorless and highly viscous material (1.60 g, yield >78 %).

4.3.2 Saponification of the polymer side chain

1.0 g of the polymer **P4ac** ($8.8 \cdot 10^{-6}$ mol) was dissolved in 50 mL THF. In another vial 1.0 g LiOH (0.04 mol) was dissolved in 50 mL distilled water. Each mixture was cooled by an ice bath in order to combine them and let the mixture react at RT overnight. Subsequently 20 mL 3M HCl were added and the mixture was stirred for at least 15 min. After washed with brine and extracted with ethyl acetate, the combined organic layer were evaporated under reduced pressure to total dryness. The deprotected polymer was observed in yields of 95 %.

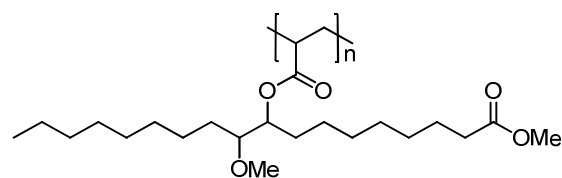
4.3.3 Miniemulsion polymerization

AIBN (0.60 mol%, 2.46 mg) was added to 1.00 g of monomer **4ac** (1 eq, 2.50 mmol). Then, water (3 mL) and sodium dodecyl sulfate (SDS) (0.01 eq, 0.025 mmol, 7.21 mg) as emulsifier were mixed and added to form a pre-emulsion by continuous stirring for 10 minutes. Then, an ultrasonic tip (Ultrasonic sonifier horn 3/8", Branson) was used to break up the monomer droplets and to obtain a homogeneous and stable miniemulsion. Cooling with an ice bath prevented pre-polymerization. Each polymerization was performed directly after ultrasonic treatment at 75 °C within a reaction time of 1.5 – 3 h.

4. Experimental part

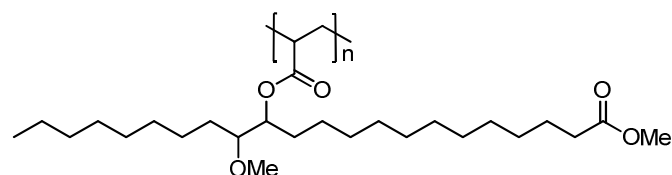
4.3.4 Synthesized polymers

Poly-methyl 9(or 10)-acryloyloxy-10(or 9)-methoxy octadecanoate

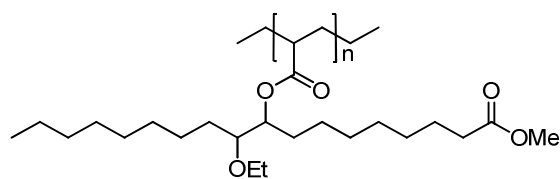


^1H NMR for **P4ac** (CDCl_3 , 300 MHz) δ = 0.88 (t, J = 6.7 Hz, 3 H, CH_3), 1.14 – 1.51 (m, 24 H, 12 CH_2), 1.52 – 1.70 (m, 4 H, 2 CH_2), 2.17 – 2.29 (m, 3 H, CH_2CO , CHCO), 3.03 – 3.20 (m, 1 H, CH), 3.28 (s, 3 H, OCH_3), 3.65 (s, 3 H, COOCH_3), 4.71 – 4.90 (m, 1 H, CH) ppm; DSC T_g = -59 $^\circ\text{C}$.

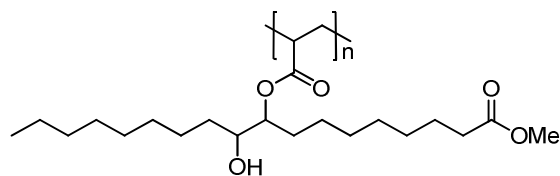
Poly-methyl 13(or 14)-acryloyloxy-14(or 13)-methoxy docosanoate



^1H NMR for **P4bc** (CDCl_3 , 300 MHz) δ = 0.86 (t, J = 6.7 Hz, 3 H, CH_3), 1.16 – 1.51 (m, 32 H, 16 CH_2), 1.54 – 1.70 (m, 4 H, 2 CH_2), 2.14 – 2.27 (m, 3 H, CH_2 , CH), 3.10 – 3.22 (m, 1 H, CH), 3.27 (s, 3 H, CH_3), 3.68 (s, 3 H, CH_3), 4.78 – 4.94 (m, 1 H, CH) ppm; DSC T_g = -63 $^\circ\text{C}$.

Poly-methyl 9(or 10)-acryloyloxy-10(or 9)-ethoxy octadecanoate (polyAMOet)

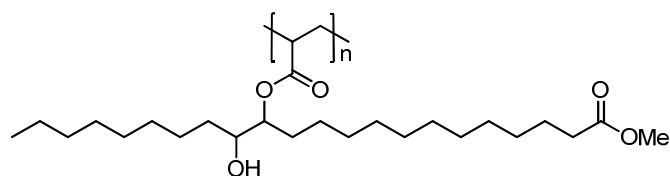
^1H NMR for **P4ad** (CDCl_3 , 300 MHz) δ = 0.85 (t, J = 6.5 Hz, 3 H, CH_3), 1.06 – 1.69 (m, 31 H, 14 CH_2 , 1 CH_3), 2.06 – 2.24 (m, 3 H, CH_2 , CH), 3.13 – 3.24 (m, 1 H, CH), 3.40 – 3.55 (m, 2 H, CH_2), 4.05 (s, 3 H, CH_3), 4.89 – 5.02 (m, 1 H, CH) ppm. DSC T_g = -59 °C.

Poly-methyl 9(or 10)-acryloyloxy-10(or 9)-hydroxy octadecanoate

^1H NMR for **P5a** (CDCl_3 , 300 MHz) δ = 0.86 (t, J = 6.07 Hz, 3 H, CH_3), 1.17 – 1.52 (m, 24 H, 12 CH_2), 1.52 – 1.76 (m, 5 H, OH, 2 CH_2), 2.18 – 2.29 (m, 3 H, CH_2 , CH), 3.55 – 3.65 (m, 1 H, CH), 3.68 (s, 3 H, CH_3), 4.82 – 4.97 (m, 1 H, CH) ppm. DSC T_g = -65 °C.

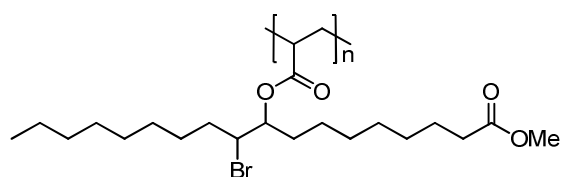
4. Experimental part

Poly-methyl 13(or 14)-acryloyloxy-14(or 13)-hydroxy docosanoate

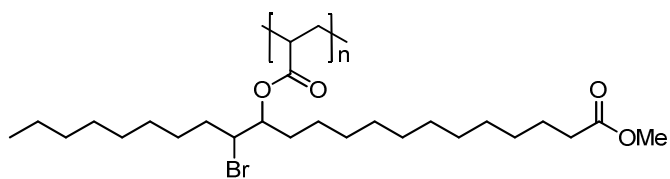


^1H NMR for **P5b** (CDCl_3 , 300 MHz) δ = 0.83 (t, J = 6.07 Hz, 3 H, CH_3), 1.11 – 1.51 (m, 32 H, 16 CH_2), 1.50 – 1.75 (m, 5 H, OH, 2 CH_2), 2.20 – 2.32 (m, 3 H, CH_2 , CH), 3.50 – 3.68 (m, 1 H, CH), 3.64 (s, 3 H, CH_3), 4.79 – 4.95 (m, 1 H, CH) ppm. DSC T_g = -69 $^\circ\text{C}$.

Poly-methyl 9(or 10)-acryloyloxy-10(or 9)-bromo octadecanoate



^1H NMR for **P6a**: (CDCl_3 , 300 MHz) δ = 0.82 (t, J = 6.6 Hz, 3 H, CH_3), 1.16 – 1.55 (m, 24 H, 12 CH_2), 1.55–1.74 (m, 4 H, 2 CH_2), 2.24 – 2.39 (m, 3 H, CH_2 , CH), 3.64 (s, 3 H, CH_3), 3.96 – 4.07 (m, 1 H, CH), 4.95 – 5.04 (m, 1 H, CH) ppm. DSC T_g = -50 $^\circ\text{C}$.

Poly-methyl 13(or 14)-acryloyloxy-14(or 13)-bromo docosanoate

^1H NMR for **P6b**: (CDCl_3 , 300 MHz) $\delta = 0.84$ (t, $J = 6.7$ Hz, 3 H, CH_3), 1.15 – 1.51 (m, 32 H, 16 CH_2), 1.53 – 1.81 (m, 4 H, 2 CH_2), 2.19 – 2.41 (m, 3 H, CH_2 , CH), 3.61 (s, 3 H, CH_3), 3.99 – 4.12 (m, 1 H, CH), 4.94 – 5.08 (m, 1 H, CH) ppm. DSC $T_g = -59$ °C.

4. Experimental part

4.4 Preparation of polymer films

In order to compare the adhesive properties of synthesized polymers the adhesive polymer films were prepared with an average film thickness of $50\pm 5\ \mu\text{m}$ for tack tests and $15\pm 2\ \mu\text{m}$ for peel tests. For tack experiments, this was achieved by coating a polymer methyl ethyl ketone (MEK) solution (60 - 80 % solid content) onto a glass slide using doctor blades with a defined gap size (0.075-0.15 mm) mounted onto an automatic film applicator ZAA 2300 (Zehntner GmbH, Switzerland, see also Figure 32). The coating speed of the film applicator was kept constant at 20 mm/s. Gap size and/or polymer concentration were varied to reach the desired polymer film thickness.

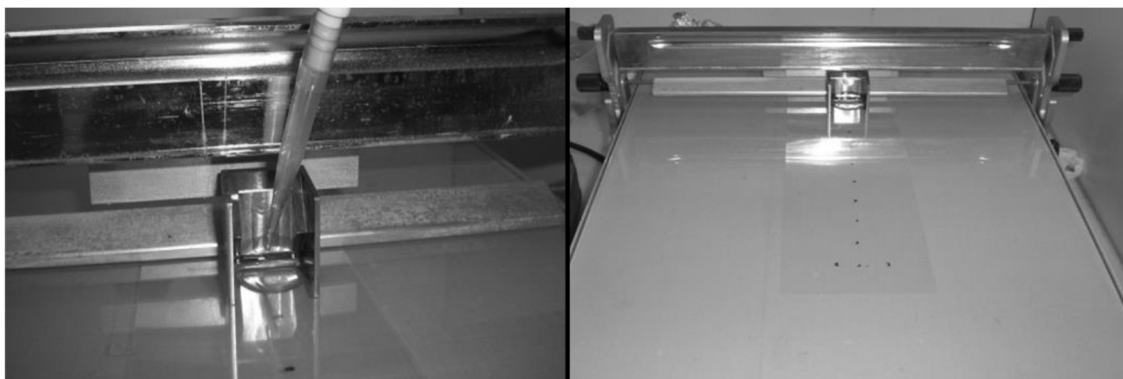


Figure 32. Film applicator. Polymer solution onto a glass slide using doctor blades with a defined gap size.

Freshly prepared films were first stored at room temperature overnight, followed by treatment at 120 °C for 1.5 h to remove the remaining solvent and to achieve a smooth polymer surface.

For peel tests, a 36 μm etched PET foil (provided by tesa SE) was coated with each polymer solution (60 - 80 % solid content) using a doctors blade at constant coating speed of 10 mm/s to gain a film thickness of $15\pm 2\ \mu\text{m}$. The prepared polymer films were directly dried at 120 °C for 1 h. The prepared samples were cut to a width of 15 mm. Prior any measurement, each sample was cooled down to room temperature (21 °C). Each polymer film was then attached to a glass plate using a 2 kg weight in 8 – 10 runs within a contact formation time of 4 min.

4.5 Experimental procedure

4.5.1 Determining tack

The experimental set-up used for determining tack and optical observation was based on a commercial device Texture Analyzer TA.XTplus (Stable Micro Systems, UK) which is shown in Figure 33 and has been already described in section 4.1.

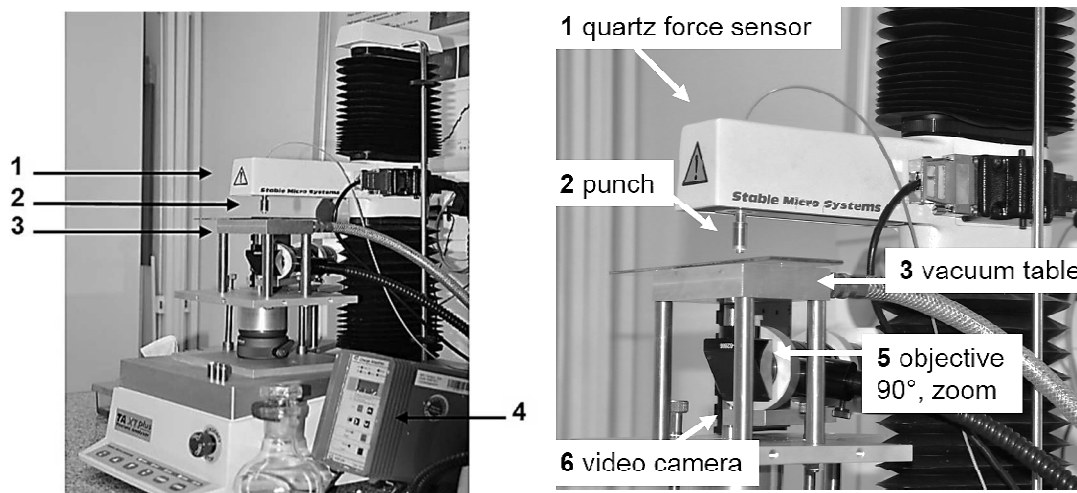


Figure 33: Experimental set-up for tack measurements with video-optical observation: 1-quartz force sensor; 2-punch (substrate); 3-vacuum table; 4- charge amplifier; 5- objective (90°); 6-video camera.

At first the zero-point (on clean glass surface) was detected and the probe height was set to 1.0 mm for each measurement. The probe was then allowed to attach the polymer film with a constant speed of 0.1 mm/s under a constant contact force of 10 N for a contact time of 1 s. Thereupon the probe was removed with a constant rate of 1.0 mm/s up to 5 mm. Simultaneously, the force-distance curves were recorded and also video images of the contact area were taken during the withdrawing process. Due to the importance of full contact of the polymer to the substrate, one was able to adjust the angle of contact by changing the height of the table in two dimensions. This had to be performed until full contact could be observed in pre-tests.

The debonding of PSAs is accompanied by the cavitation. Cavities occur at the interface between the substrate and the polymer and they are affected by the interfacial parameters. The detailed analysis of the cavitation can allow to quantify the influence

4. Experimental part

of the interfacial parameters on the adhesion of PSAs. An optical observation of the debonding allows for observation of the cavitation. Texture Analyzer TA.XTplus was equipped with a high-speed camera mounted under the vacuum table, where a transparent glass plate with the deposited sample is positioned in order to record a video sequence simultaneously with the stress-strain curves. The video images were obtained with the already mentioned high-speed camera KL MB-Kit 1M1 (Mikrotron GmbH, Germany) used in combination with a zoom objective 90° KL-Z6 and a cold light source KL3000B. The camera allowed to record 124 frames/s at maximum resolution of 1280x1024 pixels. At maximum resolution one pixel is approximately 5 μm . The images were quantitatively analyzed using Visiometrics Image Processing System (IPS) software, developed by Prof. Dr. Stephan Naser, University Darmstadt. Using IPS software one can calculate the true area of contact from the manually marked probe surface on the first image of every video sequence.

To ensure reproducible average values each sample was tested at least five times. The measured force F had to be converted to a nominal stress $\sigma = F/A$, where A is the real-time contact area, measured from the optical images. The intrinsic tack value was obtained by integration of the area under the nominal stress vs. nominal strain curve. The nominal strain also had to be calculated. This was done by using the time-dependent film thickness h , described as $\varepsilon = (h - h_0) / h_0$, where h_0 is the initial film thickness. For estimation of the initial film thickness of measured polymer films, two independent methods were used. One method was based on determining the thickness by using a standard dial gauge with a flat-ended scanner. Alternatively, the film thickness was determined directly from the force-distance curve obtained from the measurement. By calibrating the distance from the glass surface to zero, one knows the difference between the substrate position starting at 1.0 mm and the position at which the first contact with polymer material takes place, meaning the position at which a first negative force value appear which finally gives information about the initial film thickness h_0 . Both methods provided similar results, although the second method was preferred for the probe tack films. For peel films the dial gauge determination of film thickness was method of choice.

Varying probes with different substrates were used to establish the adhesive properties of the bio based polymers with respect to high and low energy surfaces (see Figure **34**).



Figure 34: Probe tack Substrates.

The substrates used for tack experiments were special treated flat-ended cylinders based on stainless steel (1, 2, 3), polyethylene (PE, 4), glass (5), wood, or Si-wafer with a diameter of 5.0 mm each (Figure 34). Furthermore stainless steel cylinders had been polished to different degrees, in order to gain various average surface roughness $R_a = 2.9, 41$ and 292 nm (1, 2, 3). Wood and gold probes were neglected.

4.5.2 Determining peel

For peel test the Texture Analyzer TA.XTplus device was changed with respect to a 90° peel device (FINAT No. 2, see Figure 35).

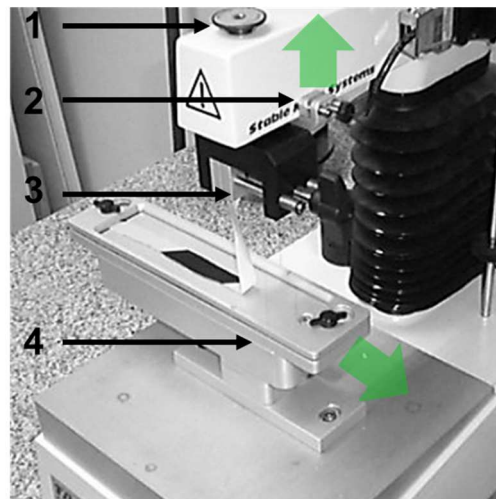


Figure 35: Experimental set-up for peel measurements: 1-standard force sensor with calibration platform; 2-wire clamp; 3-strip holder/clamp; 4-slide table.

4. Experimental part

The respective polymer films were prepared as described in section 4.4. An important fact to be mentioned by choosing a carrier foil is, that it isn't allowed to be stretched and deformed in the later test. A commercial carrier foil provided by tesaSE guaranteed desired strength for appropriate test conditions. Unfortunately there wasn't enough polymeric material to perform the standard test (ASTM D6862) requiring 20 mm wide stripes. The polymer stripes have been adjusted to a width of 15 mm and were then placed in the middle of a glass plate carrier from which they were peeled off. To ensure a sufficient contact to the carrier, a 2.0 kg weight was used and moved over the adhesive film eight times. Subsequently, the weight was placed on a second glass carrier atop the adhesive for 4 min. As it is illustrated within Figure 35, the glass carrier with the prepared polymer film was placed on a movable table (slide) and fixed by clamps under a frame.

For the measurement one end of the film was then brought in between of two brackets connected to the upper arm and to the force sensor of the device. To make sure that the peeling is proceeded in 90° angle thorough the whole measurement, the slide has to move in the same manner as the device arm gains in height. Therefore the upper arm is connected to the slide by a wire. In each measurement the peel force was detected at a constant speed of 4 mm/s in a range of 80 mm in length. Each test were performed at room temperature. The obtained force-distance plot was directly analyzed by calculating the average force in an appropriate range, starting 10-20 mm after beginning of the peel process. The Force values were noted and expressed as N/15mm.

The test conditions have been evaluated elsewhere and were proved to yield reproducible values concerning the adhesive performance of synthesized bio-polymers. Contact angle, surface energies as well as evaluation of film thickness and carrier foil type was presented as well.^[238]

4.5.3 Determining viscoelastic properties

The viscoelastic properties of polymer melts can be measured using oscillatory rheometry. The principle of the technique is to subject a specimen, held between two plates, to a sinusoidal torque or displacement determining the response of the sample

to that input. In every test method the shear storage G' and shear loss G'' moduli are determined.

Viscoelastic properties were determined by using a strain controlled Physica MCR-501 (Anton Paar, Austria, Graz) using two different oscillatory procedures. Sample preparation was as follows: After tempering to 20 °C the zero-gap was taken. Then the polymer sample was brought in between the plate/plate geometry ($d = 8$ mm) and the gap was set to 1.0 mm for each measurement. Under-filling was strictly avoided. Before each measurement the sample was allowed to relax for several minutes (15 – 30 min) depending on the viscosity grade of each sample.

In general storage and loss moduli were plotted as a function of the deformation in an amplitude sweep, where the frequency was held constant, while the strain was varied from 0.01 to 10. The region, where G' and G'' exhibit constant values, called the linear viscoelastic region, gave information about the limit deformation value. In all cases 0.01 % and 0.1 % could be used in a frequency sweep without exceeding this limit.

Frequency sweeps, where the frequency is varied, were proceeded in the range of 0.01 – 100 Hz and fixed strain of 0.01 and 0.1 at constant temperature. The range of frequency from 0.1 to 100 Hz corresponds to the wetting and creep properties of typical PSAs. The temperature has also been varied in some cases to get a master curve by using the TTS principle, leading to a better overview of the viscoelastic behavior whereas illustrating more decades. All measurements were performed at least twice, to guarantee the reproducibility of the response. As a last test method temperature sweeps were performed at a constant frequency of 1.0 Hz, 0.01 or 0.1 strain, in a range of -30 °C to 150 °C with a heating rate of 5.0 K/min. Sample preparation in this concept was performed as described.

5. OUTLOOK AND CONCLUDING REMARKS

Efficient synthesis routes were established for the successful synthesis of acrylate monomers based on methyl oleate as well as methyl erucate. A one-, two- and three-step synthesis, which were all shown to result in adequate yields and sufficient purity of the resulting monomers, are described. The results were compared to each other, revealing that the one step procedure offers the most environmentally benign approach. In addition, different monomer types could be explored. All monomers were able to react in free radical polymerization procedures and were excellent candidates for adhesive polymer base materials.

The polymerizations were mainly performed in bulk, in order to create high molecular weight bio-based homo- and copolymers for use in pressure sensitive adhesives and to a minor content in miniemulsion polymerization. The dispersions were synthesized as miniemulsions using only small amounts of emulsifier, without co-surfactant and though, they exhibited long-term stability (>2 years). Controlled radical polymerization methods were shown to work in general, but yielded adequate chain length only to a minor degree.

This work mainly focused on the pure homopolymers, which were easily tunable in their adhesive properties according to the specific demands of different PSA applications. Herein synthesized homopolymers do not contain additional additive or crosslinker as commercial PSAs. Nevertheless they are able to be processed in application, e.g. by dissolving for coating or spraying, before curing is used for reaching desired adhesive performance. As described before, the adhesive properties of a pressure sensitive adhesive are influenced by several parameters like its bulk molecular weight (M_w), dispersity (\mathcal{D}), the polymer composition and its cross-link density, as well as interfacial parameters including substrate type (high or low energy substrates) and substrate roughness (R_a). Therefore, all plant derived homopolymers as well as a copolymer were characterized with respect to their linear viscoelastic and adhesive properties. For this purpose, standard tack and peel tests were performed to judge the applicability of the synthesized polymers as PSAs.

5. Outlook and concluding remarks

The tack as well as the peel strength of the homopolymers is strongly influenced by the viscoelastic properties of the material, the surface and interfacial tensions of adhesive and adherent as it has been demonstrated in this work. Thus, the bio-based **P4ac** showed the typical dependence of adhesive performance on molecular weight as well as cross-linking density. The incorporation of acrylic comonomer in the polymer chain and the dependence on cross-linking was shown as an important factor influencing the adhesion and forcing the transition of cohesive to adhesive failure. It was also shown that **P4** as well as **P5** homopolymers are easily tunable in their viscoelastic and adhesive performance by curing at an elevated temperature due to crosslinking and network formation. At a critical curing time, tack as well as peel strength exhibit a pronounced maximum and debonding changes from cohesive to adhesive failure. In contrast, the **P6** polymers receive their low viscoelastic performance, without the formation of cross-links. Accordingly, adhesive properties can be adjusted in a wide range meeting the demands of different PSA applications.

Beyond that, the **P4ac** polymers show improved adhesion to low energy substrates as well as a good water resistance without any whitening effect, thereby demonstrating an attractive alternative with superior adhesion performance compared to common petroleum based PSAs. These specific features are attributed to the highly hydrophobic nature of the base monomer.

In general, these results might offer an opportunity to produce such bio-based acrylate monomers in sufficient yields as well as purity in industrial scales for specialty applications. With critical respect towards the polymerization process, additional optimization regarding a controlled procedure with reproducible degree of polymerization, molecular weight and conversion is necessary. Furthermore, copolymer compatibility in polymerization reactions should be investigated in detail to clearly show the possibility of substituting of common monomers, such as butyl acrylate. The pretty low T_g s of investigated polymers, especially of **P4ac**, make them an attractive alternative.

Further research should focus on bio-based resins, crosslinker or other additives to show a broad range of prospects and properties for substitution of the common market controlling fossil resource based products. Nature, especially plant oils, provides

5. Outlook and concluding remarks

suitable fatty acids in different kinds, and combined with today's excellent features in the chemical laboratories, there is a chance to enhance their prestige for application like adhesive formulations. As already emphasized, today's world is not conceivable without adhesives, which remain a growing market. Hence, it is worth a try to not only think about economic but also eco-friendly alternatives.

6. INDEX OF CONTENTS

List of Abbreviations and Symbols

°C	degrees Celsius
<i>A</i>	contact area wetted by the adhesive
Å	Ångström
AA	acrylic acid
AIBN	azobisisobutyronitrile
AMO	acrylated methyl oleate
ASTM	American Society for Testing and Materials
ATRP	atom transfer radical polymerization
<i>b</i>	width
BA	<i>n</i> -butyl acrylate
calc.	calculated
cat.	catalyst
cm	centimeter
cmc	critical micelle concentration
<i>d</i>	deuterated
Đ	dispersity
dd	doublet of doublets
<i>De</i>	Deborah number
DLS	dynamic light scattering
DMA	dynamic mechanical analysis
DSC	differential scanning calorimetry
e.g.	for example
EGDMA	ethylene glycol dimethacrylate
EHA	2-ethylhexyl acrylate
eq.	equivalent
ESO	epoxidized soybean oil

6. Index of contents

<i>et al.</i>	and others
EVAc	ethylene-vinyl acetate
<i>F</i>	tensile force
<i>f</i>	frequency
F_a	force between the surface of a flat cylindrical punch and an elastic polymer film
FAB	fast atom bombardment
FAME	fatty acid methyl esters
F_d	detaching force
FINAT	fédération internationale des fabricants et transformateurs d'adhésifs et thermocollants sur papiers et autres supports
FRP	free radical polymerization
<i>G</i>	energy release rate, shear modulus
<i>g</i>	gram
G'	storage modulus
G''	loss modulus
G_0	fracture energy
G_c	critical energy release rate
GC	gas chromatography
GPC	gel permeation chromatography
G_t	total energy
<i>h</i>	adhesive thickness, hour
<i>H</i>	gap height
HEA	2-hydroxyethyl acrylate
HFIP	hexafluoro-2-propanol
HQ	hydroquinone
Hz	hertz
<i>I</i>	Initiator, interval
i.e.	id est (that is)

IPS	image processing system
IR	infrared
J	joule
K	Kelvin
kDa	kilo dalton
kg	kilogram
k_t	termination rate constant
LSE	low surface energy
LVE	linear viscoelastic regime
m	meter, multiplet
M	monomer
MA	methyl acrylate
M_c	average molecular weight between two chemical links
M_e	entanglement molecular weight, methyl
MEK	methyl ethyl ketone
mg	milligram
min	minute
mJ	millijoule
mL	milliliter
mm	millimeter
MMA	Methyl methacrylate
mmol	millimole
M_n	number average molecular weight
mN	meganewton
MPa	megapascal
ms	millisecond
M_v	viscosity average molecular weight
M_w	weight average molecular weight
M_z	z-average molecular weight
N	Newton

6. Index of contents

<i>n</i>	normal
NBR	nitrile butadiene rubber
NBS	<i>n</i> -bromosuccinimide
nm	nanometer
NMP	nitroxide-mediated polymerization
NMR	nuclear magnetic resonance
No.	number
NR	natural rubber
<i>P</i>	adhesion energy
p(AMO)	acrylated methyl oleate polymer
ρ_0	initial cavity pressure
Pa	pascal
PC	polycarbonate
PE	polyethylene
PET	polyethylene terephthalate
PHA	poly(hydroxyalkanoate)
PIB	polyisobutylene
PLA	polylactic acid
PP	polypropylene
ppm	parts per million
PS	polystyrene
PSA	pressure-sensitive adhesive
PSTC	pressure sensitive tape council
PTFE	polytetrafluoroethylene
PVC	polyvinyl chloride
q	quartet
R	variable functional group, universal gas constant
<i>r</i>	distance
R [•]	radical

R_a	average deviation from the mean surface plane
rad	radiation
RAFT	reversible addition-fragmentation chain transfer
R_f	retardation factor
R_p	plate radius
R_p	rate of polymerization
rt	room temperature
s	second, singlet
SA	stearyl acrylate
SBC	styrene-block-copolymer
SBR	styrene-butadiene-rubber
SBS	styrene-butadiene-styrene
SDS	sodium dodecyl sulfate
SET-LRP	single-electron transfer living radical polymerization
SIS	styrene-isoprene-styrene
T	temperature, sufficient torque
t	triplet
T_g	glass transition temperature
THF	tetrahydrofuran
TLC	thin layer chromatography
TMS	tetramethylsilane
T_{Ref}	reference temperature
TTS	time-temperature superposition
U_E	elastic energy
UV	ultraviolet
V	volume
V_{deb}	rate of debonding
VOC	volatile organic compound

6. Index of contents

vs.	versus
W	work of fracture
W_A	thermodynamic work of adhesion
W_{adh}	adhesion energy
W_D	work of deformation
W_T	total work of adhesion
W_T	work of translation
wt%	percentage by weight
X_n	degree of polymerization
$\dot{\gamma}$	shear rate
γ	shear strain
γ_0	deformation amplitude
γ_l	surface or interfacial tension of the adhesive
γ_s	interfacial free energy of the adherent
γ_{sl}	interfacial free energy of the adhesive/adherent interface
δ	phase shift, chemical shift
ϵ_{max}	maximum elongation, maximum nominal strain
μm	micrometer
η	viscosity
θ	wetting angle
ϑ	movement of the probe in normal direction
ρ	density
σ_{max}	maximum nominal stress
τ	shear stress
τ_0	stress amplitude
τ_r	relaxation time
ψ	dissipated viscoelastic energy
λ_r	extension ratio

Ω	angular velocity
ω	rotational velocity
ω	peel-off angle

6. Index of contents

List of Figures

Figure 1. Chemical structure of synthesized and characterized acrylic monomers. ...	3
Figure 2. Classification of adhesive types.....	5
Figure 3. Illustration of the work needed to separate the adhesive from the adherent.	12
Figure 4. Schematic of the contact angle between adhesive and adherent.....	17
Figure 5. Schematic of a rough surface in contact with an adhesive.[].....	19
Figure 6. Schematic of a punch surface in contact with an adhesive film.....	21
Figure 7. Stages of debonding by cavity nucleation: b), cavity growth in lateral direction. c), growth in the direction of the elongation with change towards a fibril structure. d), fibril growth. e), bond failure in two ways as adhesive or cohesive break.[]	24
Figure 8. Illustration of a 90° and a 180° peel test.[27]	30
Figure 9. Failure mode explanation in a 90° peel test.[27].....	31
Figure 10. Schematic of a plate-plate fixture used in a rheometer. Ω = angular velocity [rad/s] R_p = plate radius, H = gap height, r = distance.[]	36
Figure 11. Illustration of G' and G'' as a function of deformation to determine the LVE in an amplitude sweep (log-scale).	38
Figure 12: Dynamic mechanical data of a polystyrene (220 kDa M_n). Original master curve at a reference temperature of 175°C.[]	40
Figure 13. Structure of fatty acids (e.g. sunflower oil).[]	53
Figure 14. Synthesis pathways to oleate and erucate derivatives 4ac (AMO), 4ad , 4bc , 5a,b and 6a,b	58
Figure 15. $^1\text{H-NMR}$ spectra of oleate based monomers synthesized in three-, two- and one-step procedures, measured in d -chloroform and showing respective chemical shifts of functional groups additionally illustrated by the chemical structure of monomer 4ac (bottom).	64
Figure 16. Homopolymerization to obtain polymers P4ac , P4ad , P4bc , P5a ,	66
Figure 17. Respective NMR spectra (CDCl_3) of P4ac	68

Figure 18. Deprotection of the methyl ester functionality in the side chains of polymer P4ac	70
Figure 19. Storage modulus vs. temperature of bulk and miniemulsion homopolymers (molecular weights see Table 10) compared to a commercial acrylate co-polymer Acronal V212 provided as aqueous dispersion.....	75
Figure 20. Tack of AMO-homopolymers compared to that of the commercial acrylate co-polymer Acronal V212. Debonding rate: 1 mmxs^{-1} ; probe diameter: 5 mm.	76
Figure 21. Peel force in 90° at 4 mm/s per 15 mm width.	77
Figure 22. Work of adhesion a) and peel strength b) of P4ac homopolymers with different average molecular weight M_w and dispersity \mathcal{D} . Tack experiments were performed using a steel probe with $R_a = 3 \text{ nm}$, 1 mm/s debonding velocity and 1 s bonding time. Peel tests were performed on glass plates at a debonding velocity of 4 mm/s.....	78
Figure 23. Storage and loss modulus data of cured P4ac ($M_w = 280 \text{ kDa}$, $\mathcal{D} = 3$) by means of oscillatory shear measurements. a) G' as function of temperature at different curing times measured at 1 Hz frequency and 0.01 strain. b) G' and G'' as function of angular frequency measured at 20°C	81
Figure 24. Tack performance and peel strength of cured P4ac ($M_w = 690 \text{ kDa}$, $\mathcal{D} = 4.3$) on varying substrate types.....	82
Figure 25. Cohesive (left) and adhesive failure (right) in tack and peel measurements of P4ac ($M_w = 690 \text{ kDa}$, $\mathcal{D} = 4.3$) cured for 1.5 h (left) and 27.5 h (right).....	83
Figure 26. Tack and Peel data vs. G' at 20°C to visualize the dependence of adhesive performance on viscoelastic properties.	83
Figure 27. Tack values of cured P5a ($M_w = 290 \text{ kDa}$, $\mathcal{D} = 2.2$) and cured P6a ($M_w = 250 \text{ kDa}$, $\mathcal{D} = 3.5$). Tack tests were done using a steel probe with $R_a = 41 \text{ nm}$	84
Figure 28. Peel strength of cured P5a ($M_w = 290 \text{ kDa}$, $\mathcal{D} = 2.2$), cured P6a ($M_w = 250 \text{ kDa}$, $\mathcal{D} = 3.5$) and a mixture of P4ac+HQ ($M_w = 550 \text{ kDa}$, $\mathcal{D} = 5.1$).	85
Figure 29. Storage modulus as a function of temperature at 1 Hz and 0.01 strain for a model copolymer dispersion Acronal V212 compared to a synthesized cured homopolymer P4ac ($M_w = 280 \text{ kDa}$, $\mathcal{D} = 3$) and a non-cured copolymer p(4ac-MMA) in	

6. Index of contents

<i>a molar ratio of 80/20 ($M_w = 341$ kDa, $\bar{D} = 2.0$). Values for $p(\text{BA/MA})$ calculated from $G'(w)$ data shown in Peykova et. al.^[85]</i>	<i>86</i>
<i>Figure 30. Ratio of W_{adh} measured on PE ($R_a \approx 45$ nm) and on steel ($R_a = 41$ nm) of a cured homopolymer P4ac_5.5h and P4ac_27h ($M_w = 690$ kDa, $\bar{D} = 4$) and a non-cured copolymer $p(\mathbf{4ac/MMA})$ in a molar ratio of 80/20 ($M_w = 341$ kDa, $\bar{D} = 2.0$) compared to acrylate copolymer dispersion Acronal V212 and model solution-based copolymer $p(\text{BA/MA})$ ($M_w = 192$ kDa, $\bar{D} = 6.4$) at a debonding velocity of 1 mm/s. ^{a)}Tack data of copolymer $p(\text{BA/MA})$ taken from Peykova et. al.^[235] Note that respective measurements were performed at a debonding velocity of only 0.1 mm/s.</i>	<i>87</i>
<i>Figure 31. Remaining peel strength after 24 h water immersion of acrylate copolymer Acronal V212, a standard office tape (tesa SE product) and cured P4ac after 5.5 h and 25.5 h of curing time ($M_w = 480$ kDa, $\bar{D} = 4$).</i>	<i>89</i>
<i>Figure 32. Film applicator. Polymer solution onto a glass slide using doctor blades with a defined gap size.</i>	<i>112</i>
<i>Figure 33: Experimental set-up for tack measurements with video-optical observation: 1-quartz force sensor; 2-punch (substrate); 3-vacuum table; 4- charge amplifier; 5-objective (90°); 6-video camera.</i>	<i>113</i>
<i>Figure 34: Probe tack Substrates.</i>	<i>115</i>
<i>Figure 35: Experimental set-up for peel measurements: 1-standard force sensor with calibration platform; 2-wire clamp; 3-strip holder/clamp; 4-slide table.</i>	<i>115</i>

List of Schemes

<i>Scheme 1. Synthesis pathway in three steps towards monomer 4ac, 4ad and 4bc.</i>	<i>95</i>
<i>Scheme 2. Synthesis pathway in two steps leading to monomer 5a and 5b.</i>	<i>102</i>
<i>Scheme 3. Synthesis pathway in one step towards monomer 6a and 6b.....</i>	<i>104</i>
<i>Scheme 4. Synthesis pathway in one step towards monomer 7a.....</i>	<i>106</i>

List of Tables

<i>Table 1. Comparison of main PSA such as natural rubber (NR), styrene-butadiene-rubber (SBR), styrene-block-copolymer (SBC), Acrylics and ethylene-vinyl acetate (EVAc) and their processing.^{1]}.....</i>	<i>7</i>
<i>Table 2. List of surface tension of different Substrates.....</i>	<i>18</i>
<i>Table 3. PSA characteristics described by dynamic mechanical properties.</i>	<i>35</i>
<i>Table 4. Conversion in the ring opening of the oleate based epoxide, EMO (procedure D).....</i>	<i>60</i>
<i>Table 5. Conversion of the one-pot bromoacrylation (procedure E).</i>	<i>62</i>
<i>Table 6. Conversion of the one-pot acrylation of methyl oleate catalyzed by BF₃·Et₂O.</i>	<i>63</i>
<i>Table 7. Average number (M_n) and weight (M_w) average molecular weight as well as dispersity (Đ) of synthesized polymers according to GPC.....</i>	<i>67</i>
<i>Table 8. Number (M_n) and weight (M_w) average molecular weight as well as dispersity (Đ) of saponified polymer according to GPC.</i>	<i>71</i>
<i>Table 9. Results of miniemulsion polymerization. Left: Variation of molecular weight with initiator concentration. Right: Variation of particle size with surfactant concentration.....</i>	<i>73</i>
<i>Table 10. Number (M_n) and weight (M_w) average molecular weight as well as dispersity (Đ) of tested samples according to GPC.</i>	<i>74</i>

6. Index of contents

References

- [1] Eissen, M., Metzger, J. O., Schmidt, E., Schneidewind, U., *Angew. Chem. Int. Ed.*, **41**, 414–436, **2002**.
- [2] Meier, M. A. R., Metzger, J. O., Schubert, U. S., *Chem. Soc. Rev.* **2007**.
- [3] German Federal Ministry of Food, Agriculture and Consumer Protection, Agency of Renewable Resources, <http://www.fnr.de>.
- [4] Bozell J. J., Patel M., *Feedstocks for the Future: Renewable for the Production of Chemicals and Materials*; ACS Symposium Series 921; American Chemical Society, **2006**, Washington, DC.
- [5] Biermann U., Friedt W., Lang S., Lühs W., Machmüller G., Metzger J. O., *Angew. Chem. Int. Ed.*, **39** (13), 2206–2224, **2000**.
- [6] Lu Y., Larock R. C., *ChemSusChem*, **2** (2), 136–147, **2009**.
- [7] *Industrieverband Klebstoffe e.V.*, www.klebstoffe.com.
- [8] Benedek I., Feldstein M. M., *Pressure-sensitive Adhesives and Applications*, CRC Press, New York **2004**.
- [9] Pressure Sensitive Tape Council (PSTC), **2008**, Available from: http://www.pstc.org/files/public/PSTC_TapeDescriptions.pdf.
- [10] Wool R. P., Sun X. S., in *Bio-based polymers and composites*, Elsevier Academic Press, Amsterdam **2005**.
- [11] Shull, K. R., Ahn, D., Chen, W., Flanigan, C. M., Crosby, A. J., *Macromol. Chem. Phys.*, **199**, 489-511, **1998**.
- [12] Adams, R. D., in *Adhesive Bonding: Science, Technology and Applications*, CRC Press, New York **2005**.

- [13] Wypych, G., in *Handbook of Plasticizers*, 2nd Edition, ChemTec Publishing, Canada **2013**.
- [14] Habenicht, G., in *Applied Adhesive Bonding: A Practical Guide for Flawless Results*, John Wiley & Sons, New York, **2008**.
- [15] Benedek, I., Feldstein, M. M., ed., *Technology of Pressure-Sensitive Adhesives and Products*, CRC – Taylor & Francis, Boca Raton, London, New York, **2009**.
- [16] Khan, I., Poh, B. T., *J. of Polym. and Env.*, 19 (3), 793–811, **2011**.
- [17] Röthemeyer, F., Sommer, F., in *Kautschuktechnologie: Werkstoffe - Verarbeitung – Produkte*, Carl Hanser Verlag GmbH Co KG, München **2013**.
- [18] Foreman, P.B., in *Technology of Pressure Sensitive Adhesives and Products*, Benedek, I., Feldstein, M. M., ed., Vol. 2, Cap. 5, CRC – Taylor & Francis, Boca Raton, London, New York, **2009**.
- [19] Landau, S. I., *The New Original Webster's Student Dictionary of the English Language*, Trident Press International, USA, **1999**.
- [20] Zosel, A., *Colloid & Polymer Science*, 263 (7), 541–553, **1985**.
- [21] Dahlquist, C. A., in *Adhesion Fundamentals and Practice*, Mc. Laren, London, **1966**.
- [22] Gay, C., *Integr. Comp. Biol.*, 42, 1123-1126, **2002**.
- [23] Van Oss, C. J., Chaudhury, M. K., Good, R. J., *Chem. Rev.*, 88, 927-941, **1988**.
- [24] Taghizadeh, S. M., Mirzadeh, H., Barikani, M., Yousefi, M., *Iran. Polym. J.*, 16, 279, **2007**.

6. Index of contents

- [25] Kenney, J. F.; Haddock, T. H.; Sun, R. L.; Parreira, H. C., *J. Appl. Polym. Sci.*, **45**, 355, **1992**.
- [26] Taghizadeh, S. M., Diba G., *J. of Appl. Polym. Sci.*, **120**, 411–418, **2011**.
- [27] Benedek, I., Feldstein, M. M., ed., in *Fundamentals of Pressure-Sensitivity*, CRC – Taylor & Francis, Boca Raton, London, New York, **2009**.
- [28] Taghizadeh, S. M., Lahootifard, F., *J. of Appl. Polym. Sci.*, **90**, 2987, **2003**.
- [29] Dillard, D. A., Pocius, A. V., in *Adhesion Science and Engineering: Surfaces, Chemistry and Applications*, Elsevier, Netherlands, **2002**.
- [30] Zosel, A., *Colloid Polym. Sci.*, **263**, (7), 541, **1985**.
- [31] Zosel, A., Barwich, J., PSTC Pressure Sensitive Adhesive Tape, Conference proceedings Orlando, 175-187, **1995**.
- [32] Tobing, S. D., Klein, A., *J. Appl. Polym. Sci.*, **79**, 2230, **2001**.
- [33] Zosel, A., in Satas D., ed., *Advances in Pressure Sensitive Adhesives Technology*, Warwick, Satas & Associates, **1**, 92-127, **1992**.
- [34] Zosel, A., *J. Adhesion*, **30**, 135-149, **1989**.
- [35] Zosel, A., *Int. J. Adhes. Adhes.*, **18**, 265, **1998**.
- [36] Ferry, J. D., in *Viscoelastic Properties of Polymers*, 3rd ed. Wiley, New York, **1980**.
- [37] Doi, M., Edwards S. F., *The Theory of Polymer Dynamics*, Clarendon, Oxford, **1986**.
- [38] Czech, Z., *J. Adhes. Sci. Technol.*, **21**, 625-35, **2007**.

- [39] Do, H. S., Park, Y. J., Kim, H. J., *J. Adhes. Sci. Technol.*, 20, 1529-1545, **2006**.
- [40] Wu, G. L., Jiang, Y., Ye, L., Zeng, S. J., Yu, P. R., Xu, W. J., *Int. J. Adhes. Adhes.*, 30, 43-46, **2010**.
- [41] Zosel, A., *J. Adhes.*, 34, 201-209, **1991**.
- [42] Zosel, A., *Int. J. Adhes. Adhes.*, 18, 265-71, **1998**.
- [43] Benedek, I., *Pressure-Sensitive Formulation*, VSP, Netherlands, **2000**.
- [44] Creton, C., *Processing of Polymers*, 15, 709-741, **1997**.
- [45] Aubrey, D. W., Ginosatis, S., *J. Adhes.*, 12, 189-198, **1981**.
- [46] Lakrout, H., Creton, C., Ahn, D., Shull, K. R., *Macromolecules*, 34, 7448-7458, **2001**.
- [47] Toyama, M., Ito, T., Nukatsuka, H., *J. Appl. Polym. Sci.*, 17, 3495–3502, **1973**.
- [48] Petrie, E., *Handbook of adhesive and sealants*, McGraw-Hill, New York, **2000**.
- [49] Fox, H. W., Zisman, W. A., *J. Colloid. Interface Sci.*, 5, 514, **1950**.
- [50] Ebnesajjad, S., *Handbook of Adhesives and Surface Preparation: Technology, Applications and Manufacturing*; 1st ed., **2010**.
- [51] Cognard, P., in *Handbook of Adhesives and Sealants: Basic Concepts and High Tech Bonding*, Elsevier, 1st ed., **2005**.
- [52] Drnovská, H., Lapčík Jr., L., Bursiková, V., Zemek, J., Barros-Timmons, A. M., *Colloid. Polym. Sci.*, 281, 1025–1033, **2003**.

6. Index of contents

- [53] Lehocký, M., Drnovská, H., Lapčíková, B., Barros-Timmons, A. M., Trindade, T., Zembala, M., Lapčík Jr., L., *Colloids and Surfaces A: Physicochemical and Engineering Aspects*, 222 (1-3), 125–131, **2003**.
- [54] Husemann, M., Zollner, S., U.S. Patent 0013790-A1, January 16, **2003**.
- [55] Schellekens, M. A. J., Overbeek, G. C., Nabuur, T., Geurg, J., W.O. Patent 2009/121911-A1, October 8, **2009**.
- [56] Lee, I. S. P., U.S. Patent 4994538, February 19, **1991**.
- [57] Kim, D. J., Kim, H. J., Yoon, G. H., *Interfacial J. Adhesives*, 25, 288–295, **2005**.
- [58] Foreman, P. B., Shah, S. M., Chandran, R., Eaton, P. S., U.S. Patent 6670417, **2003**.
- [59] Caspari, D., Kura, F., Schuette, M., Seeper, K. D., E.P. Patent 1357140, October 29, **2003**.
- [60] Agirre, A., Nase, J., Creton, C., Asua, J. M., *Macromolecular Symposia*, 281 (1), 181–190, **2009**.
- [61] Agirre, A., Nase, J., Degrandi, E., Creton, C., Asua, J. M., *Journal of Polymer Science: Part A: Polymer Chemistry*, 48, 5030–5039, **2010**.
- [62] Zosel, A., *J. Adhes. Sci. Technol*, 11, 1447–1457, **1997**.
- [63] Pocius, A. V., in *Adhesion and Adhesive Technology*, Carl Hanser, München, **2002**.
- [64] Kendall K., *J. Phys. D: Appl. Phys.*, 4, **1971**.
- [65] Gent, A. N., *Rubber Chem. Technol.*, 67 (3), 549–558, **1994**.
- [66] Creton, C., Hooker, J., Shull, K. R., *Langmuir*, 17 (16), 4948–4954, **2001**.

- [67] Tirumkudulu, M., Russel, W. B., Huang, T. J., *Physics of Fluids*, 15 (6), 1588, **2003**.
- [68] Lakrout, H., Sergot, P., Creton, C., *J. Adhes.*, 69, 307–359, **1999**.
- [69] Lindner, A., Lestriez, B. et al., *J. Adhesion*, 82 (3), 267–310, **2006**.
- [70] Brown, K., Hooker, J. C., Creton, C., *Macromol. Mater. Eng.*, 287 (3), 163–179, **2002**.
- [71] Chiche, A., Dollhofer, J., Creton, C., *Soft matter*, 17 (4), 389–401, **2005**.
- [72] Gay, C., Leibler, L., *Physical Review Letters*, 82 (5), 936–939, **1999**.
- [73] Gent, A. N., Lindley, P. B., *Ser. A: Math. Phys. Sci.*, 249 A, 195–205, **1959**.
- [74] Yamaguchi, T, Morita, H., Doi, M., *Eur. Phys. J.*, 20, 7–17, **2006**.
- [75] Creton, C., Fabre, P., in *Adhesion Science and Engineering, Vol.I: The Mechanics of Adhesion*, Dillar D.A. and Pocius A.V., Elsevier, Amsterdam, **2002**.
- [76] Lakrout, H., Creton, C., *J. Adhesion*, 69, **1999**.
- [77] Lakrout, H., Creton, C., *J. polym. Sci.*, 38, 965, **2000**.
- [78] Gay, C., Leibler, L., *Phys. Today*, 52, 48–52, **1999**.
- [79] Shull, K. R., Creton, C., *J. Polym. Sci. Part B: Polym. Physic.*, 42, 4023–4043, **2004**.
- [80] Chicina, I., Gay, C., *Phys. Rev. Lett.*, 85, 4546–4549, **2000**.
- [81] Brown, K., Creton, C., *Eur. Phys. J. E: Soft Matter Biol. Phys.*, 9, 35–40, **2002**.

6. Index of contents

- [82] Yamaguchi, T., Koike, K., Doi, M., *Europhys. Lett.*, 5 (11), 64002, **2007**.
- [83] Zosel, A., *J. Adhesion*, 30, 135–149, **1989**.
- [84] Zosel, A., in *Satas D, editor. Advances in Pressure Sensitive Adhesives Technology*, Vol.1. Warwick, RI: Satas & Associates, 92–127, **1992**.
- [85] Peykova, Y., Guriyanova, S., Lebedeva, O. V., Diethert, A., Müller-Buschbaum, P., Willenbacher, N., *Int. J. of Adh. and Adhes.*, 30 (4), 245–254, **2010**.
- [86] Gent, A. N., Tompkins, D. A., *J. Polym. Sci. Part A-2: Polym. Phys.*, 7, 1483, **1969**.
- [87] Nase J., Creton C., Ramos O., Sonnenberg L., Yamaguchi T., Lindner A., *Soft Mater*, 6, 2685–2691, **2010**.
- [88] Yamaguchi T., Koike K., Doi M., *Europhys. Lett.*, 5 (11), 64002, **2007**.
- [89] Creton, C., Leibler, L., *J. Polym. Sci. Part B: Polym. Phys.*, 34, 545–554, **1996**.
- [90] Zosel A., *J. Adhes. Sci. Technol.*, 11, 1447–1457, **1997**.
- [91] Hui C. Y., Lin Y. Y., Baney J. M., Kramer E. J., *J. Polym. Sci. Part B: Polym. Phys.*, 39, 1195–1214, **2001**.
- [92] Hui C. Y., Lin Y. Y., Baney J. M., *J. Polym. Sci. Part B: Polym. Phys.*, 38, 1485–1495, **2000**.
- [93] Hooker J., Creton C., Shull K. R., Tordjeman P., in *Proceedings of the 22nd annual meeting of The Adhesion Society*, Panama City Beach, USA, **1999**.
- [94] Chiche A., Pareige P., Creton C., *C. R. Phys.*, 1, 1197–1204, **2000**.
- [95] Saffmann, P. G., Taylor, G., in *Proceedings of the Royal Society, A Mathematical Physical and Engineering Sciences*, 245, 312, **1958**.

- [96] Crosby, A. J., Shull, K., *J. Appl. Phys.*, 88 (5), 2956–2966, **2000**.
- [97] Satas, D., in *Handbook of Pressure Sensitive Technology and Applications*, Ed. D. Satas and Satas & Associates, **2002**, Warwick.
- [98] Kaelble, D. H., *J. of Rheo.*, 3 (1), 161, **1959**.
- [99] Kaelble, D. H., *J. of Rheo.*, 4 (1), 45, **1960**.
- [100] FINAT (abbreviation of the French title: **F**édération **I**nternationale des fabricants et transformateurs d'**A**dhésifs et **T**hermocollants sur papiers et autres supports). Technisches Handbuch, 6. Aufl., **2001**.
Available from: <http://www.etika.it/servizi/finat/thduits.pdf>
- [101] ASTM International, Annual Book of ASTM Standards 15.1, American Society of Testing Materials, **2008**. Available from: <http://www.astm.org/>
- [102] PSTC, Test Methods for Pressure Sensitive Adhesive Tapes, Pressure Sensitive Tape Council, **2004**.
Available from: <http://www.pstc.org/i4a/pages/index.cfm?pageid=1>
- [103] Milker R., Czech Z., *Adhäsion Kleben und Dichten*, 9, 22–27, **2003**.
- [104] Shen, H., Zhang, J., Liu, S., Liu, G., Zhang, L., Qu, X., *J. Appl. Polym. Sci.* 107 (3), 1793–1802, **2008**.
- [105] Mayer, A., Pith, T. Hu, G., Lambla, M., *J. Polym. Sci. Part B: Poly. Phys.* 33 (12), 1793–1801, **1995**.
- [106] Rana, P.K., Sahoo, P.K., *J. Appl. Polym. Sci.*, 106 (6), 3915–3921.
- [107] Kim, H.J., Mizumachi, H., in *Advances in Pressure Sensitive Adhesive Technology-3*, ed. D. Satas, Satas and Associates, Warwick, **1998**.

6. Index of contents

- [108] Jo, H. S., Do, H. S., Park, Y. J., Kim, H. J., *J. Adhesion Sci. Technol.*, 20 (14), 1573–1594, **2007**.
- [109] Aubrey, D. W., Welding, G. N., Wong, T., *J. Appl. Polym. Sci.*, 13, 2193–2207, **1969**.
- [110] Do, H. S., Park, Y. J., Kim, H. J., *J. Adhesion Sci. Technol*, 20 (13), 1529–1545, **2006**.
- [111] Creton, C., Shull, K. R., in *Probe Tack in Adhesion Science and Engineering*, vol. I: *The Mechanics of Adhesion*, Dillar D.A. and Pocius A.V., Elsevier, Amsterdam, **2002**.
- [112] Lindner, A., Lestriez, B., Mariot, S., Creton, C., Maevis, T., Luhmann, B., Brummer, R., *J. Adhes.*, 82, 267–310, **2006**.
- [113] Carelli, C., Deplace, F., Boissonnet, L., Creton, C., *J. Adhes.*, 83, 491–505, **2007**.
- [114] Kaelble, D. H., *Rheology of Adhesion*, *J. Macromol. Sci.- Revs. Macromol. Chem.*, 6 (1), 85–112, **1971**.
- [115] Marin, G., Derail, C., *J. Adhes.*, 82, 469–485, **2006**.
- [116] Chang, E. P., *J. Adhes.*, 34, 189–200, **1991**.
- [117] Roos, A., Creton, C., *Macromol. Symp.*, 214, 147–156, **2004**.
- [118] Benedek, I., Feldstein, M. M., in *Molecular Nature of Pressure-Sensitive Adhesives*, in: *Fundamentals of Pressure-Sensitivity*, eds. Taylor & Francis, Boca. **2009**, vol. 1, cap.10.
- [119] Reiner, M., *Physics Today*, 17 (1), 62, **1964**.
- [120] Chu, S. G., Lee, L-H., *Adhesive Bonding*, Plenum Publishing, 97–115, **1991**.

- [121] Bröckel, U., Meier, W., Wagner, G., in *Product Design and Engeneering of Gels and Pastes*, Wiley-VCH Verlag GmbH & Co. KGaA; Auflage: 1. Auflage, **2013**.
- [122] Metzger, T. G., in *Das Rheologie Handbuch: Für Anwender von Rotations- und Oszillations-Rheometern.*, 2. überarbeitete Auflage, Vincentz Network, Hannover, **2006**.
- [123] Macosko, C. W., in *Rheology: Principles, Measurements, and Applications*, 1st ed., Wiley-VCH, New York, **1994**.
- [124] Ferry, J. D., in *Viscoelastic Properties of Polymers*, 3rd ed., vol.1, Wiley, New York, **1980**.
- [125] Maassen, W., „Versuch einer quantitativen Endgruppen-Bestimmung von Polystyrol mittels infrarot Spektroskopie und Bestimmung der molaren Masse mittels Rheologie“, Vertieferarbeit, Universität Karlsruhe (TH), März **2009**.
- [126] Flory, P. J., in *Principles of Polymer Chemistry*, Cornell University, New York, **1953**.
- [127] Carothers, W. H., *J. Am. Chem. Soc.*, 51, 2548, **1929**.
- [128] Allcock, H. R.; Lampe, F. W., in *Contemporary Polymer Chemistry*, 2nd Ed., Prentice Hall, New Jersey, **1990**.
- [129] Choi, K. Y., Kim, K. J., *Chem. Eng. Sci.*, 43 (4), 965–977, **1988**.
- [130] Yoon, W. J., Choi, K. Y., *J. Appl. Polym. Sci.*, 46, 1353–1367, **1992**.
- [131] Cowie, J. M. G., Arrighi, V., in *Polymers: Chemistry and Physics of Modern Materials*, 3rd ed., Scotland, CRC Press, **2008**.
- [132] Matyjaszewski, K., Davis, T. P., in *Handbook of Radical Polymerization*, Wiley, USA, **2002**.

6. Index of contents

- [133] Odian, G., in *Principles of Polymerisation*, 4th ed., Wiley, USA, **1991**.
- [134] Young, R. J., Lovell, P. A., in *Introduction to Polymers*, Chapman and Hall, London, **1991**
- [135] Stepto, R. F. T.; Gilbert, R. G.; Hess, M.; Jenkins, A. D.; Jones, R. G.; Kratochvíl P., *Pure Appl. Chem.*, *81* (2), 351–353, **2009**.
- [136] Seymore, R. B., Carraher, C. E., in *Polymer Chemistry: An Introduction*, 3rd ed. CRC Press, **2012**.
- [137] Arshady, R., *Colloid. Polym. Sci.*, *270* (8), 717-732, **1992**.
- [138] Kawaguchi, S; Ito, K., *Adv. Polym. Sci.*, *175*, 299–328, **2005**.
- [139] Lagaly, G., Schulz O., Zimehl, R., in *Dispersionen und Emulsionen: Eine Einführung in die Kolloidik feinverteilter Stoffe einschließlich der Tonminerale*, Springer Verlag, Heidelberg, **1997**.
- [140] Poehlein, G. W. (n.d.), *Emulsion polymerization mechanisms & kinetics*, paper prepared for the short courses : 1–72.
- [141] Durbin, D. P., El-Aasser, M. S., Poehlein, G. W., & Vanderhoff, J. W., *J. of Appl. Polym. Sci.*, *24* (3), 703–707, **1979**.
- [142] Gilbert, R. G., *Emulsion Polymerization*, Academic Press, **1995**.
- [143] Smith, W. V.; Ewart, R. H., *J. Chem. Phys.*, *16*, 592, **1948**.
- [144] Harkins, W. D. J., *Am. Chem. Soc.*, *69*, 1428, **1947**.
- [145] Fonseca, G. E., McKenna, T. F., & Dubé, M. a., *Chemical Engineering Science*, *65* (9), 2797–2810, **2010**.

- [146] Ugelstad, J., EL-Aasser, M. S., Vanderhoff, J. W., *J. Polym. Sci. Lett. Ed.*, 11, 503–513, **1973**.
- [147] Barnette, D.T., Schork, F.J., *Chem. Eng. Prog.*, 83, **1987**.
- [148] Chamberlain, B. J., Napper, D. H., Gilbert, R. G., *J. Chem. Soc. Faraday Trans.*, 1, 591, **1982**.
- [149] Schork, F., *Colloids and Surfaces A: Physicochemical and Engineering Aspects*, 153 (1-3), 39–45, **1999**.
- [150] Schork, F. J., & Guo, J., *Macromolecular Reaction Engineering*, 2 (4), 287–303, **2008**.
- [151] Antonietti, M., *Progress in Polymer Science*, 27 (4), 689–757, **2002**.
- [152] Asua, J. M., *Progress in Polymer Science*, 27 (7), 1283–1346, **2002**.
- [153] Choi, Y. T., El-Aasser, M. S., Sudol, E. D., & Vanderhoff, J. W. *Polymerization of styrene miniemulsions*, *J. of Polym. Sci.: Polym. Chem. Ed.*, 23 (12), 2973–2987, **1985**.
- [154] Schork, F. J., Luo, Y., Smulders, W., Russum, J. P., Butté, A., & Fontenot, K., *Soft Matter Sciences I*, 129–255, **2005**.
- [155] Eissen, M., Metzger, J. O., Schmidt, E., Schneidewind, U., *Angew. Chem. Int. Ed.*, 41, 414–436, **2002**.
- [156] German Federal Ministry of Food, Agriculture and Consumer Protection, Agency of Renewable Resources, <http://www.fnr.de>.

6. Index of contents

- [157] Bozell, J. J., Patel, M., ACS Symposium Series 921; American Chemical Society, Washington, DC, **2006**.
- [158] Peters, S., in *Materialrevolution: Nachhaltige und multifunktionale Materialien für Design und Architektur*, Birkhäuser GmbH, **2011**.
- [159] FAOSTAT, Food and Agriculture Organization of the United Nations Statistics Division. Available from: <http://faostat3.fao.org/home/E>
- [160] USDA, United States Department of Agriculture, Foreign Agricultural Service, Available from: <http://www.fas.usda.gov/>
- [161] Gunstone, F.D., Harwood, J. L., Dijkstra, A. J., *The Lipid Handbook*, 3rd ed., CRC Press, Taylor & Francis Group, **2007**.
- [162] Gunstone, F. D., *Fatty Acid and Lipid Chemistry*, Springer US, **2012**.
- [163] Thomas, A., in *Fats and Fatty Oils. Ullmann's Encyclopedia of Industrial Chemistry*, Wiley-VCH, Weinheim, **2002**.
- [164] Sahasrabudhe, M. R., *J. of the Am. Oil Chem. Soc.*, **54** (8), 323–324, **1977**.
- [165] Dupont, J. White, P. J., Johnston, H. A. McDonald, B. E. Grundy, S. M. Bonanome, A., *Journal of the American College of Nutrition*, **8** (5), 360–375, **1989**.
- [166] Biermann, U., Friedt, W., Lang, S., Lühs, W., Machmüller, G., Metzger, J. O., Schneider. *Angew. Chem. Int. Ed.*, **39** (13), 2206–2224, **2000**.
- [167] Lu, Y., Larock, R. C., *Chem. Sus. Chem.*, **2** (2), 136–147, **2009**.
- [168] Güner, F.S., Yagci, Y., Erciyes, A.T., *Prog. Polym. Sci.*, **31**, 633–670, **2006**.
- [169] Huber, G. W., Iborra, S., Corma, A., *Chem. Rev.*, **106**, 4044–4098, **2006**.

- [170] Piazza, G. J., Foglia, T. A., *J. Am. Oil Chem. Soc.*, 82, 481–485, **2005**.
- [171] Orellana-Coca, C., Camocho, S., Adlercreutz, D., Mattiasson, B., Hatti-Kaul, R., *Eur. J. Lipid Sci. Technol.*, 107, 864–870, **2005**.
- [172] Rüschen Klaas, M., Warwel, S., *Ind. Crops Prod.*, 9, 125–132, **1999**.
- [173] Aranyi, C., Gutfreud, K., Hawrylewicz, E.J., Wall, J. S., US Patent No. 3607370; **1971**.
- [174] Nordqvist, P., Khabbaz, F., Malmström, E., *Int. J. of Adh. and Adhes.*, 30, 72, **2010**.
- [175] de Koning, G. J. M., van Bilsen, H. M.M., Lemstra, P. J., Hazenberg, W., Witholt, B., Preusting, H., van der Galiën, J. G., Schirmer, A., Jendrossek, D., *Polymer*, 35, 2090, **1994**.
- [176] Babu, G. N., Hammar, W. J., Rutherford, D. R., Lenz, R. W., Richards, R., Goodwin, S. D., *Proceedings of the 1996 International Symposium on Bacterial Polyhydroxyalkanoates*, Davos, Switzerland, 48– 55, **1996**.
- [177] Takano, A., Morio, S., Kogure, M., Saitoh, T., United States Patent No. 5658646; **1998**.
- [178] Meier, M. A. R., Metzger, J. O., Schubert, U. S., *Chem. Soc. Rev.*, 36, 1788–1802, **2006**.
- [179] Arbaoui, A., Redshaw, C., *Polym. Chem.*, 1 (6), 801–826, **2010**.
- [180] Minam, M., Kozaki, S., *US Patent 6 559 275*, **2003**.
- [181] Lander, M. R., Zhang, J., Severtson, S. J., Pressure Sensitive Tape Council (PSTC);
Available from: <http://www.pstc.org/i4a/pages/index.cfm?pageID=4402>.

6. Index of contents

- [182] Ishimoto, K.; Arimoto, M.; Ohara, H.; Kobayashi, S.; Ishii, M.; Morita, K.; Yamashita, H.; Yabuuchi, N. *Biomacromolecules*, *10*, 2719-2723, **2009**.
- [183] Shin, J., Martello, M. T., Shrestha, M., Wissinger, J. E., Tolman, W. B., & Hillmyer, M., *Macromolecules*, *44* (1), 87–94, **2011**.
- [184] Khot, K., La Scala, J. J., Can, E., Morye, S. S., Williams, G. I., Palmese, G. R., Wool, R. P., *J. Appl. Polym. Sci.*, *82* (3), 703–723, **2001**.
- [185] Rüschen Klaas, M., Warwel, S., *J. Am. Oil Chem. Soc.*, *73*, 1453-1457, **1995**.
- [186] Vlcek, T., Petrovic, Z. S., *J. Am. Oil Chem. Soc.*, *83*, 247–252, **2006**.
- [187] Eren, T. and Küsefoğlu, S. H., *J. Appl. Polym. Sci.*, *91*, 2700–2710, **2004**.
- [188] La Scala, J., Wool, R. P., *J Appl Polym Sci*, *95*, 774–783, **2005**.
- [189] Williams, G. I., Wool, R. P., *Appl. Compos Mater*, *7*, 421–432, **2000**.
- [190] Wool, R. P., Bunker, S. P., *J. Polym. Sci: Part A: Polym. Chem.*, *40* (4), 451–458, **2002**.
- [191] Koch, C. A., *Patent WO/2008/144703*, **2008**.
- [192] Ahn, B. K., Kraft, S., Wang, D., Sun, X. S., *Biomacromolecules*, *12*, 1839–1843, **2011**.
- [193] Ahn, B. K., Sung, J., Rahmani, N. *et al.*, *J. of Adhes.*, *89* (4), 323–338, **2013**.
- [194] Li, Y., Wang, D., Sun, X. S., *RSC Advances*, *5* (35), 27256–27265, **2015**.
- [195] Khot, S.N.; M.S. Thesis, University of Delaware, **1998**.

- [196] Wu, Y., Li, A., Li, K., *J. Am. Oil Chem. Soc.*, 92, 111–120, **2015**.
- [197] Bunker, S. P., Staller, C., Willenbacher, N., Wool, R. P., *Int. J. Adhes. Adhes.*, 23, 29–38, **2003**.
- [198] Klapperich, C. M., Noack, C. L., Kaufman, J. D., Zhu, L., Bonnaillie, L., Wool, R. P., *J. Biomed. Mater. Res.*, 91 (2), 378–384, **2008**.
- [199] Agency for Toxic Substances and Disease Registry, *Toxicological Profile for Chromium*, PB2013-105788, U.S. department of health and human service, Public Health Service, Atlanta, GA, **2012**.
- [200] Warwel, S., Rüschen, Klaas, M., *J. Mol. Catal. B*, 1, 29-35, **1995**.
- [201] Samukawa, T., Kaieda, M., Matsumoto, T., Ban, K., Kondo, A., & Shimada, Y., *J. of Biosci. And Bioeng.*, 90 (9), 180–183, **2000**.
- [202] Törnvall, U., Orellana-Coca, C., Hatti-Kaul, R., & Adlercreutz, D., *Enzyme and Microbial Technology*, 40 (3), 447–451, **2007**.
- [203] Zlatanić, A., Lava, C., Zhang, W., Petrović, Z. S., *J. Polym. Sci., Part B: Polym. Phys.*, 42, 809–819, **2003**.
- [204] Dai, H., Yang, L., Lin, B., Wang, C., Shi, G., *J. Am. Oil Chem. Soc.*, 86, 261–267, **2009**.
- [205] Öztürk, C., Mutlu, H., Meier, M. A. R., Küsefoğlu, S. H., *European Polymer Journal*, 47 (7), 1467–1476, **2011**.
- [206] Montero de Espinosa, L., Ronda, J. C., Galiá, M., Cadiz, V., *J. Polym. Sci: Part A: Polym. Chem.*, 47, 1159–1167, **2009**.
- [207] Wool, R. P., Küsefoğlu, S. H., Palmese, G., Khot, S., Zhao, R., *U.S. Pat.* 6,121,398, **2000**.

6. Index of contents

- [208] Guo, A., Cho, Y., Petrovic, Z. S., *J. Polym. Sci: Part A: Polym. Chem.*, 38, 3900–3910, **2000**.
- [209] La Scala, J., Wool, R. P., *J. of the Am. Oil Chem. Soc.*, 79 (1), 59–63, **2002**.
- [210] Zhang, P., Zhang, J., *Green Chemistry*, 15 (3), 641, **2013**.
- [211] Peter, D., *Neue Synthesewege zu acryliertem Methyloleat und Derivaten*, Bachelor Thesis, KIT, Karlsruhe, Februar **2014**.
- [212] Ritter, J.J., Minieri, P.P., *J. of the Am. Chem. Soc.*, 70 (12), 4045–4048, **1948**.
- [213] Biermann, U., Metzger, J.O., *Lipid/Fett*, 92 (4), 133–134, **1990**.
- [214] Zhang, P., J. Xin, and J. Zhang, *ACS Sustainable Chemistry & Engineering*, 2, 181–187, **2013**.
- [215] Sheldon, R.A., *Green Chem.* 9, 1273-1283, **2007**.
- [216] Sharma, V., Kundu, P. P., *Prog. Polym. Sci.*, 31, 983–1008, **2006**.
- [217] Benedek, I., ed., *Development and Manufacture of Pressure-Sensitive Products*, CRC Press, New York, 205, **1998**.
- [218] Reyes, Y., Asua, J. M., *Macromol. Rapid Commun.* 32, 63–67, **2011**.
- [219] Heatley, F., Lovell, P. A., Yamashita, T. T., *Macromolecules*, 34, 7636, **2001**.
- [220] Junkers, T., Barner-Kowollik, C., *J. Polym. Sci. A: Polym. Chem.*, 46, 7585, **2008**.
- [221] Schmidt, A., “*Reversible-Deactivation Radical Polymerization of Acrylated Methyl Oleate*”, bachelor thesis, Karlsruhe Institute of Technology (KIT), Germany, **2014**.

- [222] Jenkins, A. D., Kratochvíl, P., Stepto, R. F. T., Suter, U. W., *Pure and Appl. Chem.*, 68, 2287–2311, **1996**.
- [223] Buddrus, J., *Grundlagen der Organischen Chemie*, 4th ed., Walter de Gruyter Verlag, Berlin, **2011**.
- [224] Fineman, M., Ross, S. D., *J. Polym. Sci.*, 2, 259-262, **1950**.
- [225] Kelen. T., Tüdös, F., *J. Macromol. Sci. Chem.*, 9 (1), **1975**.
- [226] Osmani, A., “*Determination of Monomer Reactivity Ratios for the Free-Radical Copolymerisation of renewable Monomers*”, bachelor thesis, Karlsruhe Institute of Technology (KIT), Germany, **2014**.
- [227] Ferrick, M. R., Murtagh, J., Thomas, J. K., *Macromol.*, 22, 1515, **1989**.
- [228] Kajtna, J., Golob, J., Krajnc, M., *Int. J. of Adh. & Adhes.*, 29 (2), 186–194, **2009**.
- [229] Khan, I., Poh, B. T., *J. of Appl. Polym. Sci.*, 120 (5), 2641–2647, **2011**.
- [230] Maaßen W., Oelmann S., Peter D., Oswald W., Willenbacher N., Meier M. A. R., *Macromol. Chem. Phys.*, 216, 1609–1618, **2015**.
- [231] Tung, C. M., Dynes, P. J., *J. of Appl. Polym. Sci.*, 27 (2), 569–574, **1982**.
- [232] Neiman, M. B., ed., *Aging and Stabilization of Polymers*, Springer, **1965**.
- [233] Balci, S., Birer, O., Suzer, S., *Polymer*, 45 (21), 7123–7128, **2004**.
- [234] Jovanivic, R., Dube, M. A., *Ind. Eng. Chem. Res.*, 44 (17), 6668–6675, **2005**.
- [235] Peykova, Y., Lebedeva, O. V., Diethert, A., Müller-Buschbaum, P., Willenbacher, N. , *Int. Int. J. of Adh. & Adhes.*, 34, 107–116, **2012**.

6. Index of contents

- [236] Jensen, A. T., Sayer, C., Araújo, P. H. H., Machado, F., *Eur. J. of Lipid Sci. and Tech*, 116 (1), 37–43, **2014**.
- [237] Lucena, I. L., Silva, G. F., Fernandes, F. A. N., *Int. Eng. Chem. Res.*, 47, 6885–6889, **2008**.
- [238] Oswald, W., “*Schälfestigkeitsmessungen von Haftklebstoffen auf Basis nachwachsender Rohstoffe*”, Studienarbeit, Karlsruher Institut für Technologie (KIT), **2013**.

7. APPENDIX

List of publications and conference contributions

Publications in peer-reviewed journals

Maaßen W., Oelmann S., Peter D., Oswald W., Willenbacher N., Meier M. A. R., *Novel insights into pressure sensitive adhesives based on plant oils*, *Macromol. Chem. Phys.*, 216, 1609–1618, **2015**.

Maaßen W., Meier M. A. R., Willenbacher N., Unique adhesive properties of pressure sensitive adhesives from plant oils, *Int. J. of Adh. & Adhes*, **2015**. Accepted.

Conference contributions

W. Maassen, N. Willenbacher, M. A. R. Meier, *Pressure sensitive adhesives from renewable resources*, 37. Münchener Klebstoff- und Veredelungs-Symposium, München, Germany, 23. Oktober, 2012.

W. Maassen, N. Willenbacher, M. A. R. Meier, *Haftklebstoffe auf Basis nachwachsender Rohstoffe*, 12. Kooperationsforum Kleben im Automobilbau, Nürnberger Akademie, Nürnberg, Germany, 5. Juni, 2013.

7. Appendix

W. Maassen, N. Willenbacher, M. A. R. Meier, *Pressure sensitive adhesives from renewable resources*, Adhesion´13, National Science Learning Centre, University of York, York, UK, Sep 04-06, 2013.

W. Maassen, N. Willenbacher, M. A. R. Meier, *Pressure sensitive adhesives from renewable resources*, 37. Münchener Klebstoff- und Veredelungs-Symposium, München, Germany, 22. Oktober, 2014.

Poster-presentations as conference contribution

W. Maassen, N. Willenbacher, M. A. R. Meier, *Pressure sensitive adhesives from renewable resources*, 6th Workshop on Fats and Oils as Renewable Feedstock for the Chemical Industry, Karlsruhe, Germany, March 17-19, 2013.

W. Maassen, N. Willenbacher, M. A. R. Meier, *Pressure sensitive adhesives from plant oils: Synthesis and Adhesive Properties*, 8th Workshop on Fats and Oils as Renewable Feedstock for the Chemical Industry, Karlsruhe, Germany, March 29-31, 2015.